PROF. DR STEFAN CZARNECKI DIED IN WARSAW ON 1 SEPTEMBER, 1982

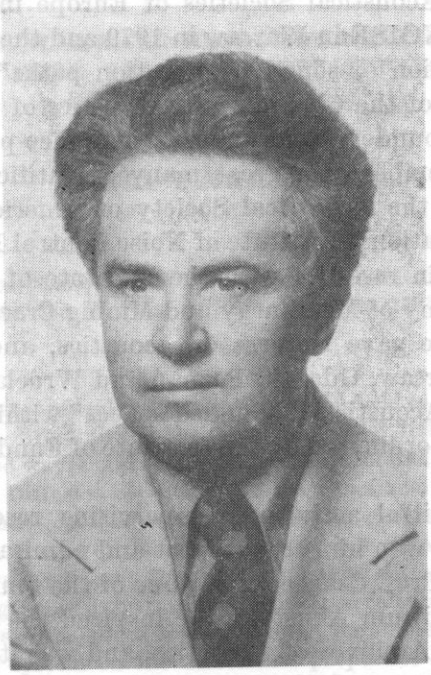

Stefan Czarnecki (born in 1925) graduated from Gdańsk Technical University in 1949 as an electronic engineer with specialization in acoustics. After several years of work at the Central Laboratory of the Polish Radio and at Warsaw Technical University, in 1953 he began work at the Institute of Fundamental Technological Research of the Polish Academy of Sciences, where in 1957 he became head of the Analogy Department. In 1963 he moved with the Department to the Institute of Automation and returned to the Institute of Fundamental Technological Research in 1974 to become head of the Department of Aeroacoustics.

His doctoral dissertation, which he defended at Warsaw Technical University in 1958, was devoted to problems of nonlinear acoustic transients in interiors, whereas the subject of his habilitational dissertation, submitted at the Institute of Fundamental Technological Research in 1965, was the analysis of the interaction of Helmholtz resonators with an acoustic medium. He was appointed assistant professor in 1972 and full professor in 1980.

The main field of his research comprised problems of aeroacoustics, room acoustics and identification of vibration transfer paths. In addition to fundamental research in this field he carried out research and development work, cooperating with industry in noise control. He published about 80 papers in Poland and abroad. He was active internationally, representing Poland at numerous conferences abroad and organizing international symposia and congresses of high scientific rank. Of these, the most important events were The Second Congress of the Federation of Acoustical Societies of Europe in Warsaw in 1978, the international INTER NOISE in Warsaw in 1979 and the International Summer Workshop "Identification of sound propagation paths" at Jabłonna in 1981. He was vice-president of the Committe on Acoustics of the Polish Academy of Sciences, one of the founders, and subsequently vice-president, of the Polish Acoustical Society, member of a great many Scientific Societies: in 1980 he was elected Fellow of the Acoustical Society of America and member of the executive of the International Institute of Noise Control Engineering. In Poland he cooperated closely in research with the Institute of Mechanics and Vibroacoustics of the Academy of Metallurgy and Mining Cracow, with Music Academy, Warsaw, where he gave lectures on acoustics, and also with acoustical research centres in Warsaw, Gdańsk, Poznań and Wrocław. He was the coordinator of the problem "Acoustics of bounded spaces" within the Interdepartmental Problem MR-1-24 coordinated by the Institute of Fundamental Technological Research.

His extremely fruitful activity in supervising research and stimulating scientific investigations won him true respect and admiration in the community of Polish acousticians. Prof. Czarnecki was one of the founders, and, since 1966, Editor-in-Chief of Archiwum Akustyki. He inspired the establishment in 1976 of the English version, Archives of Acoustics, and was its Editor-in-Chief since the very beginning. He created the present character of this quarterly and its authority at home and abroad. He always saw to the high level of this periodical, demanding high scientific level of its papers. He was interested not only in the general supervision but also helped authors in preparation of their papers.

His death is an irretrievable loss for Polish acoustics, and particularly painful for the whole Editorial Committee and Board of Archiwum Akustyki (Archives of Acoustics).

Editorial Committee and Board

ARCHIVES OF ACOUSTICS
7, 3-4, 173-182 (1982)

A GEOMETRICAL-NUMERICAL METHOD FOR THE DETERMINATION OF THE ACOUSTIC FIELD PROPERTIES RELATED TO THE DIRECTIONS OF REFLECTED WAVES*

MARIA TAJCHERT

Institute of Radioelectronics, Warsaw Technical University
(00-665 Warsaw, ul. Nowowiejska 15/19)

A method for theoretical determination of the field in enclosures is presented. To analyse the directivity of the field, the spatial distributions of the directions of the reflected waves and their energy are calculated using the geometrical-numerical method. Diffusion coefficients of the directions, energy and ray energy are introduced. These coefficients characterize in general the directional properties of the field at a given point and determine in detail the values of energy reaching the observation point from different parts of the space. An algorithm for a computer program and the results of numerical calculations for a rectangular room which illustrate the effect of the different parameters of the source-room-observation point system on the directional properties of the field are given.

1. Introduction

The methods for the evaluation of the field directivity used to date have mainly been based on measurement results [1], while theory has so far failed to provide effective tools for this purpose [2]. Such possibilities are provided by the geometrical method for field analysis which uses a computer and consists in the determination of an array of image sources [3] and in further processing of data which result from the shape of the array. Paper [3] proposed an energy approach to directivity, which defines only the mutual relations among the energies of waves reaching different points of the field but does not give information of the directions from which the waves reach a given point.

* This work was supported by the Polish Academy of Sciences as a part of the research project MR.I.24.

When application, and not the cognitive aspects, is taken into account, this energy approach can in general be considered sufficient in noise control but is insufficient in architectural acoustics in which it is necessary to know also the directions from which the energy reaches a point. In the geometrical-numerical method for field analysis this problem can be solved in a rather simple way. When an array of image sources has been determined for a given source, it is possible to construct an algorithm for the determination of the directions from which particular reflected waves reach the observation point. The question arises as to whether it is necessary to determine each direction in the form of a versor or directional cosines, or whether it is sufficient to determine the number of directions in which the waves propagate in successive parts of the space. The determination of the directional cosines of all waves which reach the observation point would permit theoretical development of a directional-energy image of reflections analogous to the saw-tooth shape obtained from measurements using a directional microphone [2]. Such an image — in particular when given in spatial form — is clear and easy to interpret for one point. It is, however, more difficult to interpret it for several points. It seems therefore useful to gather information of all reflected waves in larger groups which include the waves which reach the observation point from a certain part of the space. This gives information in more compact form, which it is thus easier to use further without additional processing. When the number of the parts of the space in which the directional properties are determined decreases, in the limits information is gained which is expressed by one number for a given observation point. Such generalized information makes it easier to compare or evaluate, but also makes difficult the work towards the introduction of desired changes, since this requires detailed information. It seems that a reasonable compromise is the giving of generalized information with possible access — as the need arises — to detailed information. Such a solution has been assumed in the development of theoretical determination of the directivity of the field using a computer.

2. The method for the determination of the field directivity

Since the present method is based on geometrical analysis of the field using image sources, it satisfies the same assumptions as the analysis does:

(1) acoustic waves — represented in the form of sound rays — radiated by point image sources reach the observation point;

(2) the energy of particular sound rays sums up at the observation point.

Conceptually the method is based on the following two assumptions:

(1) the space is divided into parts in which some parameters of the field are calculated;

(2) the directional properties of the field in a point are determined by the number of the directions in which the waves propagate in successive parts of

the space, by the energy reaching the observation point and by the energy of rays in the same parts of the space.

The centre of the coordinate system xyz is placed at the observation point. The system divides the entire space into eight parts by the planes $x = 0$, $y = 0$ and $z = 0$ (Fig. 1). The number of rays K_i which reach the observation point,

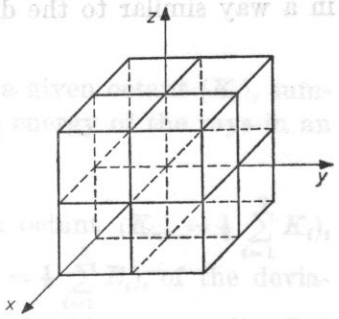

Fig. 1. The division of the space into octants by the planes $x = 0$, $y = 0$ and $z = 0$

the energy E_i carried by these rays and the mean energy corresponding to a ray, $p_i = E_i/K_i$, are determined for each ith octant. From the above values the deviations D_{ki} and D_{ei} of these quantities from the mean values for the entire space are determined from the relations

$$D_{ki} = \frac{K_i - K_{\text{av}}}{K_{\text{av}}}, \quad \text{where } K_{\text{av}} = \frac{1}{8}\sum_{i=1}^{8} K_i; \tag{1}$$

$$D_{ei} = \frac{E_i - E_{\text{av}}}{E_{\text{av}}}, \quad \text{where } E_{\text{av}} = \frac{1}{8}\sum_{i=1}^{8} E_i. \tag{2}$$

The value of the deviation D_{ki} can fall in the range $[-1, 7]$, where $D_{ki} = -1$ no ray reaches the observation point from the ith octant; $-1 < D_{ki} < 0$ fewer rays than follows from their mean number reach the observation point from the ith octant; $D_{ki} = 0$ the mean number of rays reach the observation point from the ith octant (when for all i $D_{ki} = 0$, the distribution of directions is uniform in the entire space); $0 < D_{ki} < 7$ more rays than follows from their mean number reach the observation point from the ith octant; $D_{ki} = 7$ all the rays concentrate in the ith octant.

Analogous interpretation is valid for the energy deviation D_{ei} in the ith octant.

In defining quantitatively the spatial distribution of directions and energies, the measured values of K_i and E_i and their deviations permit the distribution to be shaped at a given point by changing the parameters of the source-room-observation point system. Such detailed information of the spatial directivity in the form of several dozens of numbers for one observation point are little

useful in comparing the directional properties of the field at different points. In view of this, the diffusion coefficients — of direction d_k and of energy d_e — which characterize the directional properties in a more compact way have been introduced. The diffusion coefficients average the directional properties for all octants, expressing these by two numbers for a given point, and thus permit comparison of different points of the field. These coefficients are defined in a way similar to the directional diffusion coefficients [4],

$$d_k = 1 - \frac{\frac{1}{8}\sum_{i=1}^{8} |K_i - K_{av}|}{K_{av}}, \tag{3}$$

$$d_e = 1 - \frac{\frac{1}{8}\sum_{i=1}^{8} |E_i - E_{av}|}{E_{av}}. \tag{4}$$

The diffusion coefficients d_k and d_e take values from the range $[-0.75, 1]$; d_k(or d_e) $= -0.75$ corresponds to the field concentrated in one octant, while d_k(or d_e) $= 1$ corresponds to a dispersed field, i.e. one with a uniform distribution of directions and energies (with an accuracy of an octant). When the space is divided into more than eight parts, the range will extend, tending on the left side to -1 with $i \to \infty$.

The present computational method for the determination of the directional properties of the field permits rather easy calculation of the diffusion coefficients of directions and energy for a given point, i.e. permits a general evaluation of the directivity. It at the same time gives detailed data on particular octants of the space, thus permitting the desired shaping of the spatial distribution of directions and energies by choosing the parameters of the source-room-observation point system.

3. A short description of the programme

The programme was written in FORTRAN, while calculations were performed on a CYBER CDC 6000 system computer. A flow chart of the program is given below for a rectangular room.

data

↓

calculation of one coordinate defining the distance of the image source from the observation point and of the number of reflections from each of the two walls perpendicular to the axis along which the coordinate is calculated

↓

calculation of the distance between the image source and the observation point, of propagation and reflection losses and of the sound pressure level of reflected waves

↓

determination of the sign of the coordinates x, y, z in a new coordinate system, related to the observation point and subordination of the reflected wave to a certain octant

↓

counting of waves reaching the observation point in a given octant (K_i), summing up of their energies (E_i) and calculation of the energy of the rays in an octant ($p_i = E_i/K_i$)

↓

calculation of the mean number of reflections in an octant ($K_{\mathrm{av}} = \frac{1}{8} \sum_{i=1}^{8} K_i$), of the mean energy corresponding to the octant ($E_{\mathrm{av}} = \frac{1}{8} \sum_{i=1}^{8} E_i$), of the deviations of the number of directions and of energy for the ith octant (D_{ki}, D_{ei})

↓

calculation of the diffusion coefficients of direction (d_k) and of energy (d_e)

The input data of the programme are: the dimensions of the room, the coordinates of the sound source and of the observation point, the absorption coefficients of the walls, the sound pressure level of the direct wave at a distance of 1 m from the source, the coefficient of energy attenuation in the air and the order of the reflections considered. The calculated results are given in two tables. Table 1 gives the values of the number of waves reaching the observation point K_j, of their summary energy E_j, of the level of this energy L_{ej} and of the energy of the rays p_j. The index j takes values from 1 to 27, since the waves reaching the observation point along the axes Ox, Oy and Oz of the system and the planes xy, xz and yz are treated individually. The a priori subordination of the axes and planes to specific octants, since it masks some information, prevents effective control of the directivity of the field by varying the input data. In addition it would be incorrect to calculate the values of the means and deviations for each of 27 parts of the space, since each of these parts is treated as equivalent, irrespective of whether it is an octant or half-axis. These results, which are detailed information, are therefore only an intermediate stage. Table 2 gives the final results, i.e. the above-mentioned quantities K_i, E_i, L_{ei}, p_i, D_{ki} and D_{ei} calculated for particular octants and the diffusion coefficients d_k and d_e for a given observation point. The waves which reach the observation point in the planes xy, xz and yz are divided between the two octants adjacent to them, while the waves which propagate along the axis are separated among the four adjacent octants. The octants are numbered in the following way: from 1 to 4 for $z > 0$ counter-clockwise, where octant 1 lies between the planes determined by the positive half-axes of the system; from 5 to 8 for $z < 0$, where octant 5 lies

underneath octant 1. The programme is so built that it does not limit the order of reflections considered. The restriction on the order results from the time limit only and thus from calculation cost.

4. Calculated results and their interpretation

Calculations were performed for a rectangular room with dimensions $15 \times 25 \times 10$ m, with an active point sound source which radiated a wave of 100 dB sound pressure level at a distance of 1 m. Fig. 2 shows the position of the enclosure in the coordinate system. The coefficient of energy attenuation $m = 0.004$ was taken. The values of the absorption coefficients of the walls, α, varied from 0.1-0.6. The calculations took into account reflected waves up to the seventh order.

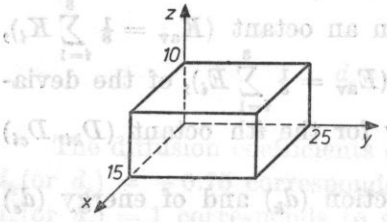

Fig. 2. The position of the room in the coordinate system

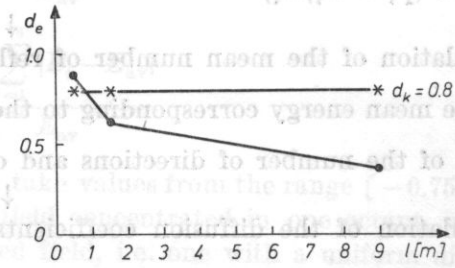

Fig. 3. The effect of the distance of the observation point from the wall on the energy uniformity of the field expressed by the diffusion coefficient of energy d_e

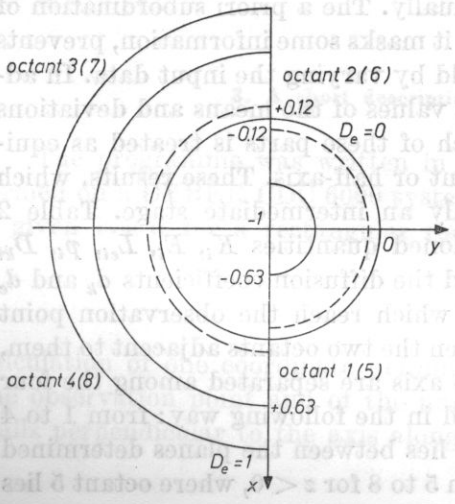

Fig. 4. The energy deviation D_e in octants for two positions of the observation point: far from one of the walls and close to it. Calculations were performed for the following parameters: the absorption coefficients of the walls $\alpha = 0.1$; the coordinates of the source placed in the centre of symmetry of the area (7.5; 12.5; 5.0 m); a solid line represents D_e calculated for an observation point with the coordinates (7.5; 16.0; 5.0 m) a dashed line expresses that for the coordinates (7.5; 24.5; 5.0 m). The solid circle marks 0 scale for $D_e = 0$

Investigations were performed on the directional properties of the field defined by the diffusion coefficients of direction and energy by always varying only one parameter of the source-room-observation point system so that it would be possible to interpret the results in a clear way.

The effect of the position of the observation point with a constant position of the source at the centre of symmetry of the room. The shift of the observation point along the Oy axis towards the wall does not change the dispersion coefficient of direction but improves, instead, the dispersion of energy (Fig. 3). This can be explained by the effect of high-energy reflections from the close wall. This is also illustrated by Fig. 4 which shows the energy deviation $D_{ei} = \Delta E_i / E_{av}$ for four octants; for the other octants the plot is the same because of the geometrical symmetry of the system. The value of the deviation D_e in a given octant is constant, which is represented in the polar coordinate system in the form of a quadrant: plotted in a solid line for an observation point at a distance of 16 m from the wall $y = 0$, in dashed line for an observation point at a distance of 0.5 m from the opposite wall. The solid circle marks the scale in the form of a circle $D_e = 0$ and $D_e = 1$. The results of the calculations permit a quantitative approach, as opposed to the only qualitative one previously, to the effect of the close wall on the energy at the observation point.

The effect of the symmetry of the position of the observation point with respect to the source placed in the centre of symmetry of the room. Investigations were performed on the cases in which the symmetry of the position of the observation point was maintained with respect to the source, e.g. when the source and the observation point differed only in one coordinates and on the cases when there was no regular position — the source and the observation differing in all the three coordinates. From the point of view of the uniformity of the field, the symmetrical position of the observation point with respect to the source is more convenient, since then both the dispersion coefficients of direction and of energy are closer to 1 than in the case of an arbitrary position of the observation point.

The effect of the geometrical asymmetry of the position of the source and the observation point in the room. Keeping a constant between the source and the observation point the directional properties of the field were compared for a symmetrical position of this pair of points in the area with the source at the centre of symmetry and the observation point on an axis parallel to the wall and for a random position. It was found that the diffusion of directions slightly decreases for a random position of the source and the observation point; the diffusion coefficient of energy, however, increases very greatly, i.e. the energy uniformity of the field decreases (e.g. d_e reduces from 0.37 to -0.05).

The effect of change in the position of the source and the observation point. In view of the geometrical symmetry of the system, the diffusion coefficient of direction, d_k, does not change, whereas the same values of the deviations D_{Ki}

are subordinated to different octants, i.e. the coordinate system undergoes rotation. In turn, the diffusion of energy changes, being greater when the source is closer to the centre of symmetry of the area.

The effect of the arrangement of the sound-absorbing materials. The introduction of differentiated absorption coefficients α of the walls does not change the diffusion of directions but reduces the uniformity of the field ($d_e \searrow$). This second conclusion is rather evident qualitatively but it is essential that quantitative relations are obtained. The magnitude of change in the diffusion coefficient of energy, d_e, depends on two factors: on the absolute change in the coefficient α and on whether the wall of another value of the absorption coefficient is close to or far from the source (Fig. 5). It was also found that the effect of the same change in the coefficient α is stronger for a field of higher nonuniformity, i.e. the diffusion coefficient of energy decreases to a greater extent if it is small before α is changed.

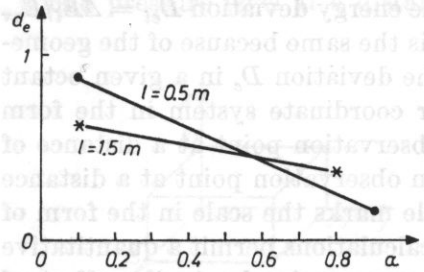

Fig. 5. The dependence of the diffusion coefficient of energy d_e on the variation of the absorption coefficient α of walls for different distances l between the observation point and the walls

The effect of the order of reflections assumed on the calculated directional parameters of the field. In order to determine the error which results from the limitation of the order of reflections up to the seventh one, calculations were performed for the tenth order. The number of reflected waves reaching the observation point increased from 575 to 1561 and the calculation time more than doubled; the diffusion coefficients however, increased only slightly. The differences of the order of hundredths of a part between the values of the diffusion coefficients are so small that it is possible to take as reliable the results calculated when the seventh order is considered.

The analysis of the calculated results will conclude with an example of the effect of two factors of opposite impact. This effect equilibrates in the calculation of the diffusion coefficient of energy, d_e, but it is, however, not balanced in particular octants. These factors are the shift of the source towards the centre of symmetry of the enclosure, which causes an increase in the diffusion of energy ($d_e \nearrow$), and the introduction of differentiated coefficients α of the walls, which decreases the diffusion of energy ($d_e \searrow$). With a correct selection of parameters the diffusion coefficient d_e may remain constant but the deviations in energy

in the octants will vary (Fig. 6). It can be concluded from this example that only an agreement among all the three diffusion coefficients for systems with different parameters makes it possible to assume the identity of the directional properties of the field. The establishment of several parameters and the change in one permit, in turn, a rather precise evaluation of change in directivity.

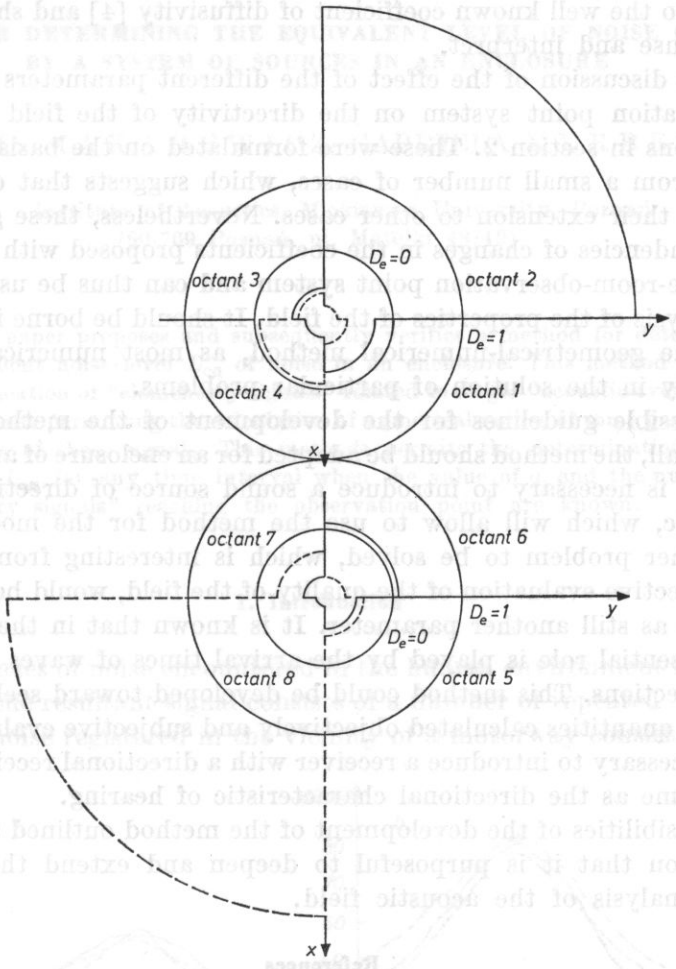

Fig. 6. The values of the energy deviation $D_{ei} = \Delta E_i/E_{av}$ in particular octants for two source room-observation point systems

The diffusion coefficient of energy $d_{e1} = d_{e2} = 0.11$ for both cases, the diffusion coefficient of direction $d_{k1} = d_{k2} = 0.7$, the diffusion coefficient of the energy of the rays with different values: $d_{p1} = 0.37$ and $d_{p2} = 0.35$. A solid line represents D_e calculated for the parameters: the coordinates of the source (7.0; 16.0; 5.5 m); the coordinates of the observation point (7.5; 12.5; 5.0 m); the absorption coefficients of the walls $\alpha = 0.1$. A dashed line represents, respectively, the coordinates (7.5; 12.5; 5.0 m) and (7.0; 16.0; 5.5 m); the absorption coefficient of the wall $y = 0$ is $\alpha = 0.06$, that of the others is $\alpha = 0.1$. The solid circle marks the scale for $D_e = 0$ and $D_e = 1$

5. Conclusion

The present method for the determination of the directional properties of the field expands the theoretical possibilities of application of the geometrical-numerical analysis.

The results of this paper show that it is useful to calculate the diffusion coefficients of direction energy and the energy of rays which express the spatial and directional features of the field. These coefficients, determined numerically, are similar to the well known coefficient of diffusivity [4] and should therefore be easy to use and interpret.

A short discussion of the effect of the different parameters of the source-room-observation point system on the directivity of the field brought some generalizations in section 2. These were formulated on the basis of the results calculated from a small number of cases, which suggests that care should be exercised in their extension to other cases. Nevertheless, these generalizations show the tendencies of changes in the coefficients proposed with given changes in the source-room-observation point system and can thus be useful in further general analysis of the properties of the field. It should be borne in mind, however, that the geometrical-numerical method, as most numerical methods, is useful mostly in the solution of particular problems.

The possible guidelines for the development of the method are readily seen. Above all, the method should be adapted for an enclosure of arbitrary shape. Secondly, it is necessary to introduce a sound source of directional radiation characteristic, which will allow to use the method for the modelling of real cases. Another problem to be solved, which is interesting from the point of view of subjective evaluation of the quality of the field, would be the introduction of time as still another parameter. It is known that in the perception of sound an essential role is played by the arrival times of waves reflected from different directions. This method could be developed toward seeking a relation between the quantities calculated objectively and subjective evaluation. It then would be necessary to introduce a receiver with a directional receiving characteristic the same as the directional characteristic of hearing.

The possibilities of the development of the method outlined above warrant the conclusion that it is purposeful to deepen and extend the geometrical-numerical analysis of the acoustic field.

References

[1] V. FURDUYEV, *Izmerenye difuznosti zvukovo pola v pomeshchenyakh metodom napravlennovo mikrofona*, Akust. Zh., **5**, 1 (1960).

[2] I. MALECKI, *Theory of waves and acoustic systems* (in Polish), PWN, Warsaw 1964.

[3] M. TAJCHERT, *Investigation of the directional properties of the acoustic field in perpendicular-walled enclosures using the geometrical method of field analysis* (in Polish), Archiwum Akustyki, **13**, 4 (1978).

[4] H. KUTTRUFF, *Room acoustics*, Applied Science Publishers Ltd., London 1973.

Received on November 21, 1980; revised version on March 26, 1982.

ARCHIVES OF ACOUSTICS
7, 3-4, 183-196 (1982)

A METHOD FOR DETERMINING THE EQUIVALENT LEVEL OF NOISE GENERATED BY A SYSTEM OF SOURCES IN AN ENCLOSURE

RUFIN MAKAREWICZ, GABRIELA KERBER

Institute of Acoustics, Mickiewicz University, Poznań
(60-769 Poznań, ul. Matejki 48/49)

This paper proposes and subsequently verifies a method for determining the equivalent noise level L_{eq} of noise in an enclosure. This method requires the identification of "elementary signals" related to single "acoustic events" and measurements permitting the calculation of numerical values of some parameters a_i for each of these signals. This methods permits the determination of the values of L_{eq} for any time interval when the value of a_i and the number of "elementary signals" reaching the observation point are known.

1. Introduction

In many cases of noise encountered in the human environment it is possible to notice that the resultant signal consists of a number of repeated "elementary signals". E.g. noise registered in the vicinity of a motorway consists essentially

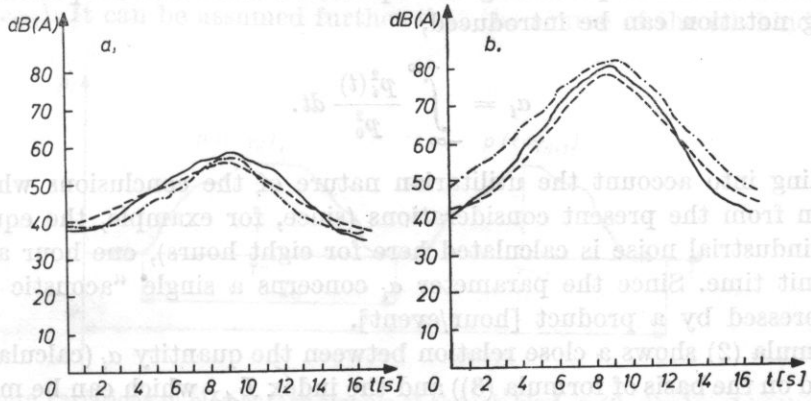

Fig. 1. Sound level variations, in dB (A), due to the traffic of single light (a) and heavy (b) vehicles

of two classes of "elementary signals": those generated by light vehicles and those generated by heavy vehicles. Single light and heavy vehicles generate distinctly different "elementary signals", while differences among signals emitted by particular light and heavy vehicles are considerably smaller (Fig. 1).

It is therefore possible to consider, in the first approximation, only two kinds of "elementary signals", corresponding to two different "acoustic events" caused by the passages of a light vehicle and a heavy vehicle, respectively. Considering different types of vehicle, their different speeds (more generally, ways of operation), traffic lanes etc., it is possible to increase the number of kinds of "elementary signals" (acoustic events) [4]. It is, however, necessary then to establish a precise criterion of the similarity of "elementary signals".

This similarity can be measured using the index of noise evaluation which is called the *Single Event Noise Exposure Level* [2],

$$L_{AX}^{(i)} = 10 \log \int_{t_p}^{t_k} 10^{0.1 L_i(t)} dt, \tag{1}$$

where $L_i(t)$, in dB (A), is the time history of the "elementary signal" of the ith kind, t_p and t_k are the limits of the time interval in which the instantaneous value of $L_i(t)$ is not lower by 10 dB (A) than its maximum value. It is possible to assume in (1) that $t_p = -\infty$ and $t_k = +\infty$ which involves error below 1 dB. On the basis of the definition of sound level

$$\int_{-\infty}^{+\infty} \frac{p_i^2(t)}{p_0^2}\, dt = 10^{0.1 L_{AX}^{(i)}}, \tag{2}$$

where $p_i(t)$ is the pressure corrected by the curve $A-40$ phons and p_0 is the reference pressure.

The integral on the left side of equation (2) is related to the energy of "an elementary signal" of the ith type. It will be shown below that this integral occurs in formulae for predicting the equivalent level. For simplification the following notation can be introduced,

$$a_i = \int_{-\infty}^{+\infty} \frac{p_i^2(t)}{p_0^2}\, dt. \tag{3}$$

Taking into account the utilitarian nature of the conclusions which can be drawn from the present considerations (since, for example, the equivalent level of industrial noise is calculated here for eight hours), one hour as taken is the unit time. Since the parameter a_i concerns a single "acoustic event", it is expressed by a product [hour/event].

Formula (2) shows a close relation between the quantity a_i (calculated and measured on the basis of formula (3)) and the index L_{AX} which can be measured using the latest, i.e. least available, Brüel-Kjaer equipment.

In a general case of noise being a superposition of individual acoustic events (particularly, industrial noise which is the object of consideration in the present paper), division of "elementary signals" into particular classes is determined by the value of the parameter a calculated from formula (3). (This problem is disscused in greater detail in section 2.1).

One of the numerous indices currently used for noise evaluation is the equivalent level L_{eq} [2],

$$L_{eq} = 10 \log \frac{1}{T} \int_0^T 10^{0.1L(t)} dt, \tag{4}$$

where T is the averaging time and $L(t)$ the instantaneous sound level of the resultant signal in dB (A).

According to definition (2), this expression can be rewritten in the form

$$L_{eq} = 10 \log \frac{\langle p^2 \rangle}{p_0^2}, \tag{5}$$

where

$$\langle p^2 \rangle = \frac{1}{T} \int_0^T p^2(t)\, dt. \tag{6}$$

Papers [5,6] gave a method for the determination of the time average intensity of the resultant signal which is a superposition of "elementary signals". This method can be used to determine $\langle p^2 \rangle$ and subsequently the equivalent level L_{eq} of signals generated by the noise sources in an enclosure.

2. Theory

It can be assumed that the "elementary signals" reaching the observation point within an arbitrary bounded region can be divided into several kinds ($i = 1, 2, \ldots,$). It can be assumed further that the source of the ith kind emits

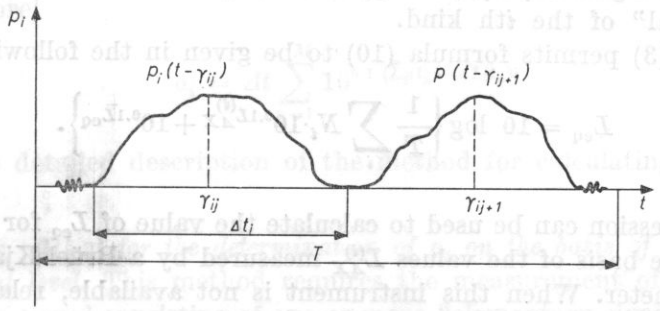

Fig. 2. Pressure variations in elementary signals of the ith kind, $p_i(t)$, displaced in time with respect to one another

an "elementary signal" at the times $\gamma_{i,1}, \gamma_{i,2}, \gamma_{i,j+1}, \ldots$, of the pressure time history $p_i(t)$ (Fig. 2). The instantaneous value of the pressure of the resultant signal is the sum of the pressures of all "elementary signals"

$$p(t) = \sum_i \sum_j p_i(t-\gamma_{i,j}) + \overline{p}(t), \tag{7}$$

where $\overline{p}(t)$ is the pressure of the acoustic background and the quantity $\gamma_{i,j}$ denotes the time shift of the jth "acoustic event" of the ith kind.

When "elementary signals" are incoherent, formula (7) yields

$$p^2(t) = \sum_i \sum_j p_i^2(t-\gamma_{i,j}) + \overline{p}^2(t). \tag{8}$$

Assuming that N_i "accoustic events" of the ith kind occurred in the time T, i.e. N_i "elementary signals" characterized by $p_i(t-\gamma_{i,j})$, where $0 < \gamma_{i,j} < T$, reached the observation point, formulae (6)-(8) give

$$\langle p^2 \rangle = \frac{1}{T} \sum_i N_i \int_{-\infty}^{\infty} p_i^2(t)\,dt + \langle \overline{p}^2 \rangle, \tag{9}$$

where $\langle \overline{p}^2 \rangle$ is the time average square background pressure.

Relation (9) is valid when the duration of the resultant signal, T (the averaging time), is much longer than the duration of the elementary signal Δt_i (Fig. 2).

It follows from the definition of the equivalent level (5) and (6) that

$$L_{eq} = 10 \log \left\{ \frac{1}{T} \sum_i N_i a_i + 10^{0.1 \overline{L}_{eq}} \right\}, \tag{10}$$

where

$$a_i = \int_{-\infty}^{\infty} \frac{p_1^2(t)}{p_0^2}\,dt = \int_{-\infty}^{\infty} 10^{0.1 L_i(t)}\,dt, \tag{11}$$

is a parameter related to the energy of the ith signal and $\overline{L}_{eq}$ is the equivalent level of the background; $L_i(t)$ being, in dB (A), the time history of the "elementary signal" of the ith kind.

Relation (3) permits formula (10) to be given in the following form

$$L_{eq} = 10 \log \left\{ \frac{1}{T} \sum_i N_i \cdot 10^{0.1 L_{AX}^{(i)}} + 10^{0.1 \overline{L}_{eq}} \right\}. \tag{12}$$

This expression can be used to calculate the value of L_{eq} for the any time interval on the basis of the values $L_{AX}^{(i)}$ measured by a Brüel-Kjaer 2218 type sound level meter. When this instrument is not available, relation (10) can be used to determine the value of L_{eq}. In such a case, it is necessary to know the values of the parameters a_i.

2.1. The method for the determination of a_i on the basis of measurement of the sound level of a single "elementary signal". The method described below requires knowledge of the sound level $L_i(t)$, in dB (A), of a pure "elementary signal", i.e. only connected with the ith "acoustic event". When in the time of measurement the acoustic background is characterized by the mean level L_0, the signal $\tilde{L}_i(t)$ registered is slightly higher, since

$$\tilde{L}_i(t) = 10 \log\{10^{0.1L_i(t)} + 10^{0.1L_0}\}.$$

If $\{t_p, t_k\}$ is a time interval defined in the same way as for L_{AX} (formula (1)), relation (11) using discrete values gives

$$a_i = \Delta t \sum_{n=1}^{M} 10^{0.1\tilde{L}_i(t_n)} - \{t_k - t_p\} 10^{0.1L_0}, \tag{13}$$

where $t_n = t_p + n\Delta t$ and $t_k = t_p + M\Delta t$ (Fig. 3).

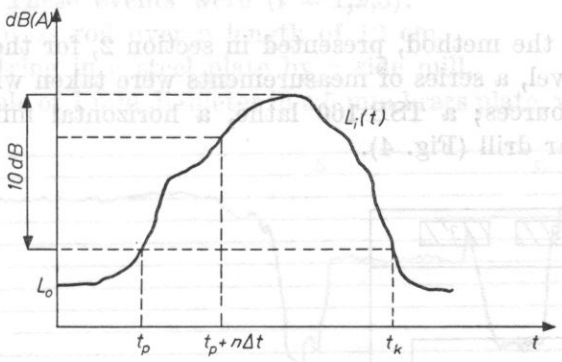

Fig. 3. Time history of the sound pressure level of a single "elementary signal"

The presence of the acoustic background of the level L_0 can also be considered otherwise, by introducing the tabulated correction ΔL [1]. Like the instantaneous values of the level $L_i(t_k)$, this correction varies in time — $\Delta L(t_k)$ and, therefore,

$$a_i = \Delta t \sum_{n=1}^{M} 10^{0.1\{\tilde{L}_i(t_n) - \Delta L(t_n)\}}. \tag{14}$$

A more detailed description of the method for calculating a_i is given in paper [4].

2.2. The method for the determination of a_i on the basis of measurement of the equivalent level. This method requires the measurement of the equivalent level L_{eq} of a signal consisting of one or more "elementary signals" of the same kind.

When a background is constant in time and has the level L_0, its equivalent level $\bar{L}_{eq} = L_0$. Formula (10) gives

$$a_i = \frac{T}{N_i}\{10^{0.1L_{eq}} - 10^{0.1L_0}\}. \tag{15}$$

Knowing the averaging time T, the number of the "acoustic events" N_i which occurred in this time, L_{eq} and L_0, it is possible to determine the value a_i more easily than by the method based on relations (13) or (14).

Since the "elementary signals" related to the same event are not fully identical, it is necessary, to measure at least several time pressure histories related to events of the same kind.

This method is given in greater detail in the following section of this paper.

3. Data on the parameter

To illustrate the method, presented in section 2, for the determination of the equivalent level, a series of measurements were taken within the enclosure with the noise sources; a TSB-160 lathe, a horizontal milling machine and a WS – 13 pillar drill (Fig. 4).

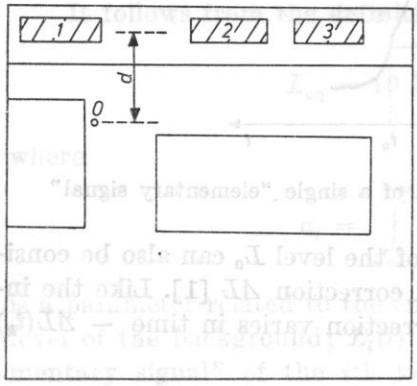

Fig. 4. Location of the noise sources
1 – lathe, *2* – milling machine, *3* – drill, and of the measurement point 0

The room had dimensions $4.10 \times 4.80 \times 3.50$ m^3. The measurements were taken using a Brüel-Kjaer instrument: a 4145 condenser microphone of $2.54 \cdot 10^{-2}$m (1″) diameter, a 2204 sound level meter and a 2304 level recorder with a 50 dB potentiometer. The microphone was placed at a height of 0.8 m. The distance of the observation point 0 from the noise sources was $d = 0.9$ m (Fig. 4).

As could be expected, the "elementary signals" emitted during the work of a single machine resembled each other very much when the same job was

performed on the same material. Fig. 5 shows the "elementary signals" registered at the observation point 0 when drilling a 7 mm diameter hole in a brass plate 5 mm thick.

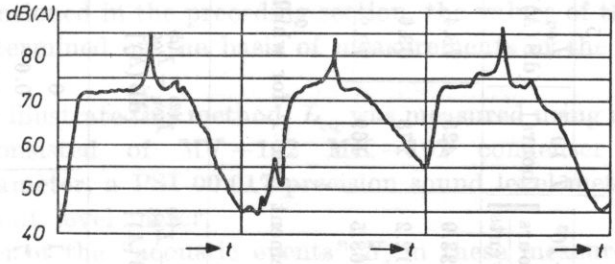

Fig. 5. Typical time histories of sound pressure level obtained for drilling

It was assumed initially, for the sake of simplicity, that each of these machines was the source of only one "elementary signal" related to only one "acoustic event". These events were ($i = 1,2,3$):

1. turning a brass rod over a length of 12 cm,
2. milling a string in a steel plate by a side mill,
3. drilling a hole of 7 mm diameter in a 5 mm brass plate, with manual feed.

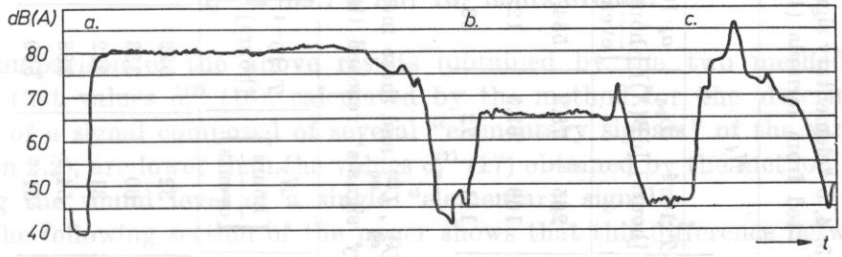

Fig. 6. Typical time histories of sound pressure level obtained for turning (*a*), milling (*b*) and drilling (*c*)

Fig. 6 shows typical time histories of "elementary signals". Each "elementary signal" was registered 15 times. In the course of measurements the acoustic background was constant and its level was 43 dB (A). Using subsequently the method discussed in section 2.1 (formula (13)), $a_{ij} (j = 1, 2, \ldots, 15)$ was calculated for each signal and the mean value $m_i = 15$ was determined from the formula

$$a_i^{(1)} = \frac{1}{m_i} \sum_{j=1}^{m_i} a_{ij}. \tag{16}$$

The following values of $a_i^{(1)}$ were obtained for the "acoustic events" $i = 1, 2, 3$:

$$a_1^{(1)} = (781 \pm 46) \cdot 10^3 \text{ hours/events}, \quad a_2^{(1)} = (15.7 \pm 1.7) \cdot 10^3 \text{ hours/events},$$
$$a_3^{(1)} = (78 \pm 27) \cdot 10^3 \text{ hours/events}, \tag{17}$$

Table 1. L_{eq} values for the time T for which $N_i = 1, 2, 3, 4, 5$ "elementary signals" reached the point 0. The values of a_i were calculated from formula (15)

i	N_i = 1			N_i = 2			N_i = 3			N_i = 4			N_i = 5		
	$T \cdot 10^{-4}$ [hours]	L_{eq} [dB(A)]	$a_i \cdot 10^{-3}$ [hours/events]	$T \cdot 10^{-4}$ [hours]	L_{eq} [dB(A)]	$a_i \cdot 10^{-4}$ [hours/events]	$T \cdot 10^{-4}$ [hours]	L_{eq} [dB(A)]	$a_i \cdot 10^{3}$ [hours/events]	$T \cdot 10^{-4}$ [hours]	L_{eq} [dB(A)]	$a_i \cdot 10^{3}$ [hours/events]	$T \cdot 10^{-4}$ [hours]	L_{eq} [dB(A)]	$a_i \cdot 10^{3}$ [hours/events]
1	88	78	578.4	181	78.4	624.6	265	78.2	584.2	350	78.6	533.9	425	78.4	588.1
2	58	63.5	13.1	108	63.9	13.3	169	63.3	12.1	222	63.4	12.2	278	63.6	12.7
3	42	70.8	50.1	67	72.8	63.5	111	72	58.7	144	72.7	68.5	169	72.2	57.5

Table 2. Comparison of the calculated values $L_{eq}^{(1)}$, $L_{eq}^{(2)}$ and those measured $L_{eq}^{(z)}$ in the measurement time T for which N_i "elementary signals" reached the observation point

Measurement	$L_{eq}^{(z)}$ [dB(A)]	N_i [hours/events]	N_2 [hours/events]	N_3 [hours/events]	$T \cdot 10^{-4}$ [hours]	$L_{eq}^{(1)}$ [dB(A)]	$L_{eq}^{(2)}$ [dB(A)]	$L_{eq}^{(1)} - L_{eq}^{(z)}$ [dB(A)]	$L_{eq}^{(2)} - L_{eq}^{(z)}$ [dB(A)]
1	70.8	16	32	32	622	71.9	70.8	1.1	0
2	72.9	30	60	60	333	74.6	73.5	1.7	0.6
3	75.4	62	31	31	322	77.1	76	1.7	0.6
4	72.8	27	82	54	368	74.3	73	1.5	0.2
5	74.8	51	51	51	590	76.5	75.4	1.7	0.6

characterizing successively the processes: of turning $a_1^{(1)}$; of milling $a_2^{(1)}$ and of drilling $a_3^{(1)}$. (The standard deviations are given in the brackets.) It can be seen that the highest value of Δa_i, compared to the value of a_i, occurs for drilling ($i = 3$).

As was mentioned in the preceding section, the values of the parameters a_i can also be determined on the basis of measurements of the equivalent level (section 2.2).

In order to illustrate this method, L_{eq} was measured using a system of RFT instruments consisted of MV−102 MK−102 condenser microphone of $2.28 \cdot 10^{-2}$ m diameter, a PSI 00 017 precision sound level meter and PSM 101 00 005 equivalent level meter.

The number of the "acoustic events" N_i in these measurements was 1-5, respectively. The duration of measurement T was registered each time. The constant sound level of the background was 45 dB (A).

The measured results and also the values of the parameters $a_i^{(2)}$ calculated according to relation (15) are shown in Table 1.

The mean values of the parameters $a_i^{(2)}$ (formula (16)) with $m_i = 15$) for each of the "acoustic events" discussed here and their standard deviations are:

$$a_1^{(2)} = (602 \pm 26) \cdot 10^3 \text{ hours/events}, \quad a_2^{(2)} = (12.66 \pm 0.54) \cdot 10^3 \text{ hours/events},$$
$$a_3^{(2)} = (59.7 \pm 7.0) \cdot 10^3 \text{ hours/events}. \tag{18}$$

Comparison of the above results (obtained by the two methods here) shows that values $a_i^{(2)}$ (18), calculated by the method for the determination of L_{eq} of a signal composed of several "elementary signals" of the same kind (section 2.2), are lower than the values $a_i^{(1)}$ (17) obtained by the method of registering the sound level of a single "elementary signal".

The following section of the paper shows that this difference between the values $a_i^{(1)}$ and of $a_i^{(2)}$ does not lead, however, to very high errors in the calculation of the equivalent level.

4. Experimental verification of the method for determining the equivalent level

Formula (10), derived in section 2, permits to determine the equivalent level L_{eq} of the resultant signal in an enclosure when the numbers of the "acoustic events" N_i, the time T, the values of the parameters a_i and the background equivalent level $\bar{L}_{eq}$ are known.

In order to verify this relation, five direct measurements of $L_{eq}^{(z)}$ were taken at the point 0 (Fig. 4), using the same instruments as in the measurements of a_i (section 3). Substitution into formula (10) of numerical values of $a_i^{(1)}$ and $a_i^{(2)}$ and the quantities T and N_i corresponding to measurement conditions gave the values of $L_{eq}^{(1)}$ and $L_{eq}^{(2)}$. The results are shown in Table 2.

This table shows that a better agreement between theory and experiment can be achieved when the values $a_i^{(2)}$ (18) obtained by the method proposed in section 2.2. are inserted into formula (10). This fact can be explained by that direct measurements of $L_{eq}^{(2)}$ and measurements permitting the determination of the values $a_i^{(2)}$ (15) were performed by the same measuring system. As was mentioned above, the sound level time history on the basis of which $a_i^{(1)}$ were calculated had been registered by other instruments.

In general case, differences between the measured values $L_{eq}^{(z)}$ and the calculated ones $L_{eq}^{(1)}$, $L_{eq}^{(2)}$ are caused by that the "acoustic events" of the same kind (turning, milling and drilling) are different from one another. This signifies that the "elementary signals" reaching the observation point in the measurements permitting the calculation of a_i are different from the signals registered in direct measurements of the equivalent level, which is caused by differences in the processes of turning, milling etc. themselves.

Table 2 shows that differences between measured values and those calculated according to formula (13) do not exceed 1.7 dB (A). Assuming that this deviation is admissible, it can be claimed that the method proposed here for determining the equivalent level in an enclosure is valid.

5. Remarks on the measuring procedure

The method proposed in this paper requires measurements of the sound level of single "elementary signals" (section 2.1), or measurements of the equivalent level of several "elementary signals" (section 2.2), or measurements of L_{AX} (formula (12)). The accuracy of the present method increases as the number of these measurements increases, since for $m_i \to \infty$ formula (16) defines the most probable value of the mean $\bar{a}_i$. For a finite number of m_i the values of a_i obtained from (16) are different from $\bar{a}_i$, which causes error in the case when the values of L_{eq} are determined from formula (10). This error increases as the difference $\delta a_i = a_i - \bar{a}_i$ increases. On the other hand, an increase in the number of measurements, m_i, causes the method to become very time-consuming and, therefore, hardly useful in practice.

This difficulty can be avoided by defining a minimum number of measurements m_i for which error committed in determining L_{eq} is less than k dB with the probability p.

According to the law of error propagation [3], the error ΔL_{eq} depends on the quantity δa_i in the following way

$$\Delta L_{eq} = \left[\sum_{i=1} \left(\frac{\partial L_{eq}}{\partial a_i}\,\delta a_i\right)^2\right]^{1/2}. \tag{19}$$

It follows from formula (10) and the condition $L_{eq} < k$ that

$$\frac{10(\log e)\left[\sum_i (N_i \delta a_i)^2\right]^{1/2}}{\sum_i N_i a_i + T \cdot 10^{0.1 \bar{L}_{eq}}} < k. \tag{20}$$

When the values of a_{ij} $(j = 1, 2, \ldots, m_i)$ have a normal distribution, the following relation is satisfied [3]

$$\delta a_i = \frac{t_p^{(i)} \Delta a_i}{m_i}, \tag{21}$$

where $t_p^{(i)}$ is the value obtained from the t distribution for the probability p with $m_i - 1$ degrees of freedom (m_i is the number of measurements of a_{ij}), while Δa_i is the standard deviation.

Substitution of (21) into (20) gives the following inequality

$$\sum_i \frac{a_i}{m_i^*} < A, \tag{22}$$

where

$$a_i = (N_i t_p^{(i)} \Delta a_i)^2, \; A = \left[0.1(\ln 10) k \left(\sum_i N_i a_i + T \cdot 10^{0,1 \bar{L}_{eq}}\right)\right]^2. \tag{23}$$

It is possible to derive from inequality (22) the number of measurements of "elementary signals", m_i^*, for which the mean values of a_i (formula (16)) are different from the values $\bar{a}_i$ by δa_i, where the value $L_{eq}(a_i)$ calculated from formula (10) is different from the real quantity $L_{eq}(\bar{a}_i)$, with the probability p, by, at most, k[dB].

In order to determine m_i^*, it is necessary to take a pilot series of measurements of $a_{ij}(j = 1, 2, \ldots, m_i)$ and define a_i according to formula (16). It is subsequently necessary to find the values $t_p^{(i)}$ for given k and p. When the number N_i of "acoustic events" in the time T is known, it is possible to calculate a_i, A and m_i^* from formulae (22) and (23).

EXAMPLE. It can be assumed that the values a_i (formula (17)) are the results obtained from the pilot series. The number of measurements of a_{ij} of each "elementary signal" was $m_i = 15$ for both turning ($i = 1$), milling ($i = 2$) and drilling ($i = 3$). It can be assumed that it is necessary to define such values of m_i^* for which L_{eq} calculated from formula (10) will differ by $k = 0.5$ dB from the real value $L_{eq}(\bar{a}_i)$ with the probability $p = 0.999$. Let the number of "acoustic events" in 8 hours be $N_1 = 500$, $N_2 = 600$ and $N_3 = 700$, respectively, and the background equivalent level $\bar{L}_{eq} = 40$ dB A.

From the t distribution for $m_i - 1 = 14$ degrees of freedom $t_{0.999}^{(i)} = 4.14$. Insertion of numerical values into formulae (23) gives

$$a_1 = 9.06 \cdot 10^{15}, \quad a_2 = 1.78 \cdot 10^{13}, \quad a_3 = 6.12 \cdot 10^{15}, \quad A = 2.73 \cdot 10^{15}.$$

Inequality (22) takes the form

$$\frac{9.06}{m_1^*}+\frac{1.78\cdot 10^{-2}}{m_2^*}+\frac{6.12}{m_3^*}<2.73.$$

Assuming that $m_1^*=m_2^*=10$, then $m_3^*=4$. This result means that the pilot series of measurements of a_{ij} $(j=1,2,\ldots,15)$ performed here is sufficient for determination of the mean values of a_i on the basis of which the value of the equivalent level L_{eq} differs from its real value by 0.5 dB. The probability of obtaining this value of L_{eq} is $p=0.999$.

6. Conclusions

The aim of this paper was an illustration (section 3) and a verification (section 4) of the method proposed in section 2 for determining the equivalent level L_{eq} in an enclosure. For a given room the values of the parameters a_i do not only depend on the operations performed on particular machines (these operations being called here "acoustic events") but also on the location of the observation point (x, y). It can be assumed that there are M different "acoustic events". Thus, formula (10) can be generalized to the form

$$L_{eq}(x,y)=10\log\left\{\frac{1}{T}\left(\sum_{i=1}^{M}N_i a_i(x,y)+10^{0.1\bar{L}_{eq}}\right)\right\}. \tag{24}$$

It can be assumed that numerical values of $a_i(x, y)$ and the equivalent level of the background are given. Let L_{eq}^* be the value of the equivalent level for T hours which must not be exceeded. Thus, from formula (24),

$$\sum_{i=1}^{M}N_i a_i(x,y)=T(10^{0.1L_{eq}^*}-10^{0.1\bar{L}_{eq}}). \tag{25}$$

It is possible to obtain from this equation the numerical values N_i^* which define the admissible number of "acoustic events". In other words: when the inequality $N_i<N_i^*$ $(i=1,2,\ldots,M)$ is satisfied, the value of L_{eq} over T hours in the observation point (x, y) is less than L_{eq}^*.

It can be seen that the present method for determining the equivalent level may be useful in controlling technological processes so that the conditions of good acoustic climate are met in industrial interiors.

EXAMPLE. The numerical values of the parameters a_i, given in section 3 (18), were obtained at the point 0 (Fig. 4). It can be assumed that $L_{eq}^*=80$ dB (A) is an equivalent level which should not be exceeded for $T=8$ hours of work. Let the equivalent level of the background be $\bar{L}_{eq}=60$ dB (A). There are three kinds of machinery: lathe, mill and drill on which turning, milling and

drilling can be performed. The respective technological processes related to these three kinds of machinery are characterized by the numbers N_1^*, N_2^* and N_3^*.

For instance, the production of screws in hall would require N_1^* turnings, N_2^* millings and N_3^* drillings. To answer the question whether the production of screws will not cause the standard $L_{eq}^* = 80$ dB (A) to be exceeded, it is sufficient to put N_1^*, N_2^*, N_3^* and $L_{eq}^* = 80$ dB (A), $L_{eq} = 60$ dB (A), $T = 8$ hours and $M = 3$ into formula (25). This gives

$$781N_1^* + 15.7N_2^* + 78N_3^* \approx 792 \cdot 10^3. \tag{26}$$

The authors wish to thank Prof. S. CZARNECKI for his assistance in preparing this paper.

References

[1] J. T. BROCH, *Acoustic noise measurement*, Brüel-Kjaer, Naerum, 1975.

[2] J. R. HASSALL, K. ZAVERI, *Acoustic noise measurement*, Brüel-Kjaer, Naerum, 1979.

[3] D. J. HUDSON, *Statistics, lectures on elementary statistics and probability*, Geneva 1969.

[4] R. MAKAREWICZ, G. KERBER, *A method of predicting noise equivalent level value in urban structure*, Archives of Acoustics, **3**, 4, 231-248 (1978).

[5] R. MAKAREWICZ, *Time average intensity of the sound field generated by moving source*, Acoustics Letters, **1**, 133-138 (1978).

[6] R. MAKAREWICZ, *A method for determining the equivalent level* L_{eq}, Archives of Acoustics, **2**, 2, 83-94 (1977).

Received on March 27, 1980; revised version on January 16, 1981.

ARCHIVES OF ACOUSTICS
7, 3-4, 197-206 (1982)

APPLICATION OF AN AUTOMATIC AUDIOMETER IN THE MEASUREMENT OF THE DIRECTIONAL CHARACTERISTIC OF HEARING

JAN ŻERA, TOMIRA BOEHM, TOMASZ ŁĘTOWSKI

Chopin Academy of Music (00-368 Warsaw, ul. Okólnik 2)

This paper describes a new version of the automatic audiometer with electronic level control, adopted for the measurement of the directional characteristic of hearing. It also presents the results of the preliminary investigations of the directionality of hearing under the conditions of the threshold stimulation by a tone and by narrow-band noise.

1. Introduction

The construction of a Bekesy automatic audiometer based on electronic circuits has provided the conditions for more accurate and comprehensive investigations of the hearing threshold. This is above all related to the technical abilities of the measurement apparatus used in the construction of the audiometer. These abilities are provided by the broad-range control of such parameters as the attenuation rate in the stimulus signal level (3, 10, 30, ..., ..., 100 dB/s), the variation rate in the frequency of a stimulus (20 Hz-20 kHz – from 10s to above 100 h), or of the rate and dynamic scale of recording (10, 25, 50, 70 dB). A selection of values of these parameters makes it possible both to obtain the entire threshold curve of hearing as a function of frequency and to choose a certain narrow frequency band to record the threshold curve with large accuracy [3]. It is also possible to analyze precisely the variation of the threshold as a function of time [3-5].

Knowledge of the directional characteristic of hearing is of great significance in many fields of acoustics, particularly in the room acoustics and the recording technique using the artificial head. In most papers [1, 2, 9] the magnitude of the acoustical pressure at the inlet of the auditory canal using a microphone probe is measured as a function of selected values of the angle of the position of the sound source. In some papers, e.g. [8], a method analogous to

that used in a classical clinical audiometer is also used. There are, however, no measurement techniques suitable for fast and at the same time precise determination of the characteristics mentioned above.

This paper aims to present a new version of the electronic automatic audiometer adopted for measurements of the directional dependence of the hearing threshold. The results of preliminary investigations of the directionality of hearing with the stimulation by a tone and by narrow-band noise are also given.

2. Measurement apparatus

The automatic audiometer for the measurement of the directional characteristic of the threshold of audibility was set up using standard laboratory Brüel-Kjaer equipment. This audiometer is a version of the audiometer described in paper [7]. A block diagram of this device is shown in Fig. 1. In the system in Fig. 1 the amplitude of the stimulus signal is changed using a control ampli-

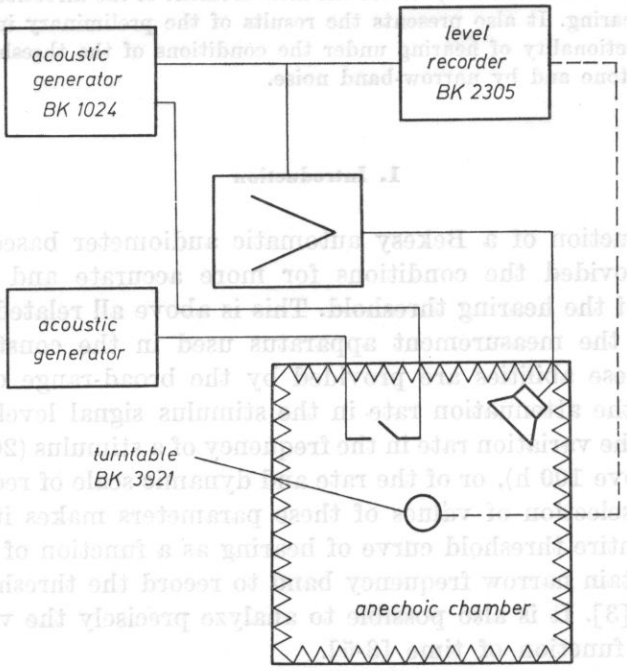

Fig. 1. A schematic diagram of an automatic audiometer for measurements of the directional characteristic of the threshold sensitivity of hearing

fier of a BK 1024 generator and an external generator. With a button the listener feeds a control signal with constant amplitude to the compressor input of the generator. Through the control amplifier this signal affects the ampli-

tude of the stimulus signal, causing a decrease in its level at a specific rate. A break in feeding the control signal (by the release of the button) causes an opposite effect, a rise in the level of the stimulus signal at the same rate. The performance of the system for electronic level control of the output signal in the automatic audiometer is described in detail in paper [7]. The element which makes the present system different from that described in paper [7] is a BK 3921 turntable. The character of the measurement requires the stimulus to be presented binaurally in the free field. In the present case, measurements were performed in an anechoic chamber using a dynamic GK 1245 loudspeaker as the sound source. The position of the elements of the system with respect to one another is shown in Fig. 1.

3. Measurement procedure

In the course of the measurement the person examined sat on a stool made fast to the turntable with his or her head still. This situation is close to the real conditions of listening, with the conscious head movements eliminated. When the table was turning the listener's task was to keep the magnitude of the signal received at the threshold level by adjusting the control signal. The level of the stimulus signal corresponded to the threshold level of hearing sensitivity under the conditions of binaural perception and signal was registered by a recorder voltmeter as a function of variation in the position of the sound source and the listener in a horizontal plane with respect to each other.

The listener kept the stimulus signal at a level corresponding to the threshold sensation by causing a decay in the signal when it entered the level range above the threshold and, conversely, by causing a rise in the signal when it lowered below the audibility threshold*. This is a common technique used in automatic audiometry. The result was registered in the form of a polar curve of the level variation about the threshold value as a function of the angle of the position of the sound source with respect to the listener. The table did not turn for the first 40-60 s of a measurement session. In this time the listener adjusted the signal presented so as to keep it on the threshold level. When the threshold value was established, the table began to turn and the registration of the signal level was started. The variation in the signal for two successive full turns of the table was registered.

In the investigations directional characteristics were determined for tones and narrow-band noise with the width $\Delta f = 300$ Hz. The measurements were performed for frequencies of 1, 2, 5, 7 and 10 kHz. The variation rate in the

* A full measurement instruction for the listener, which is also used in the present investigation, is given in paper [3].

signal level was taken to be 10 dB/s. The table turned counterclockwise at a velocity of 0.75 rpm*, i.e. a double turn lasted about 160s. In all, one measurement took about 3.5 min. This procedure of the experiment prevented both the effect of the unstability of the threshold in the initial stage of signal exposition [4] and the effects of hearing fatigue which begin to be essential after about 5 min of signal presentation. At the same time a sufficiently precise recording of the variation in the hearing threshold was obtained (Fig. 2) [5].

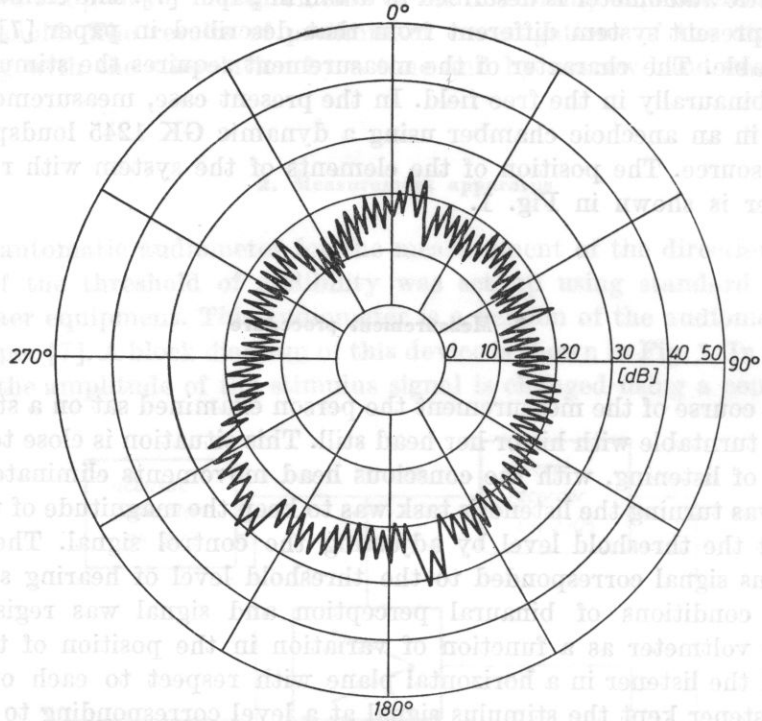

Fig. 2. A directional audiogram obtained for the stimulation by a tone of 5 kHz. The rise and decay rate of the signal was 10 dB/s. Listener *TB*

The listeners were five persons aged 22-27, students or members of the staff of the Chopin Academy of Music, Warsaw, who had a large experience in psychoacoustic investigations. All had audiologically normal hearing.

4. Measurement results

As an example, Fig. 2 shows a directional audiogram. The angle 0° corresponds to the position of the sound source in front of the listener, in the plane of symmetry of the head. The angles 90° and 270° correspond, respectively,

* It is the only rotation velocity of the BK 3921 turntable.

to the right and the left side of the listener, while the angle 180° corresponds to the sound source at the back of the listener.

The threshold value was approximated by a line lying at middle of the saw-tooth recording. This procedure seems to be most justified by the conditions assumed for the investigations [5].

It should be stressed that, similar to the previous version of the electronic automatic audiometer, here higher levels recorded correspond to a lower hearing sensitivity. This is different from the traditional registration used in clinical audiometry in which higher levels correspond to a higher sensitivity. The differences in the nature of recording result from the properties of the apparatus used and have no effect on the interpretation of results.

In the investigations 3 to 16 threshold recordings were taken for particular persons and frequencies. In order to determine an average characteristic of the hearing threshold, points distant by 30 angular degrees (i.e. corresponding to the directions 0°, 30°, 60° etc.) were selected. This procedure is justified by the preliminary character of the investigations performed whose results only provide an illustration of the present measurement method and are not expected to determine a normalized threshold curve.

The pilot investigations showed that for the participants in the experiment the differences in hearing sensitivity between the right and the left ears do not exceed 5 dB for each of the frequencies investigated. On this basis, the assumption of a symmetry of the directional characteristic of hearing with respect to the medial plane of the head was found to be admissible. This permits

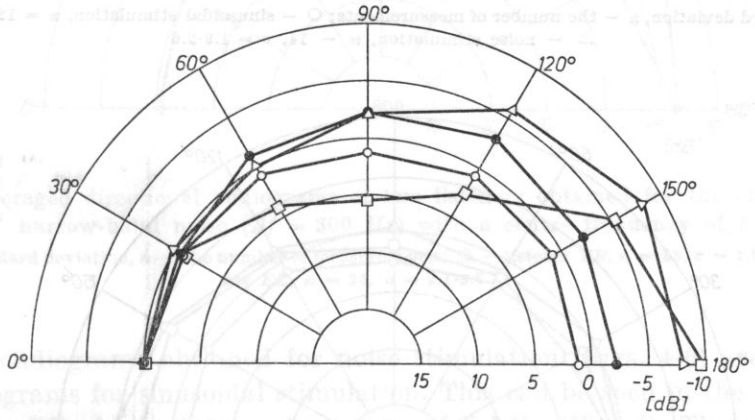

Fig. 3. Averaged directional audiograms for the stimulation by a tone. Listeners *TB*, *MB*, *KK* and *AM*

f – the stimulation frequency, σ – the standard deviation, n – the number of measurements; ○ – f = 1 kHz, n = 6, σ = 1.1-2.6; ● – f = 2 kHz, n = 6, σ = 0.5-2.1; △ – f = 5 kHz, n = 6, σ = 0.9-2,7; □ – f = 7 kHz, n = 6, σ = 2.4-5.7

the values of points lying symmetrically on both sides of this plane (0°, 30°, 330°, 60-300° etc.) to be averaged and a directional audiogram to be represented in

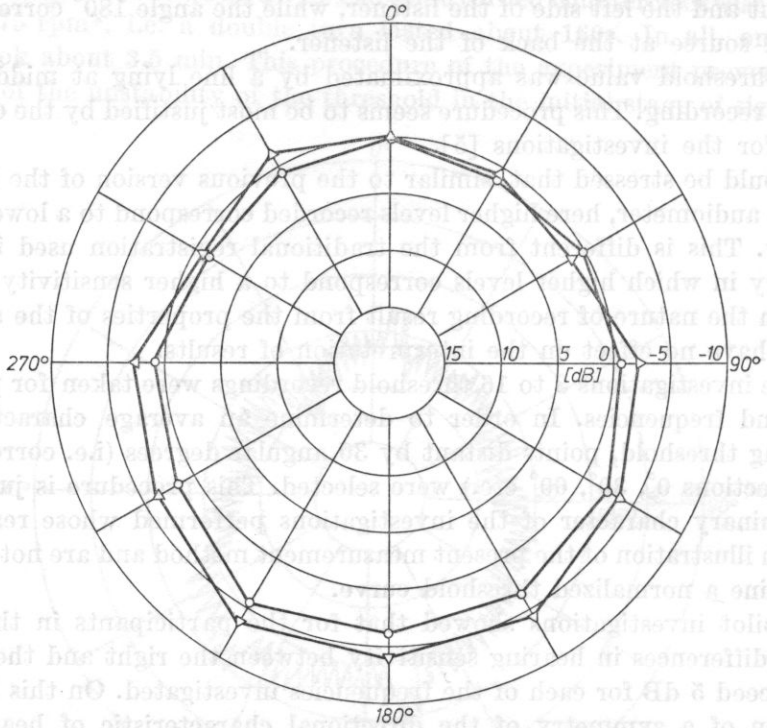

Fig. 4. Averaged directional audiograms for the stimulation of a 5 kHz tone and by narrow-band noise (Δf = 300 Hz) with a centre frequency of 5 kHz. Listener *TB*

σ — the standard deviation, n — the number of measurements; ○ — sinusoidal stimulation, n = 12, σ = 1.2-1.9; △ — noise stimulation, n — 14, σ = 1.9-2.6

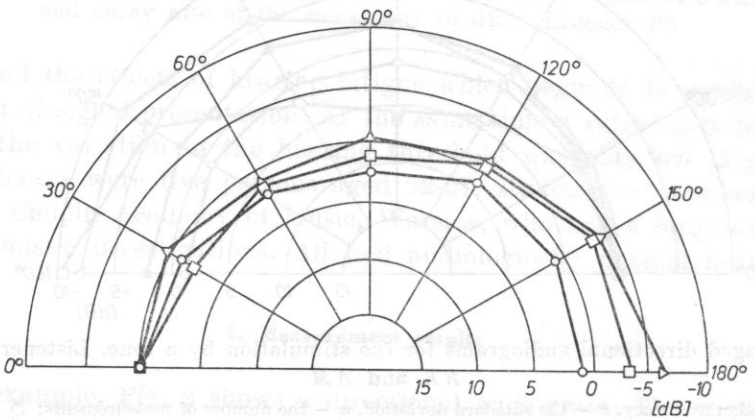

Fig. 5. Averaged directional audiograms for the stimulation by narrow-band noise (Δf = 300 Hz). Listener *TB*

f — the centre frequency of the noise band, σ — the standard deviation, n — the number of measurements; ○ — f = 1 kHz, n = 18, σ = 1.3-2.2; △ — f = 5 kHz, n = 28, σ = 1.9-2.6; □ — f = 7 kHz, n = 18, σ = 0.7-3.3

the form of a diagram which occupies half a full angle. In this situation each point of the individual audiograms given below was defined by 6-32 measurement results. Fig. 3 shows the audiograms obtained for the listener group examined with the stimulation by a tone. The plots show an omnidirectional hearing characteristic for medium acoustic frequencies (1 kHz and 2 kHz). For a frequency of 2 kHz an increase in the threshold value — by about 2 dB — becomes significant for the incidence of the wave from the back of the listener. A distinct deepening of this effect occurs for frequencies 5 kHz and 7 kHz (the significant between the front and the back of the head is about 10 dB). For a frequency of 7 kHz a significant lowering in the hearing threshold — by about 5 dB — can be observed for directions lateral with respect to the direction facing the listener. For the listener *TB* this effect also occurs for noise stimulation (Fig. 4). The question whether this feature is characteristic of hearing in this frequency range must, in view of the small set of data gathered from a group only four listeners, be left unanswered until futher, wider investigations have been performed.

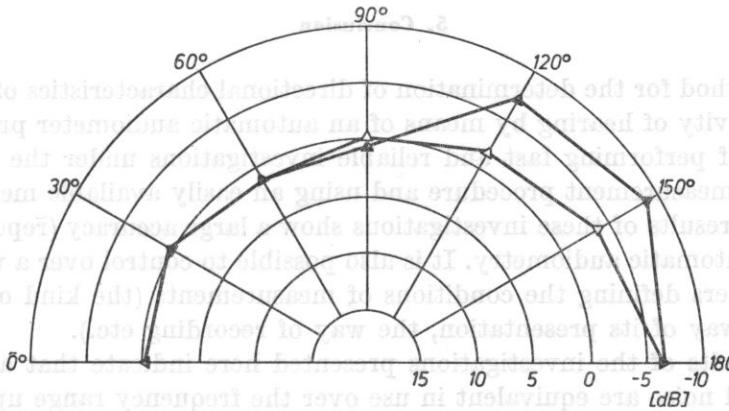

Fig. 6. Averaged directional audiograms of two listeners obtained for the stimulation by narrow-band noise (Δf = 300 Hz) with a centre frequency of 5 kHz

σ — the standard deviation, n — the number of measurements; △ — listener *TB*, n = 28, σ = 1.9-2,6; ▲ — listener *EZ*, n = 28, σ = 2.1-3.7

The audiograms obtained for noise stimulation (Figs. 4-6) are similar to the audiograms for sinusoidal stimulation. This can be seen in the audiograms of listener *TB* obtained for a frequency of 5 kHz (Fig. 4). These curves are presented for the range 0-360°. The differences between the threshold values on both diagrams do not exceed 2.5 dB.

For medium frequencies, e.g. 1 kHz, the curves of the two audiogram types are close to omnidirectional (Fig. 5). For higher frequencies, e.g. 5 or 7 kHz, the conditions of hearing signals from the back of the head become worse (Figs. 5 and 6).

It is interesting to note the large individual differences observed the audiograms of listeners *TB* and *EZ* (Figs. 5 and 6). For a frequency of 5 kHz these differences are related to the waves from the back of the head and are quantitative, while the shape of the characteristic remains unchanged.

In the case of 10 kHz signals distinct differences were observed between the directional audiograms of the listeners. It can be supposed that the main reason for the differences is the effect of the acoustic shade which, increasing as frequency increases, results from the geometrical dimensions of the heads of particular listeners. In the course of measurements performed for this frequency it was possible to observe an undesired effect of the anechoic chamber where reflections of sound waves occur over this frequency range. Hence, measurements over this frequency range were distorted by side effects which are difficult to eliminate. In view of this, the data obtained for $f = 10$ kHz could not be used as the basis for essential conclusions and were neglected in the analysis.

5. Conclusion

The method for the determination of directional characteristics of the threshold sensitivity of hearing by means of an automatic audiometer provides the possibility of performing fast and reliable investigations under the conditions of a simple measurement procedure and using an easily available measurement set up. The results of these investigations show a large accuracy (repeatability), typical of automatic audiometry. It is also possible to control over a wide range the parameters defining the conditions of measurements (the kind of stimulus signal, the way of its presentation, the way of recording etc.).

The results of the investigations presented here indicate that a tone and narrow-band noise are equivalent in use over the frequency range up to about 5 kHz. For higher frequencies it seems better to use noise bands in view of a smaller scatter of measured results and an agreement between the type of a stimulus and the width of the critical band.

References

[1] W. E. FEDDERSEN, T. T. SAMUEL, D. C. TEAS, L. A. JEFFRES, *Localization of high-frequency tones*, JASA, **29**, 9, 988-991 (1959).

[2] J. K. HARRISON, P. DOWNEY, *Intensity changes at the ear as function of the asimuth of a tone sound, A comparative study*, JASA, **47**, 62, 1509-1518 (1970).

[3] A. JAROSZEWSKI, A. RAKOWSKI, *A Bekesy audiometer with electronic signal level control and its application to psychoacoustic measurements*, Archives of Acoustics, **1**, 3, 231-242 (1976).

[4] A. JAROSZEWSKI, A. RAKOWSKI, *Analysis of the initial fraction of Bekesy recordings in the threshold audiometry*, Archives of Acoustics, **1**, 4, 299-308 (1976).

[5] A. JAROSZEWSKI, A. RAKOWSKI, *Variability of the hearing threshold tracings in automatic audiometry beyond the initial transient phase,* Archives of Acoustics, **2**, 1, 71-82 (1977).

[6] B. MOHL, *Bekesy audiometry with standard equipment,* B-K Technical Review, **1** (1973).

[7] A. RAKOWSKI, A. JAROSZEWSKI, T. ŁĘTOWSKI, *A Bekesy audiometer using conventional laboratory equipment* (in Polish), Archiwum Akustyki, **4**, 3, 247-262 (1969).

[8] L. J. SIVIAN, S. D. WHITE, *On minimum audible sound fields,* JASA, 4, 288-321 (1933).

[9] F. M. WIENER, *On the diffraction of a progressive sound wave by the human head,* JASA, **9**, 1, 143-146 (1947).

Received on September 3, 1981; revised version on April 6, 1982.

ARCHIVES OF ACOUSTICS
7, 3-4, 207-224 (1982)

FUNDAMENTAL ASPECTS OF AEROACOUSTICS IN SINGING

ZYGMUNT PAWŁOWSKI, MAREK ŻÓŁTOWSKI

Department of Phoniatrics, Chopin Academy of Music
(00-368 Warsaw, ul. Okólnik 2)

The authors have modified the aerodynamic method for diagnostics of the function of the vocal and respiration organ during professional singing. The substance of the method lies in the possibility of measuring the value of the subglottal pressure without introducing a needle into the trachea and measuring the absolute value of the remaining parameters and determining their mutual correlation during phonation. The aerodynamic curve obtained permits the phenomena occurring in singing to be recorded, according to the division into 3 periods: inspiration, expiration until the moment of the formation of phonation, the further period of the expiration phase until its termination.

In the years 1975-1981, 187 vocalists were examined and on this ground the correlation between the degree of vocal preparation and the elaboration of the evaluation criterion has been defined.

1. Introduction

The development of multilateral mass media has now caused an interest in the human voice, and especially in singing. This problem is complex, for it involves many scientific and didactic disciplines. Particularly vocalists and actors attribute vital significance to a correct performance of the vocal organ, the result of which is singing as an artistic effect. On the other hand, they have well-grounded misgivings as regards the protection of the vocal organ, rational professional and pedagogic occupation. In this respect phoniatry is credited with the role of an ally, for the elaboration and application of objective diagnostic methods in clinical practice becomes a necessity. Traditional methods, such as laryngoscopy or spirometry, are insufficient for the evaluation of the complex function of the vocal and respiration organ in singing. Therefore, the examination of disorders in voice under sensation conditions was based entirely on the acoustic evaluation of the singing voice.

In respect to the diagnostics of the function of vocal and respiration organ the aerodynamic method can be, in principle, divided into two parts:

(1) a qualitative and quantitative determination of the larynx efficiency,

(2) a determination of the vocal organ efficiency which is in terms of function strictly connected with the voice producing organ.

This division is only formal and therefore the aerodynamic phenomena occurring during voice production are investigated by the present method in conjunction.

2. A review of selected literature

The aerodynamic method was developed and applied to clinical examinations of the vocal and respiration organ in singing by von LEDEN, YANAGIHARA, ISSHIKI, and KOIKE [9, 14, 15, 27]. On the basis of complex investigations these authors showed that phonation is an aerodynamic phenomenon, for the formation of voice depends, among other factors, on the mutual interaction between two physical forces and their equilibrium, i.e. subglottal air pressure and glottis resistance [14]. The character of the vocal and respiration organ performance is here based on physical parameters whose values and their mutual correlation have been obtained from aerodynamic measurements. The essential parameters include phonation volume *PV*, vital capacity *VC*, maximum phonation time *MPT*, mean flow rate *MFR*, fundamental frequency, voice intensity, expiratory power *EP*, glottal resistance and subglottal pressure *SP*.

It follows from literature that parameters connected with the vocal and respiration organ functions in singing have been measured using conventional equipment. The method of measuring the subglottal pressure by introducing a needle into the trachea below the larynx, which the authors cited have proposed and used, determines, in the present authors'opinion, its considerable limitation in practical investigations.

3. The assumption and the purpose of the present study

The present authors have performed an investigation of the correlation of the respiration and vocal organ in singing, since the mechanism of its formation has not been explained in detail. The results obtained could provide the basis for consideration of pathological cases of the larynx, i.e. after operations etc., and of rehabilitation results.

The character of the singing voice has been described rather widely in the literature from different viewpoints, depending on the kind of scientific disciplines discussing this problem.

The vocal literature seems to consider primarily the aspect of aesthetics, of the emission technique, didactic problems and the selection repertory during training [1, 18, 23-26].

Studies in the field of acoustics which are concerned with evaluation of the singing voice concentrate first of all on the function of the vocal path and also on the sound sung as the initial product which provides the material for an analysis or syntesis of the voice [2, 3, 7, 8, 10, 11, 13, 17, 21].

Phoniatry aims to determine the physiological mechanism of voice formation. The authors omit the known problems of anatomy and physiology of the larynx and lungs, concentrating chiefly on the mechanism of the cooperation between the respiration organ and the vocal one occurring in singing. The fundamental problem contained in this paper is related to the analysis of the phenomenon in terms of its 3 stages: inspiration, the beginning of expiration until the formation of voice, the further stage of the expiration phase.

For over 5 years the authors have observed the vocalists, confronting the results obtained by the aerodynamic method with anatomical and clinical conditions and with the quality of the emission of sounds sung.

The present paper aims above all to present as objectively as possible the data on the function of the respiration organ and the vocal one in singing. The diagnostics would then allow the determination of the methods of vocal training at its various stages and to begin, in emergency cases, a proper treatment and phoniatric rehabilitation.

The problem itself of diagnosing an incorrect coordination of the vocal organ and the respiration one on the basis of the aerodynamic method is of great importance for medical and pedagogic treatment in training vocalists. The purpose of this paper is to present the method elaborated by the authors and the results of investigations of the respiration organ and the vocal one in singing and also to attempt to determine the mean values of the norms of the parameters measured.

In the cases of individual deviations from average values it will be possible to set forth conclusions for the improvement of vocal technique elements or for the selection of the proper method of phoniatric procedure.

4. Selection of cases

187 persons, students of all academic years of the Vocal-Theatrical Department and candidates for vocal studies in the Chopin Academy of Music in Warsaw, were examined.

The examined students were divided into 3 basic groups, assuming as the criterion of the division the degree of advancement in training.

A group of vocalists was qualified for investigations of the respiration and vocal organs by the aerodynamic method after a previous otolaryngologic examination. In the persons examined no deflections from the normal state of nose, nosopharynx, pharynx, oral cavity, ears and larynx were found.

Table 1. Number of investigations with consideration given to the kind of voice and degree of vocal preparation

Degree of vocal preparation	Number of persons investigated	Soprano	Mezzoso-prano and alto	Tenor	Baritone	Bass
Unadvanced	75	22	14	21	14	4
Average	88	43	13	14	10	8
Well advanced	24	12	5	0	3	4
Total	187	77	32	35	27	16

5. Investigation method

To secure the most natural conditions for the person examined the authors used the known pletismographic booth used for measurements of the resistance of the respiratory system and of the residual volume [4].

This booth permits the performance of an indirect measurement of the subglottal pressure before and during phonation. The measurement method assumed was based on the relation resulting from the Boyle and Mariotte law. It was

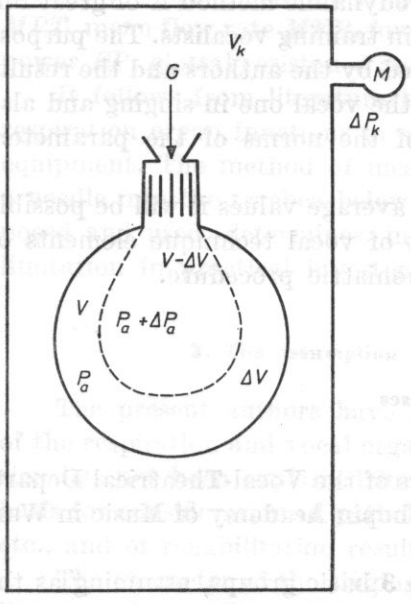

Fig. 1. A schematic diagram of the subglottal resistance measurement

G – glottis, *V* – air capacity in the lungs, *Pa* – air pressure in the lungs after inspiration, ΔV – difference in air volume in the lungs caused by initial compression, i.e. difference in the air volume contained in the pletismographic booth, $V - \Delta V$ – air volume in the lungs after initial compression, $Pa + \Delta Pa$ – air pressure in the lungs after initial compression, V_k – known booth volume, *M* – differential manometer for measurement of pressure differences in the booth with respect to the atmospheric pressure, ΔP_k – difference in pressure in the booth with respect to atmospheric pressure

assumed that the person investigated in an air-tight pletismographic booth, after having performed a maximum deep inspiration, has in the respiratory system a volume of air $V = VC + RV$, where VC is the vital capacity and RV is the residual volume. To maintain phonation the air contained in the respi-

ratory system becomes compressed by the force resulting from the tension of the diaphragma and the pressure of the abdominal muscles. This pressure, expressed in cm H_2O, depends on the glottal resistance, the intensity, and the pitch of sound. The personal qualities of the examined person cause these pressures to vary for different persons at phonation of equal intensity and pitch of sound.

The schematic diagram shown in Fig. 1 illustrates the principle assumed for the performance of measurements of the subglottal pressure.

The person examined in the pletismographic booth has in the respiratory system a volume of air V. When this air volume is compressed at closed glottis by the pressure ΔPa, it decreases by the quantity ΔV, according to the formula resulting from the Boyle and Mariotte law that $PV = \text{const}$ under isothermal conditions $PaV = (Pa + \Delta Pa)(V - \Delta V)$. Multiplication of the expressions in the brackets gives

$$PaV = PaV + \Delta PaV - Pa\Delta V - Pa\Delta V.$$

The product $\Delta Pa\Delta V$ may be neglected as very small and the equations thus reduced will take the form

$$Pa\Delta V = \Delta PaV. \tag{1}$$

Assuming that V is expressed in liters and taking $Pa = 1000$ cm H_2O ($\sim$1 At), the excess pressure in the respiratory system, ΔPa, expressed in cm H_2O, may be calculated from the formula

$$\Delta Pa = 1000\ \Delta V/V. \tag{2}$$

The air compression in the respiratory system will be accompanied by a decrease in the pressure inside the measurement booth. The manometer M controls the difference ΔP_k between the pressure in the pletismographic booth and the room pressure.

The correlation between ΔV and ΔP_k is defined precisely by the equation

$$\Delta P_k = 1000\Delta V/V_k, \tag{3}$$

where V_k is the air volume in the booth before the compression of air in the lungs of the person examined, ΔV is the difference between the booth volume after the compression of air contained in the lungs. This difference is equal to the difference ΔV in formula (2).

It follows from correlations (2) and (3) that ΔPa changes as ΔP_k changes. ΔPa may be determined by measuring ΔP_k,

$$\Delta Pa = \Delta P_k V_k/V, \tag{4}$$

where ΔP_k are pressure changes measured in the booth, V_k is the booth volume diminished by the volume of the person examined and V is the air volume in the lungs of the person examined at maximum inspiration.

Before the proper measurement the vital capacity VC of the person investigated was measured initially by a pneumotachometer with an electronic spirometer. The proper aerodynamic measurements during singing were performed in the system shown in Fig. 2.

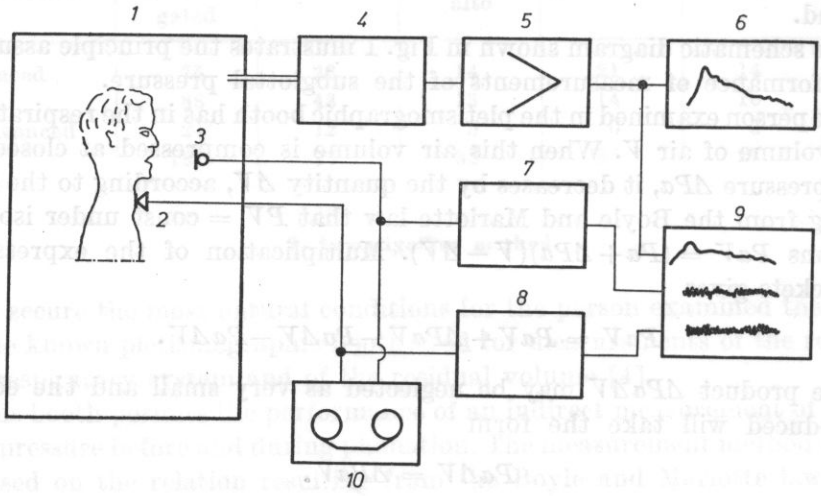

Fig. 2. A diagram of the aeroacoustic measurement system

1 – pletismographic booth, *2* – laryngophone, *3* – microphone, *4* – electro-manometer, *5* – amplifier, *6* – recorder a – y – t, *7* – microphone amplifier, *8* – laryngophone amplifier, *9* – loop oscillograph, type N-115, *10* – twochannel tape recorder, type ZK-246

Besides the ΔP_k measurements the intensity of the laryngeal sound by means of a laryngophone [2] and the sound intensity from before the mouth at a distance of about 30 cm were recorded simultaneously on a multichannel loop recorder. The signals from the laryngophone and microphone were also recorded on magnetic tape by a two-channel tape recorder for a further acoustic analysis by means of Brüel-Kjaer equipment.

6. Calculation method

The results of the measurement of the quantity ΔP_k of the acoustic pressures, the curves of the dynamics of the laryngeal sound, and of the sound emitted from before the mouth were plotted in the shape of curves synchronized in time. These results were obtained for individual persons with various kinds of phonation:

(1) phonation of sound of the mean range of scale of a given kind of voice for piano and forte;

(2) phonation of sound of the upper range of scale of a given kind of voice for piano and forte;

(3) phonation of sound sung legato from the mean range of scale to the upper one in piano and forte;

(4) phonation of sound sung legato from the upper range of scale to the mean one in piano and forte.

The interpretation of the results was based on a curve representing changes in pressure in the pletismographic booth ΔP_k. In view of the correlation between the changes in ΔP_k and the changes in ΔPa determined by equation (4), the aerodynamogram can be related to the magnitude of the subglottal pressure, to the air flow speed through the glottis and the magnitude of the glottis resistance.

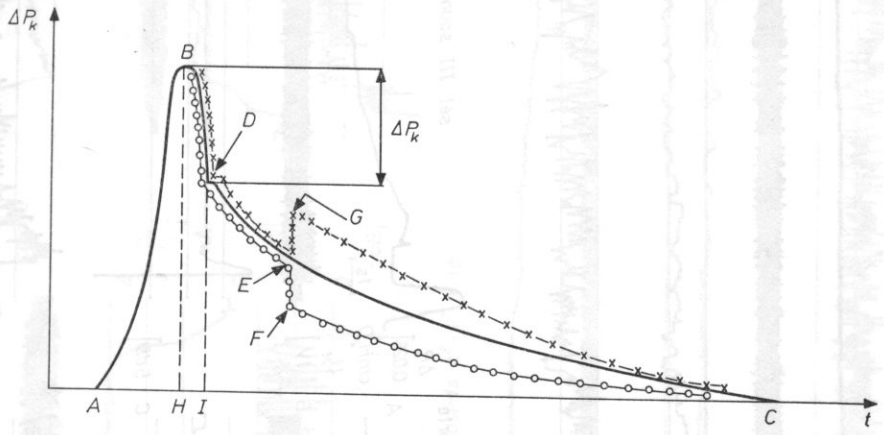

Fig. 3. A diagram of typical aerodynamograms

– – – – – – for single sound, –o–o– two sounds sung legato from the lower to the higher; –x–x– two sounds sung from the higher to the lower one. The meaning of the particular parts of the curve: AB – air inspiration, HI – initial compression period, DC – phonation period; E, F, G – characteristic points of the curve

Fig. 3 presents typical aerodynamograms. The rising part of curve *AB* corresponds to the inspiration of air. The pressure in the booth changes then in a positive direction owing to an increase in the volume of the thorax in relation to the air volume inspired (the performance of inspiration is conditioned by the formation of subpressure in the respiratory system). The difference in pressures ΔP_k permits the calculation of the subglottal pressure from formula (4). The segment *HI* defines the time of initial compression (prephonation).

The curve segment *DC* corresponds to the phonation period. The pressure changes in this part of the curve can result not only from the release from the lungs of the air initially compressed but also from the possible changes in its pressure which theoretically should be constant in order to secure a stable level of the phonation tension. The duration of phonation can be determined on the basis of measurement of the segment *IC*.

The irregularities occuring in the course of the curve suggest a change either in the subglottal pressure or in the flow speed resulting from a change in the glottis resistance.

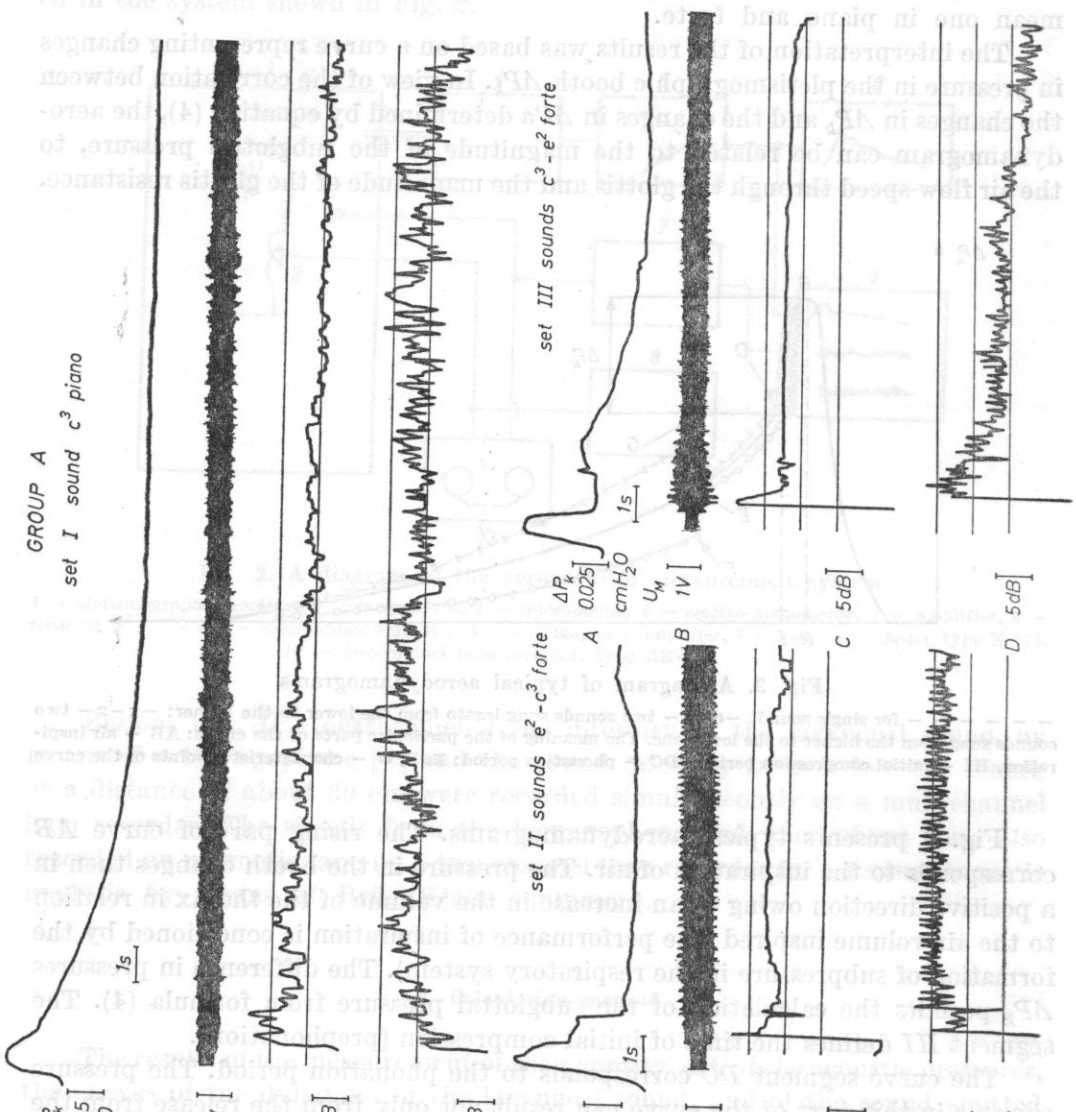
GROUP A
set I sound c³ piano
set II sounds e² - c³ forte
set III sounds c³ - e² forte
ΔPk
0.025
cmH2O
UM
1V
1s
5dB
A
B
C
D

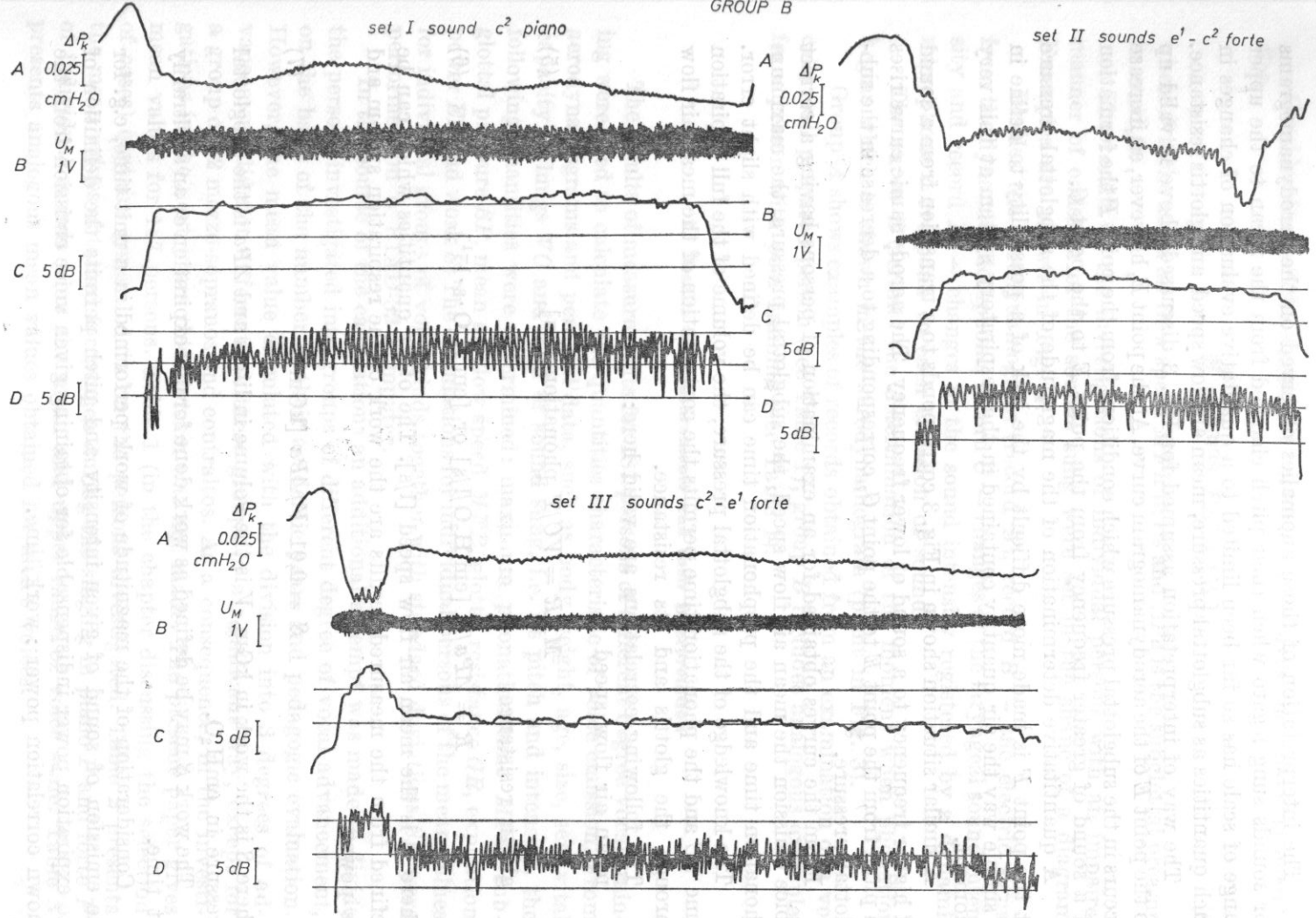

Fig. 4. Results of aerodynamic measurements

group *A* refers to a person advanced in vocal training, group *B* – to a person vocally not advanced

The interpretation of those anomalies observed on the aerodynamograms for sounds sung legato when their pitch changed from the mean to the upper range of scale has so far been limited to a qualitative evaluation of changes in such quantities as subglottal pressure, mean air flow speed, and glottis resistance.

The way of interpretation assumed for Fig. 3 discussed above is valid up to the point E of the aerodynamogram curve. At the point E, however, an increase occurs in the subglottal pressure which conditions from the point F the formation of a sound of greater frequency from the point E to the point C.

A quantitative determination of the magnitude of the subglottal pressure at the point F is made more difficult by the lack of a possibility to define in a simple way the air quantity contained in the respiratory system at this very moment.

A similar situation shown in Fig. 3 corresponds to a transition from a sound of higher frequency to a sound of lower frequency. The aerodynamic curve rises in pitch from the point E to the point G, corresponding to a decrease in the subglottal pressure.

From the curves obtained for an examination of persons having a correct voice emission the mean air flow speed, the subglottal pressure, the maximum phonation time and the prephonation time can be defined with slight error.

The knowledge of the subglottal pressure, the volume of the full expiration time VC and the phonation time permits the computation of the mean air flow through the glottis and its resistance.

The following correlations are valid here:

mean air flow speed

$$MFR = VC/T \text{ phonation } [\mathrm{l/s}], \tag{5}$$

glottis resistance

$$R = \Delta Pa/F \ [\mathrm{cm\,H_2O/l/s}] \text{ or } [\mathrm{cm\,H_2O \cdot s \cdot l^{-1}}], \tag{6}$$

where F is the mean air flow speed [l/s]. The other quantities which can be defined from the measured results are the work of the respiration system and its power.

$$S = 0{,}01 \ V/\Delta Pa \ [\mathrm{kGm}], \tag{7}$$

where S is the work in kGm, V is the volume in liters and ΔPa is the subglottal pressure in $\mathrm{cmH_2O}$.

The work S may be defined as work done for one expiration or an arbitrarily set time.

Consideration of the magnitude of work performed in a unit time, e.g. for the emission of sound of given intensity and pitch permits the definition of the expiration power indispensable for obtaining given voice emission from the known correlation power : work/time.

Consideration of the numerical coefficients involves the following correlation

$$M = 0.098\ F\Delta Pa\ [\mathrm{W}], \tag{8}$$

where F is the mean air flow speed MFR in l/s and ΔPa is the subglottal pressure in cmH_2O.

The results of the investigations of individual persons with an impaired manner of emission of the sounds sung were set in the shape of a diagram. Examples are shown in Fig. 4.

Besides the aerodynamogram (record A), record B — the electric signal from the dynamic microphone, record C — changes in the laryngeal sound intensity and record D — changes in the sound intensity registered by a dynamic microphone correspond to each emission of sound.

The curve B permits the determination of the moment when phonation begins which is shown in the aerodynamogram (point in Fig. 3).

Group A shows examples of records obtained from an examination of a vocally well prepared person (see Table 1); group B includes analogous examples for a person with poor training (see Table 1).

7. Results of measurements and their interpretation

The results of measurements for 187 persons of different degree vocal training were used to calculate the quantities characteristic of voice emission. From aerodynamograms and personal data, such as body weight, age, size, sex, vital capacity of lungs VC and kind of sound sung, i.e. its pitch and intensity, the following quantities were determined: maximum phonation time MPT, subglottal pressure SP, mean air flow speed MFR, glottis resistance GR, expiration power EP and work S. The calculations for individual persons of the mean values for individual groups of voice kinds together with standard deviations SD were performed on a RIAD-32 computer.

In the course of the calculations an additional attempt was made to divide the persons investigated into groups of different degree of vocal advancement, on the basis of the number of their academic years and pedagogic evaluation. However, the mean value calculated with the division into 3 degrees of advancement did not differentiate these groups in a significant way, except for a group of 32 mezzo-sopranos and contraltos. As a consequence, in the investigations in the next years this division was not made. The present paper gives mean values for 187 persons. Table 1 (in the chapter discussing the selection of cases) contains general data on the persons investigated. Table 2 presents the mean values obtained for women during the singing in piano P and forte F of individual sounds from the mean and upper range of voice scale. Table 3 presents analogous mean values obtained for men's voices.

Table 2. Mean values for women during singing in piano *P* and forte *F*

Parameters		Soprano		Mezzosoprano and alto	
		c_2	c_3	c_2	c_2
MPT [s]	*P*	17	12	17	15
	F	13	9	14	10
SP [cm$H_2$0]	*P*	8	9	8	13
	F	11	18	14	19
MFR [1/s]	*P*	0.20	0.28	0.23	0.20
	F	0.37	0.43	0.30	0.41
GR [cm$H_2$0/1/s]	*P*	40	42	42	55
	F	41	50	60	53
EP [W]	*P*	0.2	0.3	0.2	0.39
	F	0.4	0.8	0.43	0.88
S [kGm]	*P*	0.37	0.43	0.40	0.60
	F	0.53	0.86	0.67	0.91

Table 3. Mean values for men during singing in piano *P* and forte *F*

Parameters		Tenor		Baritone		Bass	
		c	c_1	*H*	*g*	*A*	*f*
MPT [s]	*P*	19	17	20	18	24	19
	F	13	15	19	15	21	17
SP [cmH_2O]	*P*	9	10	9	10	10	13
	F	15	23	15	21	16	21
MFR [1/s]	*P*	0.30	0.37	0.26	0.33	0.24	0.42
	F	0.39	0.48	0.30	0.39	0.28	0.44
GR [cmH_2O/1/s]	*P*	36	40	38	37	49	45
	F	48	67	59	62	64	64
EP [W]	*P*	0.24	0.34	0.25	0.38	0.25	0.53
	F	0.54	1.07	0.41	0.77	0.40	1.00
S [kGm]	*P*	0.55	0.64	0.53	0.65	0.68	0.83
	F	0.95	1.43	0.90	1.30	1.08	1.37

The numerical results obtained can be a criterion for the evaluation of the voice emission of persons investigated by this method. The determination of a correlation between such quantities as MFR, MPT and others enables a logi-

cal linking and an explanation of the cause of deviations from the values of the average results of vocal training evaluated on the basis of the academic year or years of training. A generalized characteristic of the correlation of the values of particular parameters can be given.

The correlation between *MPT* and *MFR* is characterized by a different direction of changes — *MFR* increases as *MPT* decreases. Therefore, the essential increase in the mean air flow speed (*MFR*) with increasing voice intensity, especially in the upper range of scale of a given individual, decreases the maximum phonation time.

The correlation between *MPT* and the intensity and pitch of the sound sung involves a decrease with increasing intensity and pitch of the sound. The maximum phonation time is always longer when a sound of lower pitch is sung in piano and it decreases for a sound of higher frequency in forte.

The correlation between *MFR* and *SP* (subglottal pressure) shows a common direction of changes. *MFR* increases as the subglottal pressure increases and the maximum phonation time *MPT* decreases.

Changes in the glottis resistance *GR* have a common direction of changes in the intensity and the pitch of sound sung.

The changes in expiration power *EP* and work *S* also have a common direction of changes in the intensity and pitch of the sound sung.

The interpretation of the results obtained took into account the fact that records *A*, *C* and *D* (see Fig. 4) came from 3 different measurement devices of different response characteristics. The frequencies occuring in the analysed phenomena can be divided into 3 groups:

(1) subacoustic frequencies — corresponding to the frequencies of movement of individual parts of body of the person investigated, connected with the respiratory function;

(2) fundamental frequencies of sounds;

(3) frequencies in a broad acoustic band (from the fundamental to the upper limit of the acoustic band).

The aerodynamogram obtained by a measurement of pressures in the pletismographic booth responds to the first group of frequencies, the contact microphone responds to the second and the dynamic microphone to the third. It was concluded that the aerodynamogram shape depends upon the correct work of the respiration organ and the respiration mechanism: the contact microphone upon the correctness of phonation function of the larynx (glottis) and the dynamic microphone upon the final effect, i.e. the voice quality. The fact should also be considered that the latter one, installed in the pletismographic booth with numerous resonances and its own reflections, has an irregular frequency characteristic among these three measurement systems. In this connection, the irregularities in the course of the curves *C* and *D* (see Fig. 4) have the most differentiated values for individual persons and different kinds of emission and do not always testify to the degree of preparation of a given person. It was

also found that, with vocally well prepared persons, changes in sound intensity run slower than with poorly prepared persons.

The interpretation of records in group *B*, Fig. 4, permits the discrimination in aerodynamograms of slight wavy anomalies (frequency range of 5 Hz) and thick wavy ones (frequency range of 0.1-0.2 Hz). It follows from clinical observations that slight wavy changes testify to variable values of the glottis resistance, whereas thick wavy ones indicate variations in the value of the expiration power which change the subglottal pressure. As a consequence, this is felt as a trembling voice.

8. Discussion

The measurement results obtained were compared with the results obtained by other authors which by their nature do not provide the possibility of their introduction in practical clinical examination.

The main purpose of the authors was, therefore, to develop a method which would give repeatable results under physiological conditions.

According to ISSHIKI [9], the main factors controlling the voice intensity are the glottis resistance during phonation for a low frequency and the expiration power for this frequency. A discussion of this question seems necessary because of the specificity of the function of the vocal organ and the respiration one during singing. It is assumed that for sounds sung "low" the vocal cords are slack and the glottis resistance is so small that it can be increased further which is reflected in an increase in voice intensity. And conversely, for sounds sung "high" the glottis resistance is so great, probably maximum, that this resistance cannot be increased any further without a change in the tension of the vocal cords, which as a consequence would cause a change in the pitch of the sound sung.

Thus the intensity of sound with "high" sounds must be modulated not by the glottis resistance but by the expiration power. Therefore, for "high" sound, with too weak glottis resistance, an increase in the intensity of the air flow through the glottis fissure owing to an increase in the value of the expiration power causes it to open to such a degree that the voice intensity is small and the voice itself becomes hoarse. A similar phenomenon is observed for the decay of the voice at "low" sounds. Facts confirmed by experimental observations testify that in these series where a deflection of voice occurs during phonation of "low" sounds a much higher intensity of the air flow through the glottis fissure was observed.

The univocal conclusion presented by ISSHIKI as regards the division of functions between the glottis resistance and the expiration power in the modulation of voice intensity encouraged investigations in this field. In order to explain the above problem other investigators made use of three different methods:

(1) the electromyographic method (EMG) used by KATSUKU [12], FABORG-ANDERSEN [5] and FINK [6],

(2) the *X*-ray method used by LUCHSINGER [17], LANDEAU and ZUILI [16],

(3) the aerodynamic method used by PTACEK and SANDERS [22].

Only FABORG-ANDERSEN found no essential differences in the potentials of the intralaryngeal muscles with changes in voice intensity.

A different method was used in the present paper. The pletismographic booth was used only for measurements of the subglottal pressure by an indirect method without introducing a needle into the trachea.

It should be also stated that the pletismographic booth provides the freedom of movement of the investigated person's body and makes it possible to eliminate the mask on the face during the sequence sung. Such a procedure seems reasonable, especially in carrying out routine investigations comprising, as in the present case, a greater number of people.

An important element resulting from the present method is the achievement of a record, the so-called aerodynamogram. This curve shows changes in pressure in the pletismographic booth which can be related to the value of the subglottal pressure, to the air flow speed and to the value of the glottis resistance. The aerodynamogram also enables the performance of an analysis of the phenomenon divided into 3 stages, i.e. the commencement of inspiration, the beginning of expiration and phonation and its duration until its termination. A simultaneous analysis of changes in voice dynamics synchronized in time with the course of the aerodynamic curve characterizes the function of the respiration organ and the vocal one. But, it follows from an analysis of the results, the shape and form of the aerodynamograms determine in an unambigous way the evaluation of the functions of the organs investigated. In clinical practice this is of fundamental importance and the acoustic information obtained should be treated as complementary to a subjective evaluation.

The acoustical literature, only some items of which are cited here, shows a great interest in the problem of human voice. Undoubtedly, with the developments in technical researches the acoustic methods of the investigation of vocal phenomena have over the recent years retained a high level. The directions of these investigations are many-sided as they are concerned, among other things, with the knowledge of the voice path function from an analytical and synthetic point of view.

The present authors are of the opinion that on the basis of aerodynamic investigations it is possible to determine the physiological mechanism of the formation of voice. The use of an acoustic method makes it possible to record the final effect of the vocal organ. Therefore, both methods complement each other.

Studying individual aerodynamograms and deviations from most regular changes occuring in them, the authors considered the phenomenon of the vibration of the vocal cords.

An analysis of the phenomenon according to the Bernouli law does not explain the formation of slight wavy changes as a result of the vibration of the vocal cords, even in pathological cases [19, 20].

The essence of the formation of these changes needs further studies. Since there is no correlation between the degree of advancement determined from years of learning and the results obtained from personal measurements, another criterion for the evaluation of the degree of advancement was proposed. The maximum phonation time (*MPT*), as it is conditioned by the efficiency of both the respiration and the vocal system, was assumed as the determining factor.

Such a criterion is supported by the fact that a reduction of volume of the lungs, a reduction of the efficiency of muscles of the abdominal press, the constrictor of the glottis fissure etc. effect a decrease in the phonation time.

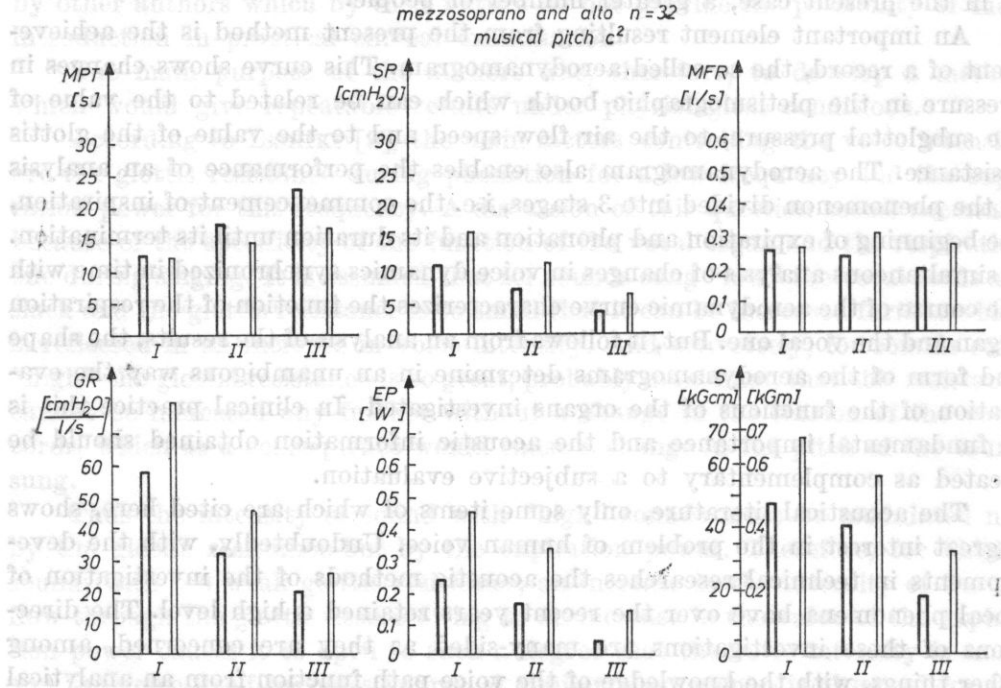

Fig. 5. Measurement results for 3 groups of vocal advancement degree for 32 women
Piano – thick line, Forte – thin line; I, II, III – degree of preparation, *MPT* – maximum phonation time, *SP* – subglottal pressure, *MFR* – mean air flow speed, *GR* – glottis resistance, *EP* – expiration power, *S* – work of respiratory organ

Only the group of 32 mezzosopranos and altos divided into different degrees of preparation according to years of learning showed a correlation between measurement results and years of learning. Fig. 5 presents a comparison of the value of the fundamental parameters.

Gross deviations from the mean values given in Tables 2 and 3 permit the determination of individual causes of deviation from norm which result, for example, from the function of larynx or the respiration system.

Beside, combination of the evaluation method above mentioned with the quality of an individual aerodynamogram gives a better idea of the mechanism of the performance of the vocal and the respiration organ during singing.

The results obtained in the present work agree with the results obtained by other methods of the authors quoted.

9. Conclusions

The modified aerodynamic method is bloodless, indirect, and repeatable in view of the fact that it eliminates the introduction of a needle into the trachea, records the values of the particular parameters from the pletismographic booth and permits repeated measurements of the phenomena occuring during singing.

The above method permits the evaluation of the teaching of singing at particular stages and the determination of the degree of vocal preparation. Therefore, it is applied fully in research and didactic work. In phoniatric practice this method permits a detailed analysis of the voice emission and proposals to be submitted for directing activities towards its improvement.

References

[1] W. Brégy, *Elements of vocal technique*, PWM, Kraków 1974.

[2] H. Ciołkosz-Łupinowa, *Some acoustic characteristics of singing* (in Polish), Central Pedagog. Art Train. Center, **148**, 1-74 (1973).

[3] H. Ciołkosz-Łupinowa, *Some problems of the formants of the singer's voice* (in Polish), PWSM J., **4**, 63-81 (1967).

[4] J. E. Cotes, *Function of lungs*, PZWL, 1969.

[5] K. Faborg-Andersen, *Electromyographic investigations of intrinsic laryngeal muscles in humans*, Acta Physiol. Scand., 41 Suppl., 140 (1957).

[6] B. R. Fink, *Tensor mechanism of the vocal folds*, Ann. Otol., **71**, 592-601 (1962).

[7] M. Hirano, Y. Takouchi, I. Hiroto, *Internasal sound pressure during utterance of speech sound*, Folia phoniat., **18**, 369-381 (1966).

[8] A. S. House, K. N. Stevens, *Analog studies of the nasalization of vowels*, J. of Speech and Hearing Disorders, **21**, 218-232 (1956).

[9] N. Isshiki, *Regulatory mechanismus of voice intensity variation*, J. Speech Res., **7**, 17-29 (1964).

[10] J. Kacprowski, *A simulative model of the vocal tract including the effect of nasalization*, Archives of Acoustics, **2**, 4, 235-255 (1977).

[11] J. Kacprowski, *Objective acoustical methods in phoniatric diagnostics of speech organ disorders*, Archives of Acoustics, **4**, 4, 289-304 (1979).

[12] Y. Katsuki, *The function of the phonatory muscles*, Jap. J. Physiol., **1**, 29-36 (1950).

[13] M. KWIEK, *Voice spectra of contralto* (in Polish), Mickiewicz University Scientific J., **2**, 47-59 (1958).

[14] H. von LEDEN, *Objective measures of laryngeal function and phonation*, Annals of the New York Academy of Sciences, **155**, 56-67 (1968).

[15] H. von LEDEN, *Objective methods of vocal analysis in singers and actors*, Reprinted from Excerpta Medica International Congress Series No. 206 (1969).

[16] M. LANDEAU, H. ZUILI, *Vocal emission and tomographs of the larynx*, The NATS' Bulletin, 6-11 (1963).

[17] R. LUCHSINGER, G. E. ARNOLD, *Lehrbuch der Stimme und Sprachheilkunde*, Springer Verlag, Wien 1959, 91.

[18] F. MARTIENSSEN-LOHMANN, *Training of the singer's voice*, PWM, Kraków 1953.

[19] Z. PAWŁOWSKI, *Objective diagnostics in the vibration of vocal cords*, Arch. Otolaryng., **82**, 195-197 (1965).

[20] Z. PAWŁOWSKI, *Objective method of investigation of the phonatory function of the larynx* (in Polish), Arch. Ac., **3**, 5, 331-352 (1970).

[21] Z. PAWŁOWSKI, T. ŁĘTOWSKI, A. RAKOWSKI, *Comparative analysis of microphone recordings registered at various points of the vocal tract*, Folia phoniat., **24**, 360-370 (1972).

[22] P. H. PTACEK, E. K. SANDER, *Maximum duration of phonation*, J. Speech Dis., **28**, 171-181 (1963).

[23] B. ROMANISZYN, *Problems of vocal art and pedagogics* (in Polish), PWM, Kraków 1957.

[24] A. STAMPA, *Atem, Sprache und Gesang*, Bärenreiter Verlag, Kassel 1956.

[25] J. TARNEAU, *La voix, sa construction et sa distruction*, Librairie Medicine, Paris 1946.

[26] P. F. TOSI, J. F. AGRICOLA, *Anleitung zur Singkunst*, Deutscher Verlag für Musik, Leipzig 1966.

[27] N. YANAGIHARA, Y. KOIKE, *The regulation of sustained phonation*, Folia phoniat., **19**, 1-18 (1967).

Received on September 16, 1981.

ARCHIVES OF ACOUSTICS
7, 3-4, 225-246 (1982)

DYNAMIC ULTRASONIC VISUALIZATION OF BLOOD VESSELS AND FLOWS

ANDRZEJ NOWICKI

Institute of Fundamental Technological Research, Polish Academy of Sciences
(00-049 Warszawa, ul. Świętokrzyska 21)

JOHN M. REID

Institute of Applied Physiology and Medicine (Seattle, USA)

This paper describes a new method for dynamic real-time visualization of blood flows. This method uses a special signal processing system (SEC) which consists in cancellation of stationary echoes from the reflections of ultrasonic waves from soft tissues with continuous measurement of the phase of signals scattered in blood.

The stationary echo cancellation system has been designed on the basis of the properties of periodic filters using quartz delay lines. A level of stationary echo cancellation above 55 dB was achieved, which, when using an original detector of the phase of signals scattered in blood, permits real-time observation of blood flow velocity profiles. This, in turn, permits the internal diameter of a vessel (the degree of constriction) to be evaluated in the site under investigation.

1. Introduction

Ultrasonic methods for the visualization of the internal anatomical structures of man use the particular properties of ultrasonic wave propagation, permitting the detection of small differences in the density and elasticity of soft tissues. The density and elasticity of tissues determine the acoustic impedance of the biological medium investigated. Knowledge of the acoustic impedance of media permits the determination of the part of the energy of ultrasonic waves incident on the boundary between the two media which is partly reflected and returns to the receiving transducer and also of the part which

penetrates into an adjacent medium. The higher the difference between the acoustic impedances of the two media is the greater is the energy on the boundary between them. The magnitude of the reflected energy also depends on the geometry of the ultrasonic beam and on the geometry of the system. For simplification, the case of the perpendicular incidence of ultrasonic waves on biological structures of different acoustic impedance has been assumed in the present discussion.

The development of the optimum system for the visualization of blood vessels requires the estimation of differences in the level of signals reflected from stationary structures and of signals scattered in blood. An exact solution of this problem would require some difficult in vivo measurements of the energy of signals reflected from all the biological structures on the path between the ultrasonic transducer and the blood vessel. Even in the latter case, however, the results obtained describe only the anatomical system related to a specific structure, thickness and distribution in the of tissues investigated ultrasonically.

In the case when the wave is reflected from a flat reflector with the energy coefficient of reflection R the intensity of the wave received by the transducer is [10]

$$I_0 = \frac{P_t A}{4x^2\lambda^2} R \exp(-4\alpha x), \tag{1}$$

where P_t is the sound power of the signal transmitted, λ is the wavelength, α is the attenuation coefficient of the wave in the medium, A is the effective area of the transducer which is equal to its geometrical area when it works in a piston mode and x is the distance from the transducer.

In the case when the ultrasonic wave is incident on a single particle (target) which is small compared to the wavelength and the width of the ultrasonic beam, the scattered wave is isotropic and propagates in the form of a spherical wave.

In the latter case, the power of the scattered wave is calculated from the product of the effective scattering surface δ and the intensity of the incident wave. The intensity of the reflected wave is thus

$$I = \left(\frac{P_t A}{x^2\lambda^2}\right)\left(\frac{\delta}{4\pi x^2}\right) \exp(-4\alpha x). \tag{2}$$

The first term represents the intensity of the wave incident on a particle with the active "scattering cross-section" δ which is at a distance x from the transducer, the other describes the propagation of a spherical wave.

In order to calculate the intensity of the isotropic wave scattered by many molecules, it is necessary to sum up the successive intensities from particular particles described by formula (2). The total active surface area of the system of particles is represented by the product of the blood volume and the effective scattering coefficient η. According to SHUNG *et al.* the coefficient η is a function

of hematocrite [12]. The total intensity of the scattered signal can thus be expressed in the form

$$I_r = \frac{P_t A^2}{x^4 \lambda^2 4\pi} \frac{c\tau\eta}{2} \exp(-4\alpha x), \tag{3}$$

where $Ac\tau/2$ is the blood volume contained in the ultrasonic pulse field in the form of a cylinder with the base area A and height of $c\tau/2$; and τ is the duration of the pulse. The ratio of the intensities of the wave scattered from blood and of that reflected on the boundary between fat tissue and the wall of the vessel can be determined by way of dividing expressions (3) and (1) by each other and subsequently substituting into the quotient the respective numerical values,

$$\frac{I_r}{I_0} = \frac{A}{\pi R x^2} \frac{c\tau}{2} \eta. \tag{4}$$

Let the duration τ of pulses be 1 μs and the diameter of the transducer $2a$ be 5 mm. For 30 % hematocrite the scattering coefficient $\eta = 11 \cdot 10^{-5}$ cm^{-1} [12]. The acoustic impedances of fat tissue and the wall of the vessel are equal, respectively, to $1.38 \cdot 10^6$ kg/m^{2}s and $1.66 \cdot 10^6$ kg/m^{2}s. The energy coefficient of reflection, R, on the boundary of the tissues mentioned above is equal to $85 \cdot 10^{-4}$. For these numerical values the ratio I_r/I_0 is equal to $6 \cdot 10^{-5}$.

In practice this signifies that successive echoes whose amplitudes differ by almost theree orders of magnitude occur at the input of the receiver system. This prevents simultaneous observation of reflected and scattered echoes. It is necessary to bear in mind that large echoes reflected from structures lying at depth corresponding to a double or even triple repetition period of pulses can also occur. This phenomenon is described by the ambiguity function $\chi(t, v)$ for $v = 0$ (stationary target) [3, 6].

2. A survey of ultrasonic methods for imaging blood vessels

The easiest method for the investigation of geometrical dimensions of a blood vessel on the oscilloscope screen is the A-mode.

In the case of such structures as fat tissue, muscles, etc. echoes on the oscilloscope screen are stationary, while echoes from moving structures such as blood vessels or the heart change their position on the time base of the C.R.T.

In the case of arteries this motion is periodic, following the beat of the heart in that the walls of the vessel go away from each other for systole and approach for diastole. This effect can be observed on the oscilloscope screen where the echoes from the walls fluctuate, moving away and approaching each other. The A-mode has not been widely used in the visualization of blood vessels; it nevertheless has been the basis for a number of interesting works, particularly that of BUSHMAN [2] concerning changes in the diameter of a carotid artery in healthy persons and those with advanced sclerosis.

In the TM (time-motion) mode the time base on the oscilloscope screen is blank when no echoes occur and brightened up only by the echoes from structures in the ultrasonic field.

Echoes are thus projected along the time base in the form of bright points, which are mobile when the ultrasonic waves is reflected from a moving structure.

The TM technique has been applied mainly in the investigations of the moving structures of the heart; it has increasingly been used recently for the visualization of the abdominal aorta, particularly of its aneurisms.

Whereas the A- and TM-modes only show a geometrical, one-dimensional image of the distribution of biological structures along the ultrasonic beam, the so-called B-scanning (for brightness) permits two-dimensional visualization of the structures examined. The B-mode uses partly the basis electronic devices applied in the A-scanner apparatus. The essential modification is in the system of mounting the probe on a special gantry with two mobile arms. Carrying the probe along the structure investigated in translatory and rotary motion, the arms of the gantry change their position and accordingly the angles θ, $\varnothing$ and α change between the arms of the gantry and the probe. Simple trigonometric relations permit the determination on this basis of the coordinates x, y of the position of the transmitted ultrasonic beam and of the one received by the ultrasonic transducer. This transformation, which changes the motion of the probe into the motion of the time base on the oscilloscope display, is implemented using a special electronic system, e.g. of the Metrop type [5]. When the ultrasonic wave encounters reflecting structures on its path, the resultant echoes are displayed on the time base of the oscilloscope tube in the form of bright points, while the brightness of these points depends on the strength of the echo. The B-mode has most widely been used in the investigations of the abdominal cavity in obstetrics, gynaecology and in the diagnostics of the eye and eye orbit.

Nevertheless, in the few recent years the technological developments which increased resolution and dynamics of apparatus permitted the application of B-scanning for the visualization of large blood vessels, particularly of aneurisms of the abdominal aorta.

In many cases B-scanning has greater diagnostic value than that of X-ray arteriography, in view of the harmlessness and repeatability of examinations essential in the monitoring of the distention of an aneurism. In arteriography examinations must not be too frequent, since they put an extra burden on the patient. Punctures of an artery, catherisation and the introduction of the bulk of contrast often damage the vessel and threaten a general shock. An additional advantage of B-scanning is the possibility of projecting the vessel in two planes, while arteriography only gives an image in one plane, which makes it difficult to interpret angiograms of aneurisms in which thrombi occur.

The other group of methods for the visualization of blood vessels includes different Doppler methods. Because of its simple apparatus and its easy clinical application, the so-called continuous-wave method (C.W. Doppler) has been

widely used in the evaluation of the state of patency of vessels, in the localization of thrombi and fistulas in arteries and veins and also, more recently, in the forecasting of the level of amputation on the basis of exact measurements of the systole pressure in peripheral vessels. Among the numerous mutations of the C. W. method, the technique for the visualization of blood vessels elaborated in 1972 by Reid and Spencer [11] seems to be particularly interesting. In view of its similarity to the imaging of vessels in *X*-ray angiography, its authors have called it Doppler angiography.

Doppler angiography is widely used, particularly in the USA, where serial production of relevant apparatus has recently been commenced (Carolina Medical Electronics, Inc.). Its buyers are clinical units engaged in diagnostics of arteriosclerosis of carotid arteries, particularly with an impending stroke. Until recently the only method for monitoring the patency of blood vessels has been that of *X*-ray angiography, which involves the high risk of complications.

A preliminary ultrasonic examination, though it does not always defines unambiguously the degree of inductability of the internal and external carotid arteries, limits the use of *X*-ray angiography only to dubious cases [14].

The transition from qualitative investigations to quantitative ones has been made possible by the development of a pulse Doppler method which permits the measurement of blood flow rate selectively at varying depth [9]. As a result, the degree of constriction of the vessel investigated can be evaluated with high accuracy (usually better than 1 mm) [6, 7].

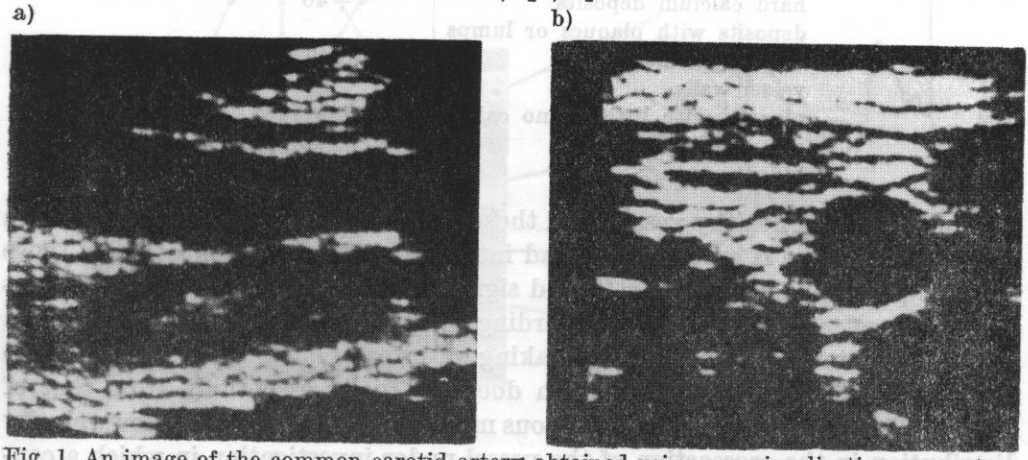

Fig. 1. An image of the common carotid artery obtained using eye visualization apparatus: a) longitudinal section, b) crossection

Several types of pulse Doppler apparatus are now produced in the world. Particular attention is due the British devices (Mavis-GEC Medical) which are equipped with 30 parallel channels permitting simultaneous registration of blood flow at different depth and French (Echovar Doppler Pulsée — Alvar Electronic) and Polish (UDP-30 — Z.D. Techpan) devices for automatic registration of blood flow profiles averaged in time [7].

Concluding this short survey of methods for the visualization of blood vessels, it is interesting to note the complementary technique which combines B-scanning with the pulse Doppler method. In Poland the first attempts to use this measurement technique were made in 1974 using a B-scanner for the visualization of the internal structures of the eye [4] and a prototype ultrasonic pulse Doppler flowmeter, UDP-30, developed by the author.

Fig. 1 shows an image of the carotid artery of a healthy, young man. The inner diameter of the vessel is displayed in the form of a blackened channel (longitudinal section) or a blackened hole (cross-section), when sharp, bright points arise on the boundary of a wall of the vessel. This results from the fact that the energy of ultrasonic waves reflected from walls of the vessel is greater by two orders of magnitude than the energy of waves scattered in blood (see Table 1).

It follows from Table 1 that the areas with fat deposits narrowing the effective inner diameter of the vessel and the areas filled with blood cause a reflection of ultrasonic waves on a similar level.

Table 1. Relative levels of ultrasonic echoes from sclerotic deposits of different type [1]

Tissue	Relative echo level [dB]
hard calcium deposits	+40
deposits with plaques or lumps of calcium deposit	0-20
vessel walls	0
plaques with little or no calcium deposit	from 0 to −40
blood	−40

In the case of healthy vessels and those narrowed as a result of hard calcium deposits the image is easy to read and interpret. With soft deposits (e.g. those with fat plaques) the level of reflected signals does not differ greatly from that of signals scattered in blood and accordingly the oscilloscope screen displays an image of less intensive brightness (making an impression of a blackened image) in the place of a constriction, which does not differ essentially from that of a vessel filled with blood. A simultaneous measurement of the blood flow velocity distribution in the crossection of the vessel under investigation in which a constriction of this type is suspected to occur can prevent the examiner from an erroneous interpretation of results.

3. The principle of dynamic visualization of blood flows by means of the moving target indicator (M.T.I.) technique

The application range of the methods described above is usually limited by structural features of apparatus, resolution of the system and time necessary for an image of the vessel investigated to be obtained.

In a continuous-wave visualization system the images obtained resemble those of vessels in *X*-ray angiography. Twodimensional projection permits the evaluation of patency of vessel only in a plane parallel to the surface of the skin over the vessel. The vessel can be projected in a plane perpendicular to the surface of the skin using a multi-channel pulse Doppler apparatus. The large number, however, of analyzing gates, necessary for good resolution and minimalization of the time of investigation of the vessel, complicates the apparatus and raises its price considerably.

The complementary system-of a real-time *B*-scan and of a single-channel pulse Doppler method – although it provides high resolution and rapid representation, is limited to only the visualization of straight sections of the vessel which lie in the plane of motion of the probe B (see Fig. 2). This limits the eva-

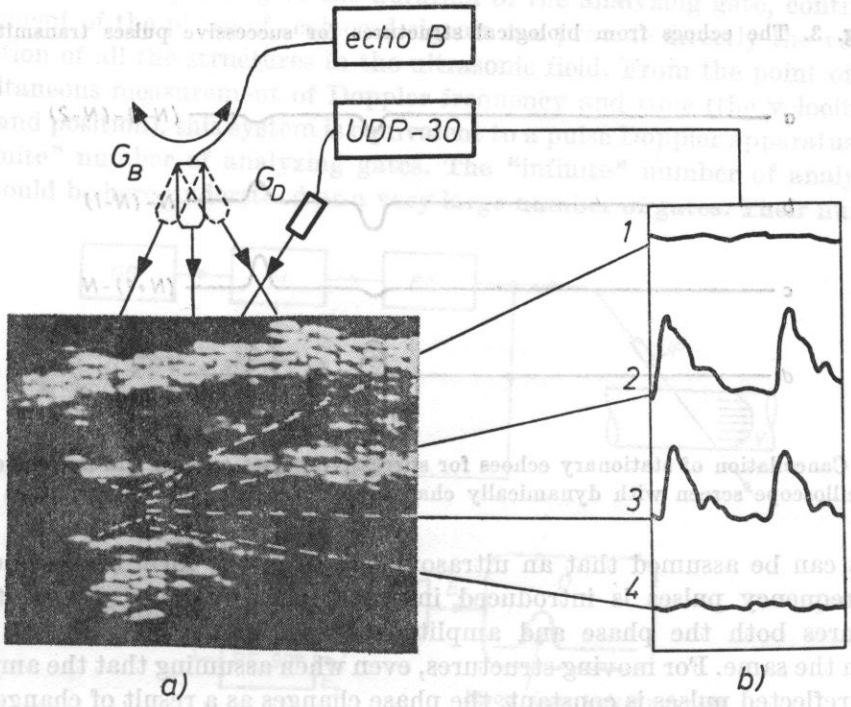

Fig. 2. Complementary visualization of blood vessels with *B*-scanning and the pulse Doppler method (UDP-30)

a) an image of a vessel part in *B*-scanning, where dashed line marks areas with soft calcium deposits; b) registration of flow velocity at different parts of a vessel cross-section; curves *1* and *4* show the lack of flow in an area with soft calcium deposits, G_B – ultrasonic probe for B-scanning, G_D – ultrasonic Doppler probe

luation of patency in vessel bifurcations, e.g. in the bifurcation of the common carotid artery into internal and external carotid arteries and in the bifurcation of the femoral artery into the femoral profunda artery.

Compared to the visualization methods discussed the method for the real-time detection of the phase of signals scattered in blood using the radar technique of stationary echo cancellation SEC [8] seems particularly attractive.

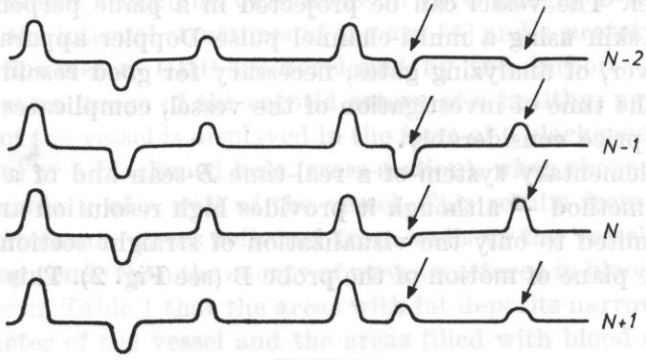

Fig. 3. The echoes from biological structures for successive pulses transmitted

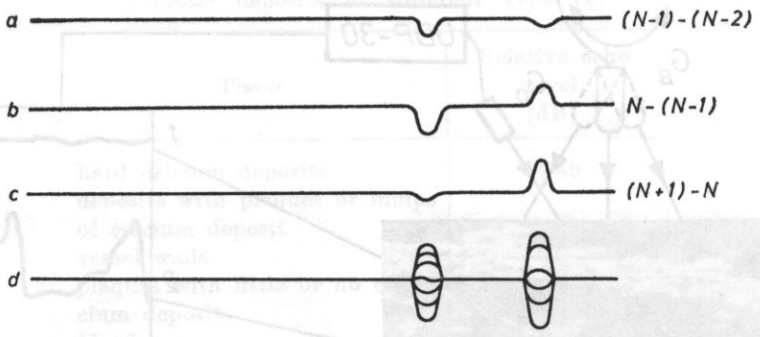

Fig. 4. Cancellation of stationary echoes for successive pulses (*a*, *b*, *c*) and an image on the oscilloscope screen with dynamically changing echoes from mobile structures (*d*)

It can be assumed that an ultrasonic signal in the form of a sequence of high-frequency pulses is introduced into the patient's body. For stationary structures both the phase and amplitude of the successive reflected pulses remain the same. For moving structures, even when assuming that the amplitude of the reflected pulses is constant, the phase changes as a result of change in the distance between the reflecting structure and the source of ultrasonic waves in the time from the transmission of the pulse N to the transmission of the pulse $N+1$.

It can be seen in Fig. 3 that most echoes do not change from pulse to pulse. They are thus reflected from stationary structures; some, marked with arrows, differ from one another because of change in phase upon reflection from moving structures. By way of signal processing, which consists in the subtraction of two consecutive echo sequences from each other, where the echo sequence from

the earlier pulse is delayed by the time T_p equal to the repetition period of transmitted pulses, it is possible to achieve the effect of cancellation of stationary echoes (Fig. 4).

In a standard pulse Doppler method the ultrasonic transducer transmits a sequence of coherent high-frequency pulses with some specific repetition frequency $F_p (F_p = 1/T_p)$. Inside the body the ultrasonic waves are reflected on the boundary of tissues with different acoustic impedance ϱc and scattered by morphotic elements of blood, with the ratio of the amplitudes of reflected and scattered signals greater possibly than 100.

Thus it can be seen that strong signals reflected from stationary or slowly moving tissues (e.g. the walls of vessels) can mask weak signals scattered in blood which contain Doppler information about its flow rate. Whereas in the pulse method the flow rate of a blood layer at chosen depth is measured in short time intervals corresponding to the duration of the analyzing gate, continuous measurement of the phase of scattered signals can provide directly the velocity distribution of all the structures in the ultrasonic field. From the point of view of simultaneous measurement of Doppler frequency and time (the velocities of motion and position), this system is equivalent to a pulse Doppler apparatus with an "infinite" number of analyzing gates. The "infinite" number of analyzing, gates should be here understood as a very large number of gates. Their number

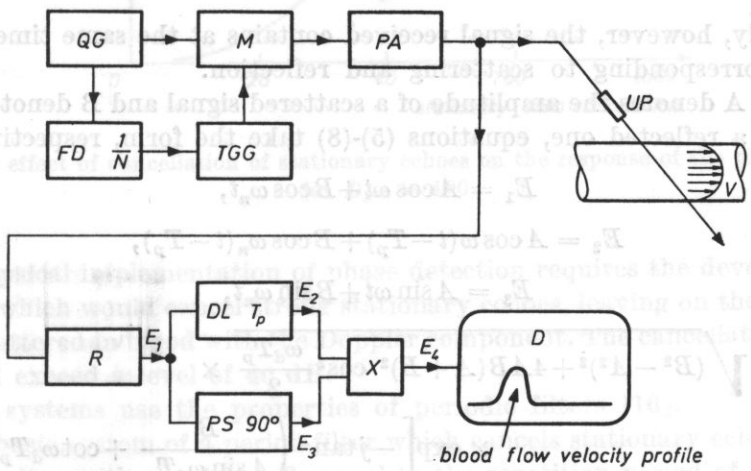

Fig. 5. A schematic diagram of the system for dynamic flow visualization

QG – quartz generator, *FD* – frequency divider, *TGG* – transmitter gate generator, *M* – modulator, *PA* – power amplifier, *UP* – ultrasonic probe, *R* – receiver, *DL* – delay line, *PS* – phase shifter, *X* – doubly balanced mixer, *D* – display

which it is difficult to determine analytically, depends mainly on the repetition period T_p and the frequency f_n of transmitted pulses. The notion of the number of analyzing gates should not be identified with the resolution of the system, which depends on the duration and shape of transmitted pulses.

An approximate number of analyzing gates corresponding to the SEC system can be determined from the expression $n \simeq T_p f_n$. For a repetition period of 64 μs and the frequency of the carrier wave $f_n = 4.37$ MHz a multi-gate system corresponding to the SEC system should contain about 280 analyzing gates. A schematic diagram of the system for the visualization of blood flow by continuous measurement of the phase of signals scattered in body is shown in Fig. 5.

In the case when only a signal scattered in blood occurs without additional stationary echoes the signals E_1, E_2, E_3 and E_4 in Fig. 5 can be represented in the form

$$E_1 = A \cos \omega t, \tag{5}$$

$$E_2 = A \cos \omega (t - T_p), \tag{6}$$

$$E_3 = A \sin \omega t, \tag{7}$$

$$E_4 = -\frac{A^2}{2} \sin \omega T_p = -\frac{A^2}{2} \sin \omega_d T_p, \tag{8}$$

where

$$\omega = \omega_n \pm \omega_d, \qquad T_p = \frac{2\pi N}{\omega_n}, \qquad \omega T_p = 2\pi N \pm \omega_d T_p.$$

Usually, however, the signal received contains at the same time the components corresponding to scattering and reflection.

When A denotes the amplitude of a scattered signal and B denotes the amplitude of a reflected one, equations (5)-(8) take the form, respectively,

$$E_1 = A \cos \omega t + B \cos \omega_n t, \tag{9}$$

$$E_2 = A \cos \omega (t - T_p) + B \cos \omega_n (t - T_p), \tag{10}$$

$$E_3 = A \sin \omega t + B \sin \omega_n t, \tag{11}$$

$$E_4 = \frac{1}{2} \sqrt{(B^2 - A^2)^2 + 4AB(A+B)^2 \cos^2 \frac{\omega_d T_p}{2}} \times \exp\left[-j \tan^{-1} \left(\frac{B}{A \sin \omega_d T_p} + \cot \omega_d T_p \right) \right]. \tag{12}$$

The signal E_4 at the output of the phase detector decreases considerably as the amplitude of stationary echoes increases and for the same level of reflected and scattered signals ($A = B$), for example, the signal at the output of the phase detector reaches an amplitude of half the level for $B = 0$. For stationary echoes stronger by a factor of a hundred than scattered echoes it is possible to observe a decrease by a factor of fifty in the signal at the output of the phase detector. An additional decrease in the sensitivity of the phase detector is related to the limitation of the linear characteristic range of the receiver for strong sig-

nals. For transmitted pulses with an amplitude of 60 V echoes scattered in blood reach an amplitude of several dozens of μV, while the amplitude of echoes from stationary structures can exceed several dozens of mV.

At the output of a typical receiver, with amplification of 60 dB, the latter echoes can achieve a level of above 10 V, exceeding the linear range.

The effect of the degree of cancellation of stationary echoes on the amplitude of the output signal from the phase detector was calculated from expression (12). The assumption was made that the amplitude of stationary echoes is larger by a factor of a hundred than that of scattered echoes, $B = 100\,A$. The calculated results are plotted in Fig. 6.

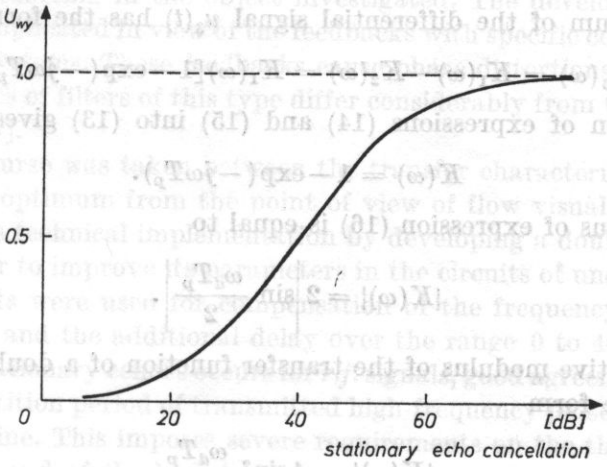

Fig. 6. The effect of cancellation of stationary echoes on the response of the phase detector for $B/A = 100$

A physical implementation of phase detection requires the development of a system which would cancel strong stationary echoes, leaving on the same level signals scattered in blood with the Doppler component. The cancellation efficiency should exceed a level of 40 dB.

SEC systems use the properties of periodic filters [16].

The basic system of a period filter which cancels stationary echoes consists of a delay line with the delay T_p equal to the repetition period of transmitted

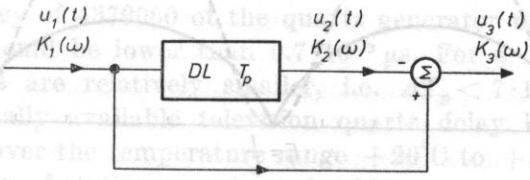

Fig. 7. The SEC system with one delay line *DL*

pulses and a differential amplifier. The frequency response of this system can be determined from its transfer function

$$K(\omega) = \frac{K_3(\omega)}{K_1(\omega)}, \tag{13}$$

where $K_1(\omega)$ and $K_3(\omega)$ are the spectra of the signals at the input and output of the filter.

The spectrum of the signal $u_2(t) = u_1(t - T_p)$ at the output of the delay line has the form, according to the theorem of the shift in the time domain,

$$K_2(\omega) = K_1(\omega)\exp(-j\omega T_p). \tag{14}$$

The spectrum of the differential signal $u_3(t)$ has the form

$$K_3(\omega) = K_1(\omega) - K_2(\omega) = K_1(\omega)[1 - \exp(-j\omega T_p)]. \tag{15}$$

Substitution of expressions (14) and (15) into (13) gives

$$K(\omega) = 1 - \exp(-j\omega T_p). \tag{16}$$

The modulus of expression (16) is equal to

$$|K(\omega)| = 2\left|\sin\frac{\omega_d T_p}{2}\right|. \tag{17}$$

The respective modulus of the transfer function of a double in series SEC system has the form

$$|K(\omega)| = 4\sin^2\frac{\omega_d T_p}{2}. \tag{18}$$

In both systems the detectability of stationary structures is a function of the Doppler frequency, this relation being sinusoidal for a single SEC system and proportional to a squared sine function for a double SEC system. It can be seen from Fig. 8 that not only echoes of zero Doppler frequency (stationary echoes) and multiple repetition frequency but also those whose frequency is

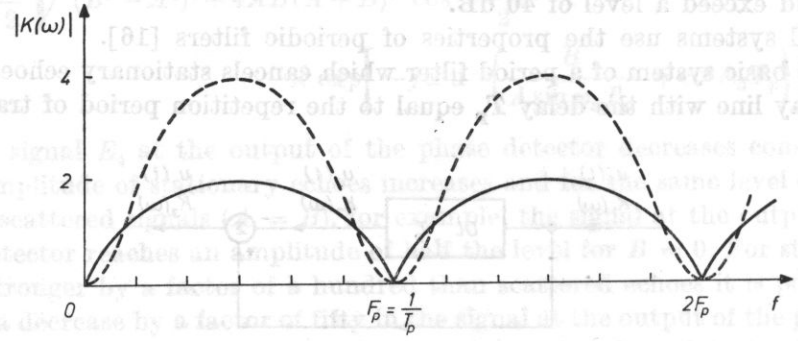

Fig. 8. The frequency response of a single (solid line) and a double (dashed line) SEC system

close to zero are cancelled. These signals usually come from slowly moving vessel walls and from blood flowing at vessel walls.

It was found experimentally that the amplitude of the Doppler signal changes according to the systole and diastole of the heart and increases for higher flow velocities (the systole phase). The probability of low velocities being detected is therefore low for the SEC system described, introducing error in the evaluation of the diameter of a vessel, particularly in the diastole. An ample theory has been developed for feedback periodic filters whose transfer characteristics are close to ideal ones, i.e. they show maximum cancellation of stationary and slowly changing echoes and a flat transfer characteristic in the velocity range occurring in the object investigated. The development of these filters is very complicated in view of the feedbacks with specific coefficients introduced into the systems. These feedbacks cause phase distortions and in general the characteristics of filters of this type differ considerably from those calculated theoretically [13].

A middle course was taken between the transfer characteristic of the SEC system which is optimum from the point of view of flow visualization and the possibilities of its technical implementation by developing a double SEC system in series. In order to improve its parameters in the circuits of undelayed signals, additional circuits were used for compensation of the frequency characteristic of the delay line and the additional delay over the range 0 to 40 ns. Since the cancellation of stationary echoes occurs for *r.f.* signals, good agreement is required between the repetition period of transmitted high-frequency pulses and the delay T_p of the delay line. This imposes severe requirements on the thermal stability of the delay line and of the high-frequency generator. A coherent sequence of high-frequency pulses with the repetition time T_p can be achieved by dividing the frequency of a signal generated by a quartz oscillator; thus the stability of the repetition period of transmitted pulses is equal to the stability of quartz.

Assumption that a 40 dB cancellation of stationary echoes is sufficient for correct performance of the phase detector for a single SEC system gives

$$\left| \sin \frac{\omega_n \Delta T_p}{2} \right| < 0.01. \tag{19}$$

For a small argument $\sin x = x$ and thus

$$\omega_n \Delta T_p < 0.02. \tag{20}$$

For a frequency of 4379060 of the quartz generator used the permissible changes in ΔT_p should be lower than $0.7 \cdot 10^{-3}$ μs. For a double SEC system these requirements are relatively smaller, i.e. $\Delta T_p < 7 \cdot 10^{-3}$ μs.

The commercially available television quartz delay lines have a delay drift of $5 \cdot 10^{-3}$ μs over the temperature range +20°C to +50°C. In this range a 40 dB cancellation of stationary echoes should be expected only for a double SEC system (or one of higher order).

4. A schematic diagram and the performance principle of the device for the visualization of blood vessels with the SEC system

A prototype pulse Doppler UDP-30 flowmeter was used in developing a model device for blood flow visualization with cancellation of stationary echoes. In its schematic diagram two functionally independent parts can be distinguished. The first part is a modified pulse Doppler flowmeter which permits the

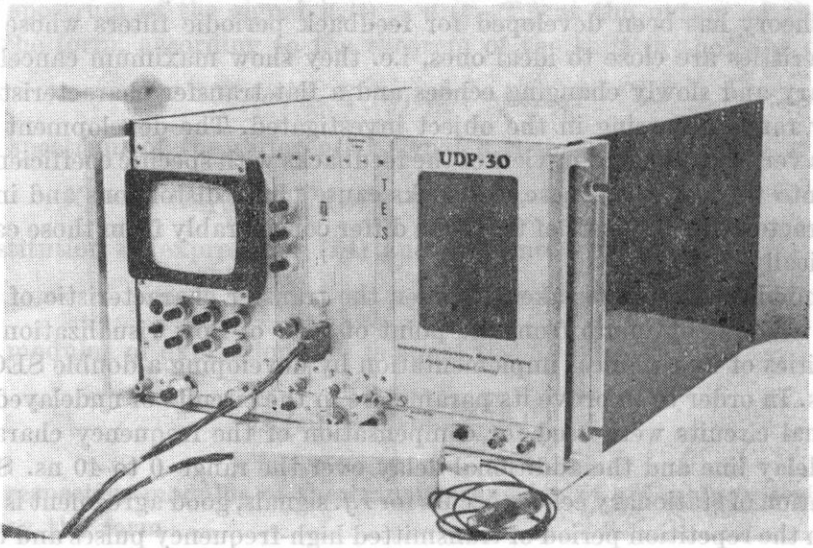

Fig. 9. A general view of an ultrasonic pulse Doppler UDP-30-TES flowmeter

measurement and registration of the instantaneous values of blood flow and of time averaged flow profiles. The second part is made of SEC systems and of phase detection of Doppler signals for the observation of blood flow dynamics in real time. The apparatus contains some common units: a high-frequency generator, a frequency divider, a power transmitter with a modulator, a limiter and a high-frequency preamplifier. A modification in these units with respect to a standard UDP-30 device consisted in replacing the generator *LC* with a quartz generator whose frequency f_n is equal to the integer multiple of the reciprocal of the delay T_p of the delay lines ($f_n = N/T_p$).

In the present device the frequency of the quartz generator $f_n = 4379060$ MHz, while in the frequency divider the division by $N = 280$ was used. The design of the high-frequency receiver was changed by introducing additionally into the existing time gain control (TGC) system a unit for gating off the preamplifier over a time of 3 μs following the transmission of the pulse. This cancels in the receiver the direct transmitted pulse and the pulses reflected in the focussing lens of the ultrasonic probe and from the surface of the skin.

The amplitudes of these signals usually exceed the linear characteristic range of the receiver. At the output of the delay line these signals undergo con-

siderable distortion both in amplitude and in phase and cause an increase in the level of third echoes in the delay line, thus decreasing the efficiency of the SEC system.

A double in-series stationary echo cancellation system was built using delay lines designed for colour TV sets. In the selection of lines attention was paid to their temperature stability, minimum cancellation of direct echoes (delay T_p) with the highest possible cancellation of third echoes (delay T_p) and of the other spurious echoes in the line [8].

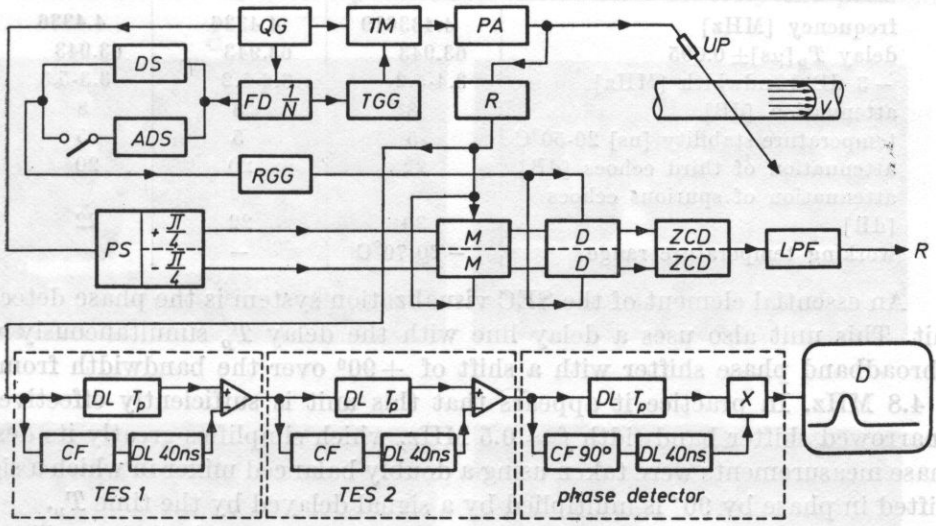

Fig. 10. A schematic diagram of the flow visualization device UDP-30-TES

QG – quartz generator, *FD* – frequency divider, *TGG* – transmitter gate generator, *TM* – transmitter modulator, *PA* – power amplifier, *UP* – ultrasonic probe, *R* – receiver, *DS* – receiver gate delaying system, *ADS* – automatic receiver gate delaying system, *PS* – phase shifter, *RGG* – receiver gate generator, *M* – mixer, *D* – detector, *ZCD* – zero-crossing detector, *LPF* – low-pass filter, *R* – register, *DL* – delay line, *CF* – correction filter, *X* – doubly balanced mixer, *D* – display

Among the delay lines now available on world market, similar parameters are characteristic of the lines manufactured by Telefunken, Andersen Laboratories Inc., Matsushita and Kinsekisha.

The delay lines from Anderson Laboratories Inc. used in the system are different from the others in their greater cancellation of third and spurious echoes, which influenced their choice.

As was mentioned above, the efficiency of the performance of the SEC system depends on the temperature stability of the delay T_p. In the delay lines it is better than 5 ns over the temperature range +20°C to +50°C; differences in delay of up to 20 ns occurred, however, among particular lines. In view of this, both in the circuit of direct signals in both cancellers and in the phase detector, additional units for precise correction of the total delay were used

over the range 0 to 40 ns. These systems used small-size delay lines with continuous delay adjustment. These lines compensate in addition for the differences in delay introduced by correction filters compensating the frequency response of quartz delay lines.

Table 2. Typical values of delay line parameters

Parameter	Andersen Lab. Inc. PDL 641E	Matsushita SFD-EN 645	Kinsekisha
frequency [MHz]	4.433619	4.4336	4.4336
delay T_p [μs] ± 0.005	63.943	63.943	63.943
− 3 dB bandwidth [MHz]	3.4-5.2	3.6-5.2	3.3-5.3
attenuation [dB]	8	8	8
temperature stability [ns] 20-50°C	5	5	5
attenuation of third echoes [dB]	22	20	20
attenuation of spurious echoes [dB]	30	22	22
working temperature range	− 20-70°C	—	—

An essential element of the SEC visualization system is the phase detection unit. This unit also uses a delay line with the delay T_p simultaneously with a broadband phase shifter with a shift of $+90^0$ over the bandwidth from 3.8 to 4.8 MHz. In practice it appears that this unit is sufficiently effective for a narrowed shifter bandwidth $f = 0.5$ MHz, which simplifies greatly its design. Phase measurements were taken using a doubly balanced mixer in which a signal shifted in phase by 90° is multiplied by a signal delayed by the time T_p.

The output of the phase detector is connected to an built-in oscilloscope which displays simultaneously dynamic flow profiles, the position of an analyzing gate and distance markers. The frequency response measured at the output of the phase detector is shown in Fig. 11.

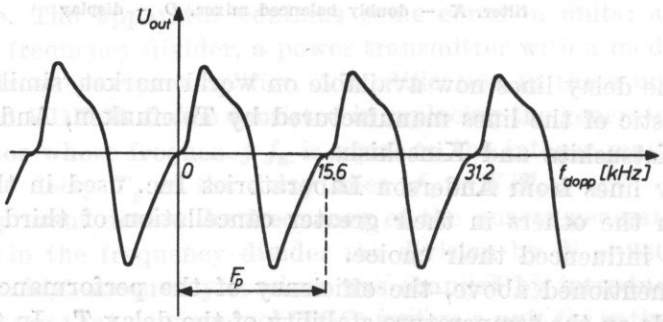

Fig. 11. The frequency response of the SEC visualization system developed by the present author

The system has a quasi-monotonous frequency-voltage characteristic over the range $-\frac{1}{4} F_p$ to $+\frac{1}{4} F_p$ (± 3.9 kHz), while outside this range the phase

of a signal varies with keeping the same sign of the Doppler frequency (discrimination of the flow direction) over the range $-\frac{1}{2} F_p$ to $+\frac{1}{2} F_p$, i.e. in the frequency range measured using a pulse Doppler flowmeter.

From this diagram it is possible to evaluate the degree of cancellation of stationary echoes (the frequency nF_p, where $n = 0, \pm 1, \pm 2, \ldots$) and of slowly moving objects whose velocity corresponds to Doppler frequencies < 300 Hz.

It is interesting to note the broadband character of the SEC system. In pulse Doppler flowmeters the maximum frequency measured cannot exceed half the repetition frequency F_p. This condition limits severely the possibility

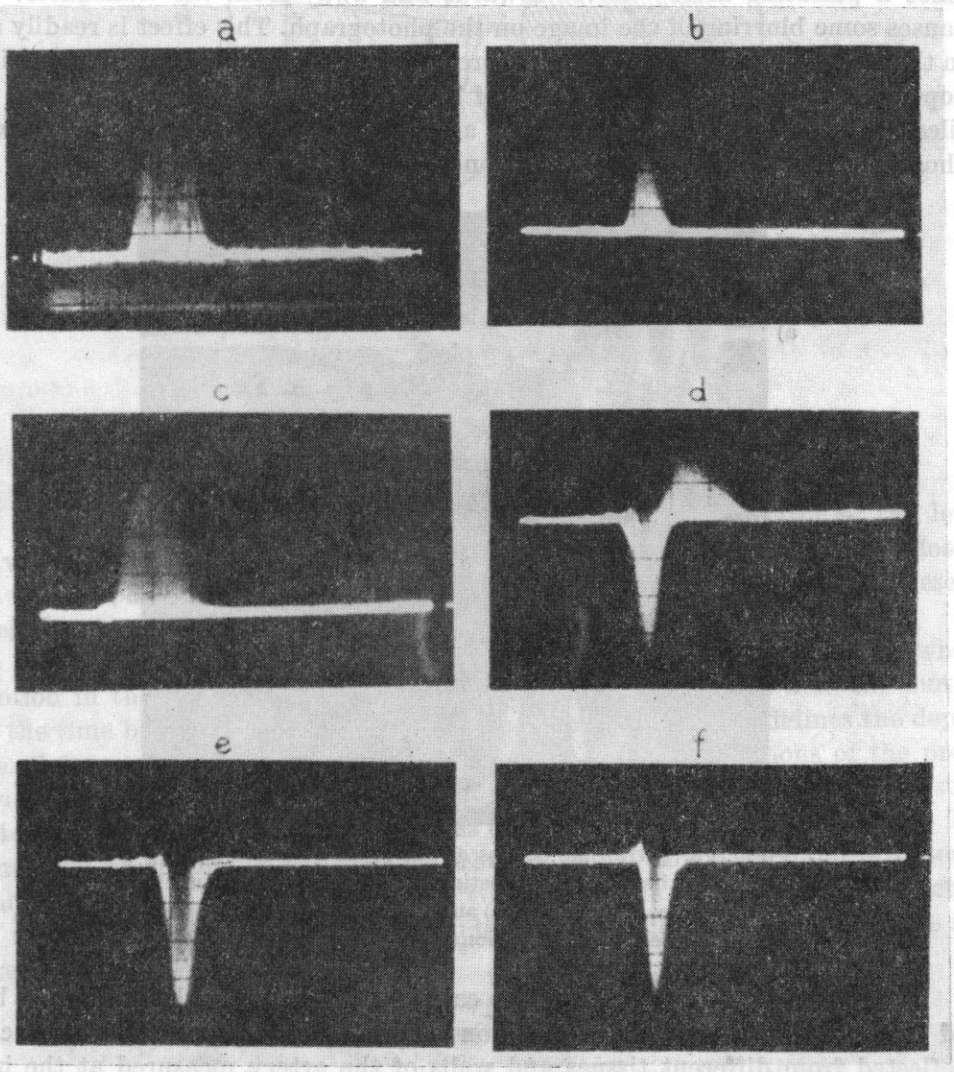

Fig. 12. Dynamic blood flow velocity profiles in common carotid artery (a), internal carotid artery (b), common femoral artery (c), simultaneously in jugular vein and carotid artery (d), subclavian vein (e) and femoral vein (f)

of evaluating the blood flow in a constriction of the carotid artery where, according to SPENCER *et al.* [15], the upper Doppler frequency may exceed 20 kHz. This restriction does not apply to the SEC visualization system whose characteristic covers a range of $\pm$ several dozens of kHz.

Fig. 12 shows photographs of typical signals corresponding to a dynamic representation of blood flow profiles on the oscilloscope tube display. The length of the time base on the oscilloscope screen corresponds to a depth of 5 cm in the body. In the case of arteries the base of the blood flow profiles displayed corresponding to the diameter of the vessel investigated is wider than in practice, since a pulsating artery moves towards and away from the transducer. This causes some blurring of the image on the photograph. This effect is readily seen in the course of observing blood flow profiles in real time, directly on the oscilloscope screen. A directional character of blood flow detection is evident: the profiles corresponding to blood flow in arteries have a positive direction, while those for flow in veins a negative one.

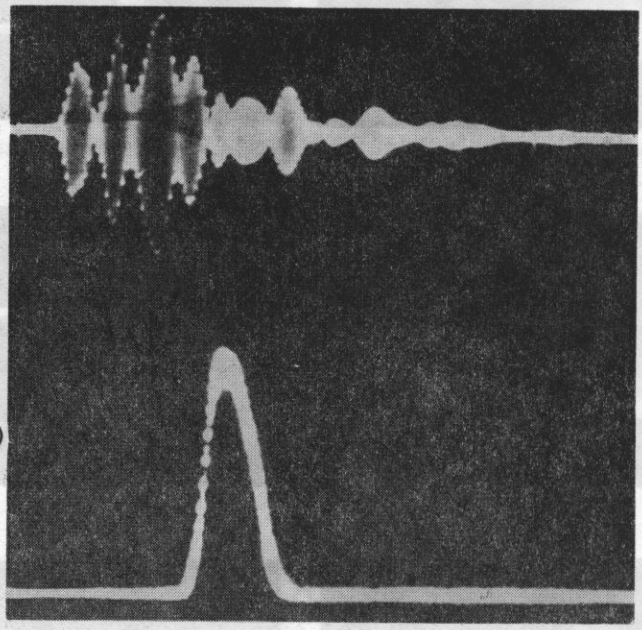

Fig. 13. Ultrasonic echoes at the input of the SEC system obtained in the investigation of blood flow in the common carotid artery (a) and a flow profile in this artery after cancellation of stationary echoes above 55 dB (b)

The efficiency of stationary echo cancellation can be evaluated on the basis of flow measurements in the common carotid artery. Fig. 13a shows echoes reflected from different tissues and walls of the artery measured at the input of the SEC system, while Fig. 13b shows a blood flow profile at the output of the phase detector after cancellation of stationary echoes in the SEC system.

The representation of blood flow profiles on the oscilloscope screen is essentially a modification of *A*-scanning where the coordinate x defines the depth and the coordinate y defines the blood flow velocity (in a typical *A*-scanning the coordinate y is proportional to the intensity of an ultrasonic signal reflected on the boundary of tissues with different acoustic impedance).

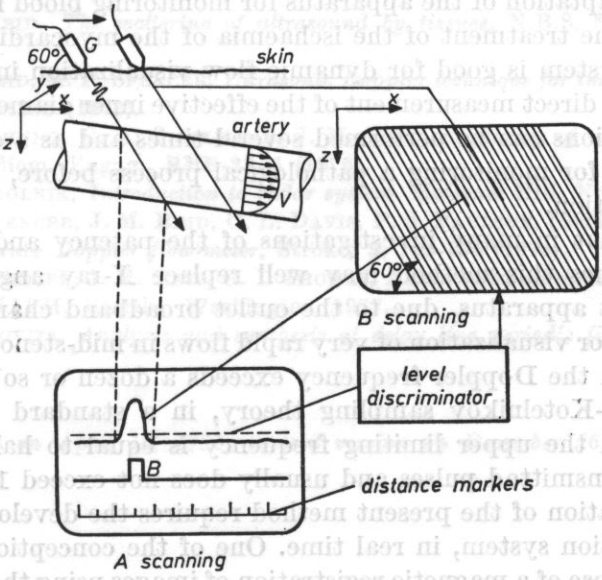

Fig. 14. The principle of the visualization of a vessel in the SEC system

A combination of a phase detection system, a discriminator of the level of velocity profiles and a system for spot brightness modulation on the oscilloscope tube display provides a system for visualization of blood vessels which resembles *B*-scanning (Fig. 14).

In this system the ultrasonic probe is mounted on a mobile arm whose motion in the x axis is transformed in the electronic system into the motion of the time base in the x direction. The coordinate z, in turn, defines the depth. Blood flow velocity profiles corresponding to successive positions of the probe over the vessel investigated are transformed in the level discriminator system into a signal modulating the brightness of spots on the oscilloscope screen. The time base on the screen is blackened when no blood flow occurs and brightened only by a signal corresponding to a velocity profile. The length of a section of the time base brightened corresponds to the diameter of a vessel at the site examined.

5. Conclusions

In view of limited material of clinical measurements, it is difficult to evaluate fully the SEC apparatus. It is now undergoing tests at the Clinic of Vascular Surgery CMKP, Warsaw (headed by Prof. Dr. Med. H. Rykowski) and at the

Department of Pathophysiology of Circulation System, Institute of Pediatrics, Academy of Medicine, Warsaw (headed by Prof. Dr. Med. A. CHROŚCICKI). The first results show that, apart from visualization of vessels, this method will be particularly useful in the evaluation of the dynamics of flows inside the heart in children's cardiology. A parallel direction of investigation concerns the adaptation of the apparatus for monitoring blood flows in vascular transplants in the treatment of the ischaemia of the myocardium.

The SEC system is good for dynamic flow visualization in real time, with the possibility of direct measurement of the effective inner diameter of the vessel. These investigations can be performed several times and as a consequence this method is good for monitoring a pathological process before, in the course of and after operation.

It seems that in many investigations of the patency and constriction of superficial arteries this method may well replace X-ray angiography.

The present apparatus, due to the outlet broadband characteristic of the system, is good for visualization of very rapid flows in mid-stenosis of the carotid artery for which the Doppler frequency exceeds a dozen or so kHz. According to the Shannon-Kotelnikov sampling theory, in a standard ultrasonic pulse Doppler method the upper limiting frequency is equal to half the repetition frequency of transmitted pulses and usually does not exceed 10 kHz.

A full aplication of the present method requires the development of a convenient registration system, in real time. One of the conceptions concerns the use for this purpose of a magnetic registration of images using the video recorder, a technique increasingly often used in the registration of images in echo-cardiotomography in real time.

References

[1] F. E. BARBER, D. W. BAKER, A. W. C. NATION, D. E. STRANDNESS, J. M. REID *Ultrasonic duplex echo-Doppler scanner*, IEEE Trans. On Biom. Engng., **BME 21**, 2 (1974).

[2] W. BUSCHMAN, *Ultrasonic imaging of arterial wall echoes*, Ultrasound in Med. and Biol., **1**, 33-43 (1975).

[3] L. FILIPCZYŃSKI, R. HERCZYŃSKI, A. NOWICKI, T. POWAŁOWSKI, *Blood flows: hemodynamics and ultrasonic Doppler measurement methods* (in Polish), PWN, Warszawa — Poznań 1980.

[4] L. FILIPCZYŃSKI, G. ŁYPACEWICZ, J. SAŁKOWSKI, T. WASZCZUK, *Automatic eye visualization and ultrasonic intensity determination in focused beams by means of electrodynamic and capacitance methods*, Proc. 2nd European Congress on Ultrasonic in Medicine, Munich 12-16 May, 1975; Excerpta Medica, Amsterdam 1975.

[5] L. FILIPCZYŃSKI, J. GRONIOWSKI, G. ŁYPACEWICZ, J. SAŁKOWSKI, T. WASZCZUK, *Design of UG-4 ultrasonograph and its application in obstetrics and gynaecology* (in Polish), Probl. Techn. Med., **6**, 231 (1975).

[6] A. NOWICKI, *Ultrasonic pulse Doppler method in blood flow measurement*, Archives of Acoustics, **2**, 4, 305-323 (1977).

[7] A. NOWICKI, *Simplified automatic measurements of blood flow by the ultrasonic pulse Doppler method*, Archives of Acoustics, **4**, 4, 359-366 (1979).

[8] A. NOWICKI, M. J. REID, *An infinite gate pulse Doppler*, Ultrasound in Med. and Biol., **7**, 41-50 (1981).

[9] P. A. PERONNEAU, F. LEGER, M. XHAARD, M. PELLET, P. V. SCHWARTZ, *Velocimetre sanguine a effect Doppler a emission ultrasonore pulse*, L'onde Electrique, **50**, 5, 369-389 (1970).

[10] J. M. REID, *The scattering of ultrasound by tissues*, N.B.S. Special Publ., **453**, 29-47 (1976).

[11] J. M. REID, M. P. SPENCER, *Ultrasonic Doppler technique for imaging blood vessels*, Science, **176**, 1235-1236 (1972).

[12] K. K. SHUNG, R. A. SIGELMANN, J. M. REID, *Scattering of ultrasound by blood*, IEEE Trans. on Biom. Engng., **BME-23**, 6 (1976).

[13] M. I. SKOLNIK, *Introduction to radar system*. McGraw Hill, New York 1962.

[14] M. P. SPENCER, J. M. REID, O. L. DAVIS, P. S. PAULSON, *Cervical carotid imaging with a continuous wave Doppler flow-meter*, Stroke, **5**, 145-154 (1974).

[15] M. P. SPENCER, J. M. REID, G. I. THOMAS, *Noninvasive cerebrovascular evaluation*, Special Publ. of IAPM, Seattle, Washington 1977.

[16] H. URKOVITZ, *Analysis and synthesis of delay line periodic filters*, IRE Trans., **CT-4**, 41-53 (1957).

Received on April 16, 1981; revised version on December 16, 1981.

ARCHIVES OF ACOUSTICS
7, 3-4, 247-252 (1982)

APPLICATION OF THE STATIONARY ECHO CANCELLATION TECHNIQUE (SEC) IN ULTRASONIC DOPPLER MEASUREMENTS OF BLOOD FLOW IN CHILDREN'S HEARTS

L. FILIPCZYŃSKI, A. NOWICKI

Department of Ultrasound, Institute of Fundamental Technological Research, Polish Academy of Sciences
(00-049 Warszawa, ul. Świętokrzyska 21)

A. CHROŚCICKI

Institute of Pediatrics, Academy of Medicine
(00-575 Warszawa, ul. Litewska 14/16)

The authors used an ultrasonic Doppler system based on the technique of the cancellation of stationary echoes (SEC) with an built-in conventional single-gate Doppler pulse flowmeter for recording blood flow rates in large vessels and cavities in children's hearts. The SEC technique facilitates considerably noninvasive investigation and identification of blood flow, as it permits the visualization of the blood velocity distribution over the whole depth of structures penetrated by an ultrasonic beam. The present system also permits records of blood velocities at chosen depths to be obtained. Examples of the visualization and records of blood velocities in large vessels and cavities of the heart are given.

The technique of the cancellation of stationary echoes (SEC), which was first developed in the radar, has recently been introduced into ultrasonic Doppler measurements of blood flow in peripheral vessels [1]. This technique is based on the subtraction of two successive pulses received, one of which is delayed with respect to the other by a time interval equal exactly to the repetition period of pulses transmitted. Stationary signals from the stationary boundaries of tissues can thus be eliminated, leaving only signals from moving structures, e.g. blood particles, which undergo further electronic processing and are represented on the oscilloscope screen. The spatial and temporal blood velocity distribution is thus given on the oscilloscope screen. A detailed description of the apparatus was given in paper [3] of NOWICKI and REID.

Fig. 1 shows the principle of the application of the SEC technique in the ultrasonic Doppler method. The UDP-30-SEC system, based on this technique, has an working frequency of 4.37 MHz, a repetition frequency of 15.6 kHz, a maximum range of 5 cm, while the maximum measured velocity is 260 m/s at a 60° angle of the inclination of the probe with respect to the flowing blood [2].

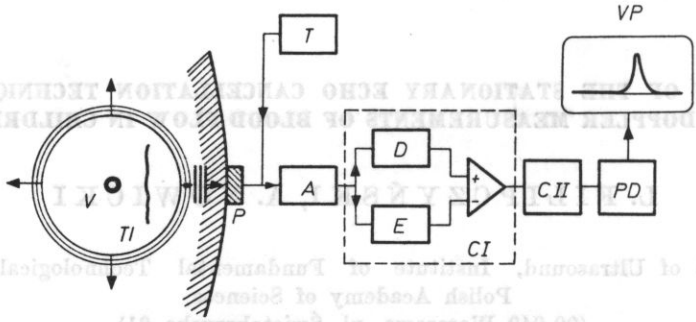

Fig. 1. The principle of the technique of the cancellation of stationary echoes (SEC)

T – transmitter, *P* – piezoelectric transducer, *TI* – the boundary of tissues at which stationary echoes occur, *V* – blood vessel, *CI* and *CII* – first and second canceller of stationary echoes, *D* – delay line, *E* – equilizer, *PD* – phase detector, *VP* – blood velocity in the vessel *V* represented on the oscilloscope screen, *A* – amplifier

Fig. 2 shows the results of an investigation by the SEC technique of two vessels in the area of the right collar-bone. At a depth of 8 to 12 mm it is possible

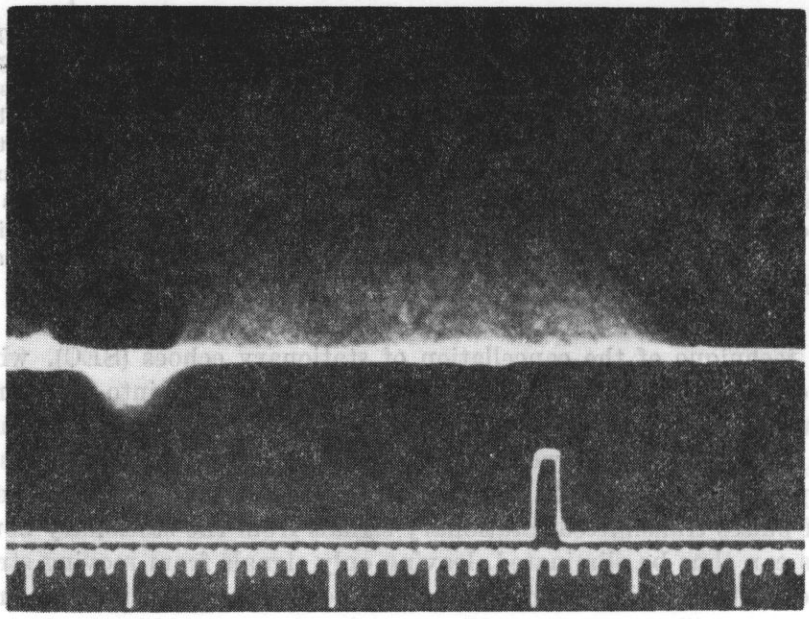

Fig. 2. The visualization by the SEC technique of blood velocities in two vessels; negative displacement – blood velocity in a jugular vein, positive displacement – blood velocity in the aorta

to see a negative velocity in the jugular vein, corresponding to the outflow of blood towards the right atrium of the heart. At a depth of 12 to 36 mm, in turn, it is possible to see a broad positive velocity corresponding to the inflow of blood in the aorta towards the probe. The depth at which the blood flow occurs can be evaluated easily using the millimetre and centimetre depth scale shown in the figure.

The flow in the aorta is strongly pulsating, which can be seen on the oscilloscope screen but which it is more difficult to show on photography in view of the exposure time of 1s.

The SEC technique seems to be very promising for applications in cardiology where the spatial and temporal blood velocity distributions are very complex. In view of this, the present authors have decided to use this technique in the children's cardiology where the penetration range is of the order of several cm. The present paper reports on the results of preliminary investigations in this field.

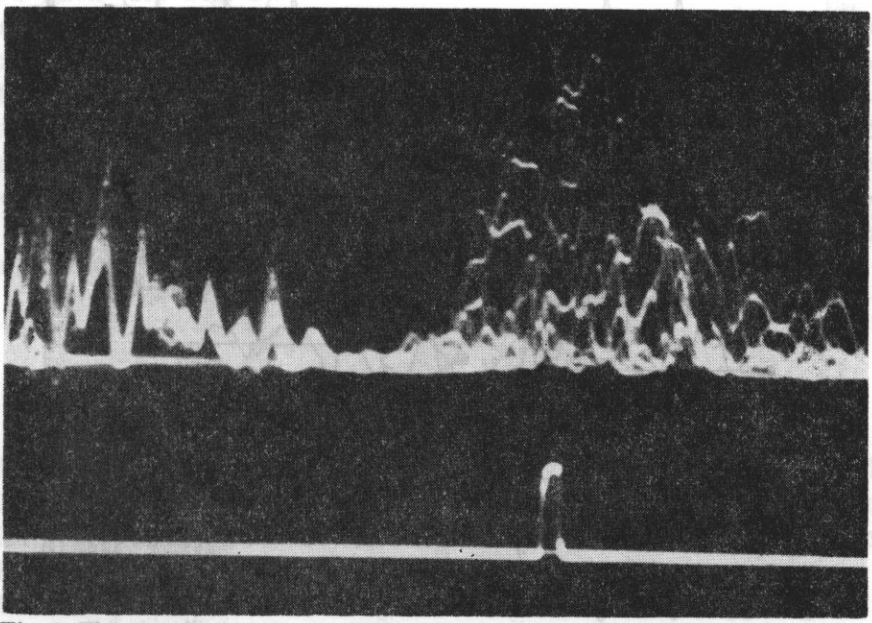

Fig. 3. The visualization by the SEC technique of blood velocity in the course of the outflow tract from the left ventricle
left the echoes from the moving structures of the heart, right – the instantaneous blood velocity distributions

Fig. 3 shows an example of the use of the SEC technique, giving the result of measurement in the course of the outflow of blood from the left ventricle of the heart. The photograph was taken with an exposure time of 0.5 ms. The slowly variable displacements farthest to the left correspond to the motion of the front wall of the left ventricle, while the displacements farthest to the right of the

oscillogram represent the instantaneous blood velocity distributions. The displacements on the left and the right of Fig. 3 differ completely in character. In the blood flow displacements it is possible to distinguish a number of successive blood velocity distribution profiles where the time interval between them is equal to a repetition period of pulses of 0.064 ms (about 8 profiles).

In view of the frequency response of the period filter and the properties of the phase detection used, the output signal depends not only on the blood velocity but also on the amplitude of the signal scattered on blood particles (see [3], formulae (8) and (12)).

For this reason, however, the SEC technique is not suitable directly for blood velocity measurements, although it may serve for the observation of the flow. Accordingly, apart from the SEC technique, a system of signals which is typical of the pulse Doppler flowmeter with one analyzing gate was used in

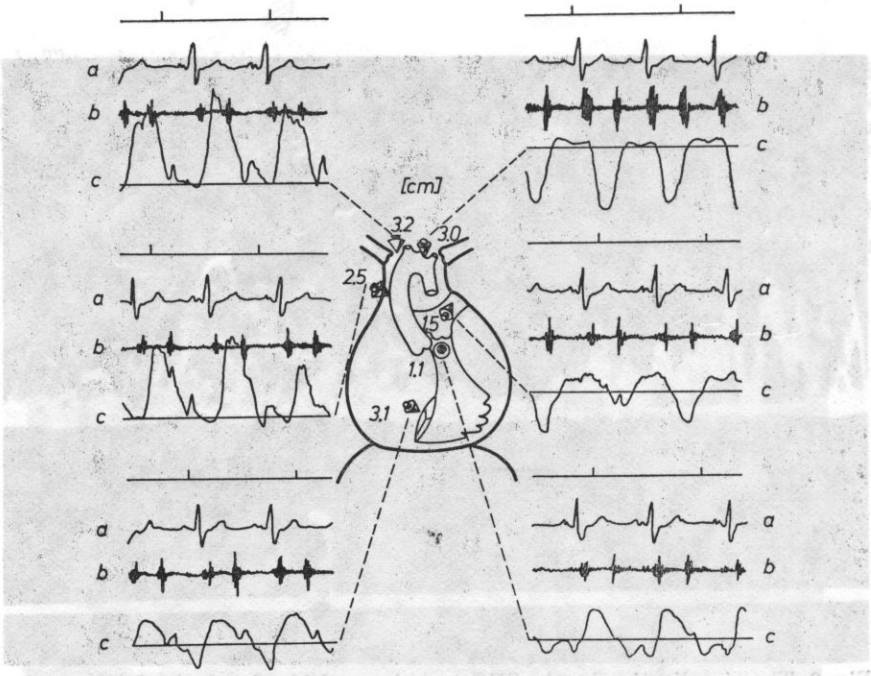

Fig. 4. The records of time markers, ECG (*a*), FONO (*b*) and of Doppler blood velocities (*c*) made at 6 points at different depth by the UDP-30-SEC apparatus

threedimensional arrows mark the place and direction of the application of the ultrasonic probe; numbers, in cm, alongside give the depth at which blood velocities have been recorded

the UDP-30-SEC apparatus in the investigations. This system uses the procedure of signal processing of the zero-crossing counter and of the determination of the direction of blood flow. This permits the measurement of the recording of the blood velocity at chosen depth by means of an analyzing gate shown in Figs. 2 and 3.

Fig. 4 shows as an example the application of the present technique on a 4-year-old child with cardiomyopathy. The recording was made noninvasively at 6 different points. Threedimensional arrows mark the place and direction of the application of the ultrasonic probe; numbers alongside give the depth at which the recording was made. Apart from a schematic diagram of the structures of the heart, the records obtained are given. The topmost line in all the 6 records is time markers of 1 s, the second line is an ECG record, the third line a phonocardiographic record from the area of the pulmonary artery, the fourth line a Doppler record of blood velocity.

In the range of venous and arterial vessels the UDP-30-SEC measuring apparatus permits the visualization and determination of the velocity and direction of blood flow and the determination of the diameter of a vessel and the depth at which it occurs. This facilitates considerably the identification of individual flows and the elimination of the motion of the anatomical structures of the heart which disturb the measurement of blood flow, giving an image different from the flow itself (see Fig. 3).

In the area of the Erb point where the anatomical relationships and the motion of the heart are very complex, velocities in the course of Doppler measurements are often obtained in a direction different from the expected one. The present authors think that this may be caused by transverse motion of flowing blood resulting from the rhythmical displacement of the heart which echocardiographic investigations show. At this stage it is also difficult to exclude the possibility of an inaccurate angular position of the ultrasonic probe with respect to the stream of flowing blood.

Conclusions

The SEC technique facilitates considerably the investigations of blood flows in the heart, permitting the identification of blood flows as a result of the visualization of the blood velocity distribution over the whole depth of structures investigated.

The combination of this technique with a conventional Doppler pulse flowmeter permitted the taking and recording of blood velocity measurements at chosen depths in large vessels and in the cavities of the hearts.

The first records of the blood flow rate obtained in children's hearts agree with previous observations made using other methods, but standards based on more examined patients must still be made.

The visualization of blood flows in blood vessels and in the heart by means of the SEC technique permits rapid and direct control of hemodynamic disorders. This may have great practical value, irrespective of the subsequent registration of blood velocity.

References

[1] A. NOWICKI, J. REID, *An infinite gate pulse Doppler*, Proc. 23-rd AIUM Meeting, San Diego 1978, p. 1719; Ultrasound in Medicine and Biology, 7, 1, 41-50 (1981).

[2] A. NOWICKI, *Ultrasonic methods of the visualization of blood vessels and flows* (in Polish), Institute of Fundamental Technological Research, Polish Academy of Sciences, 65/1979, Warsaw 1979.

[3] A. NOWICKI, J. REID, *Ultrasonic visualization of blood vessels and flows*, Archives of Acoustics, 7, 3-4, 55-75 (1982).

Received on August 25, 1980; revised version on December 16, 1981.

ARCHIVES OF ACOUSTICS
1, 3-4, 253-270 (1982)

DETECTABILITY OF BLOOD VESSELS BY MEANS OF THE ULTRASONIC ECHO METHOD USING A FOCUSED ULTRASONIC BEAM

LESZEK FILIPCZYŃSKI

Department of Ultrasound, Institute of Fundamental Technological Research, Polish Academy of Sciences
(00-049 Warszawa, ul. Świętokrzyska 21)

The detectability of a small, hypothetical cylinder-shaped blood vessel with a diameter of 0.1 mm has been considered analytically using the ultrasonic echo method. Soft tissues surrounding the vessel have been taken as homogeneous and not causing reflections of ultrasonic waves. They have been ascribed both with bulk and shear elasticity. A beam of longitudinal ultrasonic waves incident on the vessel has been taken in the form of a focused beam at the focus of which the blood vessel has been placed. It has been assumed that the reflection of ultrasonic waves from the blood vessel is caused by the difference between the velocity of waves in the tissue surrounding the vessel and that in blood.

Assuming a frequency of ultrasonic waves of 2.6 MHz, a diameter of the transmit-receive piezoelectric transducer of 2 cm, a focal length of this transducer of 10 or 8 cm, voltage of the transmitter of 250 V and sensitivity of the receiver of 10^{-5}V, the conditions of detectability have been determined.

It has been shown that the signal of an echo from the blood vessel assumed is potentially detectable. Its magnitude depends critically on the distance between the vessel and the surface of the body, resulting from the attenuation of waves in tissues penetrated.

1. Introduction

In an earlier paper [3], devoted to the detectability of blood vessels, the present author assumed that the ultrasonic beam incident on the blood vessel is parallel. The present considerations deal with a focused ultrasonic beam which is used in most modern diagnostic apparatus.

Another change in the assumptions made for the present problem is the taking of a more exact and more complex model of soft tissue in which ultrasonic waves propagate. The present author assumes that this tissue exhibits not only bulk elasticity but also shear elasticity. In the previous work [3] only the bulk elasticity of tissue was assumed.

The problem of parameters characterizing the shear elasticity of soft tissues, however, remains. One of the sources of information on this subject is the paper of FRIZELL and others [6], who measured the characteristic impedance of these tissues for transverse waves and determined on this basis the order of the velocity and absorption of transverse waves in tissues of this type. The present author used these data in obtaining the quantitative results of the analytical expressions derived.

Notation

$\boldsymbol{A}, A_z$ — vector potential of displacement
A_l — attenuation loss
a — radius of blood vessel
a_p — radius of piezoelectric transducer
B_m — constant
b — wave number for blood, dipole moment
c — velocity of longitudinal wave in tissue
c_t — velocity of transverse wave in tissue
c_b — velocity of longitudinal wave in blood
C_m, C_m^* — constants
D_m, D_m^* — constants
f — focal length
$H_m^{(2)}$ — Hankel function of second kind
h — wave number of transverse wave in tissue
J_m — Bessel function
j — $\sqrt{-1}$
k — wave number of longitudinal wave in tissue
M — mass
m — natural number
N_m — Neuman function
N_r — power of wave incident on transducer
N_t — power of wave radiated by transducer
Q_0 — volume velocity of source
p — acoustic pressure
R — reflection loss
r — distance from transducer, coordinate of polar system
S — area
s — current radius on transducer surface
T — transducing loss
t — time
$\boldsymbol{u}, u_r$ — displacement vector, its radial component
u_0, u_1, U_0, U_1 — vibration velocity of sources (instantaneous values and amplitudes)
$\boldsymbol{v}, v_r$ — vector of acoustic velocity, its radial component
w — vibration velocity of transducer surface
x — argument of cylindrical functions
Y — axis of blood vessel
y — coordinate on Y axis
Z_m — cylindrical function

$a_m(J)$, $a_m(H)$ — auxiliary constants
β_m — auxiliary constant
γ_m — auxiliary constant
$\delta_m(J)$, $\delta_m(H)$ — auxiliary constants
ε — radius tending to zero
η — displacement potential in blood
θ — azimuth
Λ — wavelength in tissue
λ — Lame constant in tissue
λ_b — Lame constant in blood
μ — Lame constant in tissue
ϱ — density of tissue
ϱ_b — density of blood
σ_{rr} — normal stresses
Φ — displacement potential in tissue
φ — velocity potential in tissue
ψ — angle
ω — angular velocity

2. Assumptions of analysis

It can be assumed that a cylinder-shaped vessel with the radius $a = 0.1$ mm is placed in the focus of an ultrasonic beam generated by a bowl-shaped focusing piezoelectric transducer (Fig. 1). The diameter of the transducer is $2a_p = 2$ cm

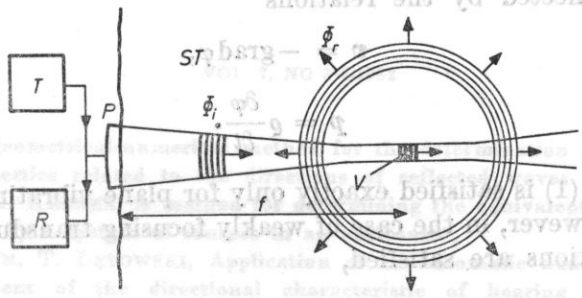

Fig. 1. A scattered reflection of ultrasonic waves from a small blood vessel
T — transmitter, R — receiver, P — ultrasonic probe with piezoelectric transducer, v — small blood vessel, Φ_i — incident wave, Φ_r — reflected wave, ST — soft tissue, f — focal length of the transducer

and its focal length is $f = 10$ cm. An ultrasonic wave of a frequency of 2.6 MHz (wavelength $\Lambda = 0.63$ mm) is incident on the blood vessel, perpendicularly to its axis. The soft tissue surrounding the vessel and the walls of the vessel are assumed to be homogeneous and to have the same characteristic acoustic impedance. In this case it can be assumed that the reflection of the ultrasonic wave from the blood vessel is caused only by a difference between the velocity of the wave in the tissue surrounding the vessel and that in blood. The densities of the tissue

and blood are assumed to be the same. The velocity of longitudinal ultrasonic waves in muscle tissue is assumed to be $c = 1.63$ km/s (uterus muscle), while that in blood is taken as $c_b = 1.57$ km/s [7].

The velocity of transverse waves in muscle tissue is known only in terms of the order of magnitude. FRIZELL and others [6] determined the velocity range of these waves to be 9-100 m/s; it is then possible to assume for calculations the velocity of transverse waves $c_t = 65$ m/s which falls within the range mentioned above.

This problem will be analyzed for steady state, as in the previous paper [3].

3. Ultrasonic field radiated by the transducer

The velocity potential of waves radiated by a plane transducer vibrating with the velocity w can be determined from the integral expression given by RAYLEIGH [10]

$$\varphi = -\frac{1}{2\pi}\int_S w\frac{\exp(-jkr)}{r}dS, \tag{1}$$

where S is the vibrating area, $k = 2\pi/\Lambda$ and r is the distance from the transducer. Expression (1) can be regarded as a quantitative representation of the Huygens principle. The acoustic velocity v, the velocity potential φ and the acoustic pressure ϱ are connected by the relations

$$v = -\operatorname{grad}\varphi, \tag{2}$$

$$p = \varrho\frac{\partial\varphi}{\partial t}. \tag{3}$$

Expression (1) is satisfied exactly only for plane vibrating surfaces; it can also be used, however, in the case of weakly focusing transducers [9] when the following conditions are satisfied,

$$a_p \ll f, \tag{4}$$

$$a_p \gg \Lambda, \tag{5}$$

where a_p is the radius of the transducer and f is its focal length.

From expressions (1) and (3) it is possible to determine the acoustic pressure at a point of the field P (Fig. 2) lying on the Y axis of the blood vessel. Let us consider the surface vibrating element dS at the point Q on the surface of the piezoelectric transducer. The distance $r = QP$ can be expressed in the following way ($s \ll f$),

$$r = f\left(1+\frac{y^2-2sy\cos\psi}{f^2}\right)^{1/2} \approx f\left(1+\frac{y^2-2sy\cos\psi}{2f^2}\right), \tag{6}$$

where $y = GP$, s is the distance between the point Q and the X axis and ψ is the angle between the Y axis and the plane 0' QG. The error resulting from simplification (6) is equal to [5]

$$\Delta r = \frac{1}{8f^3}(y^2 - 2sy\cos\psi)^2 \tag{7}$$

and in the worst case (for $s = a_p$ and $\cos\psi = -1$) it is smaller by a factor of about 60 than the wavelength. The distance r in the denominator of expression (1)

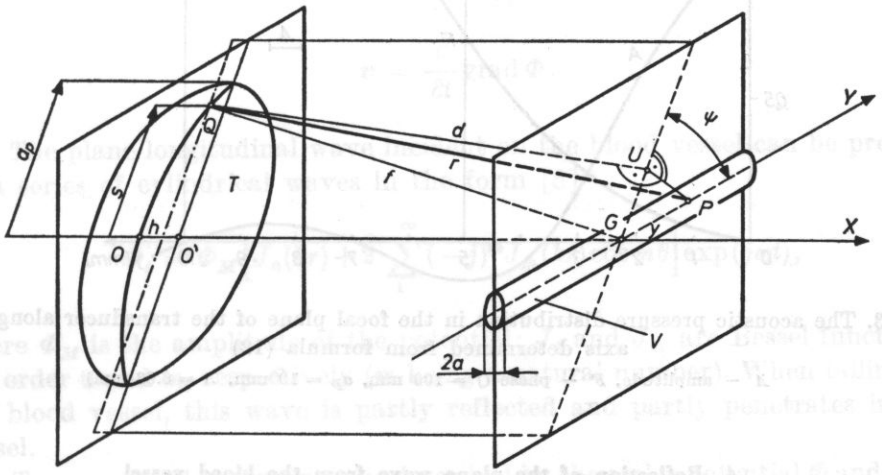

Fig. 2. The coordinate system used in the analysis
T – piezoelectric transducer, V – blood vessel, P – a point of the field under consideration, G – focus

can be replaced with f. This causes only a slight change in the amplitude of elementary waves reaching the point P under consideration from the surface of the transducer. Consideration of expressions (1), (3) and (6) gives the value of acoustic pressure

$$p = \frac{jk\varrho cw}{2\pi f}\exp\left\{j\left[\omega t - kf\left(1+\frac{y^2}{2f^2}\right)\right]\right\}\int_0^{a_p}\int_0^{2\pi}\exp\left(\frac{j\,ksy\cos\psi}{f}\right)d\psi s\,ds. \tag{8}$$

Application of the known properties of Bessel functions

$$J_0(x) = \frac{1}{\pi}\int_0^{\pi}\exp(jx\cos\psi)\,d\psi, \tag{9}$$

$$\int xJ_0(x)/dx = xJ_1(x), \tag{10}$$

$$J_1(0) = 0, \tag{11}$$

yields, from expression (8), the following acoustic pressure distribution in the focal plane of the transducer, along the Y axis,

$$p = \frac{jk\varrho cwa_p^2}{2f} \exp\left\{j\left[\omega t - kf\left(1+\frac{y^2}{2f^2}\right)\right]\right\} \frac{2J_1(ka_p y/f)}{ka_p y/f}. \tag{12}$$

This distribution is shown in Fig. 3 for the system assumed here.

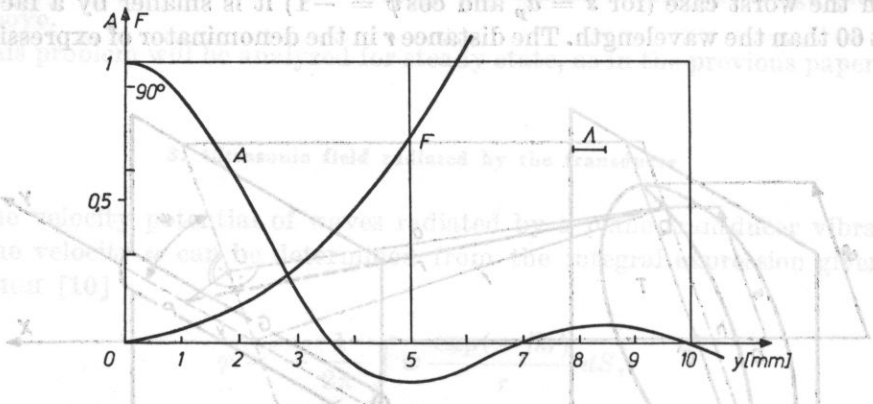

Fig. 3. The acoustic pressure distribution in the focal plane of the transducer along the Y axis determined from formula (12)

A – amplitude, F – phase ($f = 100$ mm, $a_p = 10$ mm, $\Lambda = 0.63$ mm)

4. Reflection of the plane wave from the blood vessel

In the vertical plane perpendicular to the Y axis (Fig. 2), in the vicinity of the vessel, the field radiated by the transducer can be considered plane locally, in view of the geometry of the problem ($f \gg a_p \gg \Lambda$). The case is different in the horizontal plane $0'GP$. The ultrasonic wavelength is, however, shorter by one order of magnitude than the width of the ultrasonic beam in the plane of the focus (Fig. 3). In view of this, it can be assumed with some approximation that the reflection of an ultrasonic wave in each cross-section of the vessel will be independent of the adjacent cross-sections. As a consequence, the partial contributions, obtained independently for the reflection of the wave in each plane section of the vessel, can be gathered, giving the solution of the problem of reflection which takes into account the distribution of the wave incident along the Y axis.

Analysis can be carried out in a plane system of polar coordinates where r is the radius and θ is the azimuth. The axis of the coordinate system is coaxial with the axis of the blood vessel. The present analysis will consider both the bulk and shear clasticity of the soft tissue in which the wave radiated by the transducer propagates. In view of this, it is more covenient to replace the velocity potential (employed in acoustics) with scalar and vector displacement po-

tentials (used in elasticity theory). Thus Φ denotes here the scalar potential of the displacement vector $\boldsymbol{u}$, $\boldsymbol{A}$ the vector potential of the displacement vector. The following relation then occurs,

$$\boldsymbol{u} = \operatorname{grad}\Phi + \operatorname{rot}\boldsymbol{A}. \tag{13}$$

It should be noted that in the case of the scalar displacement potential, relations (2) and (3) take other form, i.e.

$$p = -\varrho\frac{\partial^2\Phi}{\partial t^2}, \tag{13a}$$

$$\boldsymbol{v} = \frac{\partial}{\partial t}\operatorname{grad}\Phi. \tag{13b}$$

The plane longitudinal wave incident on the blood vessel can be presented as a series of cylindrical waves in the form [8]

$$\Phi_i = \Phi_M\left[J_0(kr) + 2\sum_1^\infty(-j)^m J_m(kr)\cos m\theta\right]\exp(j\omega t), \tag{14}$$

where Φ_M is the amplitude of the potential; J_0 and J_m are Bessel functions of the order 0 and m, respectively (m being a natural number). When falling onto the blood vessel, this wave is partly reflected and partly penetrates into the vessel.

Two waves, a longitudinal one described by the scalar potential Φ and a transverse one described by the vector potential $\boldsymbol{A}$, reflect from the vessel. The transverse reflected wave will have two components of the displacement vector, u_r and u_θ, and therefore, according to (13), only one component of the vector potential A_z different from zero will occur. The two reflected waves can be represented in the form of a series of cylindrical waves, i.e.

$$\Phi_r = \sum_0^\infty D_m H_m^{(2)}(kr)\cos(m\theta)\exp(j\omega t), \tag{15}$$

$$A_z = \sum_0^\infty C_m H_m^{(2)}(hr)\sin(m\theta)\exp(j\omega t), \tag{16}$$

where $h = \omega/c_t$ is the wave number for the transverse wave and $H_m^{(2)}$ is a Hankel function of the 2nd kind.

The function cos θ occurs in formula (15), since the longitudinal reflected wave is symmetrical with respect to the incidence direction of the wave ($\theta = 180^\circ$), whereas sin θ occurs in formula (16), since the transverse wave is antisymmetrical. This results from the geometry of the problem.

Only the longitudinal wave penetrates into the blood vessel. This wave

can be assumed in the form

$$\eta = \sum_{0}^{\infty} B_m J_m(br)\cos(m\theta)\exp(j\omega t), \tag{17}$$

where η is the scalar displacement potential; $b = \omega/c_b$, c_b is the velocity of the wave in blood.

The constants D_m, C_m and B_m in relations (15)-(17) can be determined from three boundary conditions which must be satisfied on the boundary of the vessel $r = a$.

The first condition is the equality of the normal stresses σ_{rr} in tissue and the acoustic pressure p in blood on the boundary of the vessel. It takes the form

$$\sigma_{rr} = \lambda \operatorname{div} \boldsymbol{u} + 2\mu \frac{\partial u_r}{\partial r} = -p, \tag{18}$$

where λ and μ are Lame constants.

The minus sign on the right side of condition (18) results from the fact that in mechanics tensile stresses are regarded as positive, while in acoustics the corresponding pressures are considered to be negative.

Consideration of (13) in (18); of the formulae

$$\operatorname{div}\operatorname{rot} = 0, \tag{19a}$$

$$\operatorname{div}\operatorname{grad} = \nabla^2; \tag{19b}$$

of the wave equations which are satisfied by the displacement potentials

$$\nabla^2\Phi + k^2\Phi = 0, \tag{20a}$$

$$\nabla^2 A_z + h^2 A_z = 0, \tag{20b}$$

$$\nabla^2\eta + b^2\eta = 0, \tag{20c}$$

where

$$k = \frac{\omega}{c} = \sqrt{\frac{\varrho\omega^2}{\lambda + 2\mu}}, \tag{21a}$$

$$h = \frac{\omega}{c_t} = \sqrt{\frac{\varrho\omega^2}{\mu}}, \tag{21b}$$

$$b = \frac{\omega}{c_b} = \sqrt{\frac{\varrho_b\omega^2}{\lambda_b}}, \tag{21c}$$

(ϱ_b being the density of blood, λ_b a Lame constant in blood), and also of the relation between the sound pressure p and the displacement potential

$$p = -\varrho\frac{\partial^2\eta}{\partial t^2}, \tag{22}$$

gives the boundary c ndition (18) for $r = a$, in the form

$$\Phi\left(\frac{2k^2}{h^2}-1\right)+\frac{2}{h^2}\Phi''+\frac{2}{h^2}\left(\frac{1}{r}A_\theta\right)' = -\frac{\varrho_b}{\varrho}\eta. \tag{23}$$

In order to simplify notation the index z was dropped in the component of the vector potential A_z. The dash in the potentials denotes differentiation with respect to r, while the index θ denotes differentiation with respect to θ.

The second boundary condition involves the disappearance of the tangential stresses on the boundary of the vessel ($r = a$). This condition has the form [2]

$$\frac{2}{r}\Phi_\theta-\frac{2}{r^2}\Phi_\theta-A''+\frac{1}{r}A'+\frac{1}{r^2}A_{\theta\theta} = 0. \tag{24}$$

The third boundary condition requires the equality of the normal displacements on the boundary of the vessel ($r = a$). Consideration of (13) gives

$$\Phi'+\frac{1}{r}A_\theta = \eta'. \tag{25}$$

Insertion into the above conditions of the sum $\Phi = \Phi_i+\Phi_r$ whose components are expressed by expressions (14) and (15) and supstitution of potentials (16) and (17) give the possibility of determining the constants D_m and C_m of interest here which describe the waves reflected from the blood vessel. In view of the orthogonality of the sine and cosine functions, these constants can be determined independently, successively for each m [8]. In calculating the derivatives of cylindrical functions it is possible to use the formulae

$$\frac{dZ_m(kr)}{dr} = k\left[\frac{m}{kr}Z_m(kr)-Z_{m+1}(kr)\right], \tag{26}$$

$$\frac{d^2Z_m(kr)}{dr^2} = k^2\left\{\left[\frac{m(m-1)}{(kr)^2}-1\right]Z_m(kr)+\frac{1}{kr}Z_{m+1}(kr)\right\}. \tag{27}$$

Thus, for $m = 0$

$$D_0 = \frac{\frac{2}{h^2}J_0''(kr)J_0'(br)-\left(\frac{2k^2}{h^2}-1\right)J_0(kr)J_0'(br)-\frac{\varrho_b}{\varrho}J_0'(kr)J_0(br)}{H_0^{(2)}(kr)\left(\frac{2k^2}{h^2}-1\right)J_0'(br)+\frac{2}{h^2}H_0^{(2)''}(kr)J_0'(br)+\frac{\varrho_b}{\varrho}H_0^{(2)'}(kr)J_0(br)}\Phi_M; \tag{28}$$

while the constant C_0 is equal to zero.

For $m \geqslant 1$, however, the following expression can be obtained,

$$D_m = \frac{-\alpha_m(J)\beta_m-\gamma_m\delta_m(J)}{\alpha_m(H)\beta_m+\gamma_m\delta_m(H)}\Phi_m, \tag{29}$$

where

$$a_m(J) = \frac{2m}{r}\left[J'_m(kr) - \frac{1}{r}J_m(kr)\right], \tag{30a}$$

$$a_m(H) = \frac{2m}{r}\left[H^{(2)\prime}_m(kr) - \frac{1}{r}H^{(2)}_m(kr)\right], \tag{30b}$$

$$\beta_m = \frac{2m}{h^2}\left[\frac{H^{(2)}_m(hr)}{r}\right]' + \frac{m}{r}\frac{\varrho_b}{\varrho}J_m(br)\frac{H^{(2)}_m(hr)}{J'_m(br)}, \tag{30c}$$

$$\gamma_m = \left[\frac{1}{r}H^{(2)\prime}_m(hr) - H^{(2)\prime\prime}_m(hr) - \frac{m^2}{r^2}H^{(2)}_m(hr)\right], \tag{30d}$$

$$\delta_m(J) = \left(\frac{2k^2}{h^2} - 1\right)J_m(kr) + \frac{2}{h^2}J''_m(kr) + \frac{\varrho_b}{\varrho}J_m(br)\frac{J'_m(kr)}{J'_m(br)}, \tag{30e}$$

$$\delta_m(H) = \left(\frac{2k^2}{h^2} - 1\right)H^{(2)}_m(kr) + \frac{2}{h^2}H^{(2)\prime\prime}_m(kr) + \frac{\varrho_b}{\varrho}J_m(br)\frac{H^{(2)\prime}_m(kr)}{J'_m(br)}, \tag{30f}$$

and $r = a$.

The constant C_m which occurs in expression (16) describing the transverse reflected waves can be determined from the second boundary condition (24). The following relation can then be obtained

$$C_m = \frac{\dfrac{2m}{r}J'_m(kr) - \dfrac{2m}{r^2}J_m(kr) - D_m\left[\dfrac{2m}{r^2}H^{(2)}_m(kr) - \dfrac{2m}{r}H^{(2)\prime}_m(kr)\right] - \dfrac{1}{\Phi_M}\Phi_M}{\dfrac{1}{r}H^{(2)\prime}_m(hr) - H^{(2)\prime\prime}_m(hr) - \dfrac{m^2}{r^2}H^{(2)}_m(hr)}, \tag{31}$$

$$r = a.$$

For the wave velocities in soft tissue and blood assumed above, the following wave numbers can be obtained: $k = 10\ \text{mm}^{-1}$, $h = 250\ \text{mm}^{-1}$ and $b = 10.4\ \text{mm}^{-1}$. When inserted into relations (30), (31) and (32), these wave numbers permit the determination of the constants D_m and C_m which are shown in Table I.

It follows therefore that the constants D_m, and accordingly the magnitudes of the longitudinal reflected waves, decrease rapidly with increasing the wave order m, whereas the constants C_m corresponding to the transverse waves show an oscillatory character, which is understandable in view of the large value of the argument $ha = 25$.

However, in view of very large attenuation, transverse waves exist only in the closest vicinity of the blood vessel. It follows from the measurements of FRIZELL and others [6] that the attenuation of these waves in soft tissues falls

within the range $(2\text{-}30)\cdot 10^3\ \mathrm{cm}^{-1}$. Accordingly, the further analysis aimed at the determination of the detectability of a blood vessel will consider only longitudinal waves and neglect the transverse waves which occur for the phenomenon of reflection. Moreover, only the first two orders of reflected waves ($m = 0.1$) will be considered. In view of the rapid decrease in the constants D_m with increasing m (see Table 1), the higher orders do not make a noteworthy contribution to the calculation of the amplitude of the longitudinal wave reflected from the blood vessel.

Table 1. The constants D_m^* and C_m^* determined from formulae (28), (29) and (31)

m	$D_m^* = D_m/\Phi_M$	$C_m^* = C_m/\Phi_M$
0	$0.0476e^{-j93°}$	0
1	$0.0068e^{-j90°}$	$0.0025e^{j43°}$
2	$0.0008e^{j176°}$	$0.0045e^{-j52°}$
3	$0.00002e^{j40°}$	$0.0023e^{+j52°}$

Insertion into formula (13a) of expression (15) and of the constants D_0 and D_1 gives the acoustic pressure of the wave reflected from the blood vessel in the form

$$p = \omega^2\varrho[D_0H_0^{(2)}(kr) + D_1H_1^{(2)}(kr)\cos\theta]\exp(j\omega t). \tag{32}$$

The acoustic velocity of the reflected wave can be determined in a similar way from expressions (13*b*) and (15),

$$v_r = j\omega\left\{-D_0kH_1^{(2)}(kr) + D_1\left[\frac{1}{r}H_1^{(2)}(kr) - kH_2^{(2)}(kr)\right]\cos\theta\right\}\exp(j\omega t). \tag{33}$$

4. Pulsating and oscillating equivalent sources of the wave reflected from the vessel

The wave reflected from the blood vessel can be substituted for by equivalent waves radiated by pulsating and oscillating sources placed on the Y axis of the vessel. Expression (32) shows that these sources will be pulsating (monopoles) and oscillating (dipoles). It can be assumed that these sources have the shape of a sphere with the radius ε tending to zero. These spheres vibrate so that points of their surfaces have the velocity

$$u_0 = U_0\exp(j\omega t), \tag{34a}$$

$$u_1 = U_1\cos\theta\exp(j\omega t), \tag{34b}$$

where U_0 and U_1 are the amplitudes of the velocities.

These velocities can be compared with the velocities defined by relation (33) for the small arguments $kr = k\varepsilon$. The Hankel functions which occur in this relation can be represented in the form

$$H_m^{(2)}(x) = J_m(x) - jN_m(x), \tag{35}$$

while for $x \to 0$ and $m > 0$,

$$J_m(x) \to 0, \tag{36a}$$

$$N_m(x) \to -\frac{(m-1)!}{\pi}\left(\frac{2}{x}\right)^m. \tag{36b}$$

It follows therefore that in the present case ($\varepsilon \to 0$)

$$H_1^{(2)}(k\varepsilon) = -\frac{2j}{\pi k\varepsilon}, \tag{37a}$$

$$H_2^{(2)}(k\varepsilon) = \frac{-4j}{\pi k^2\varepsilon^2}. \tag{37b}$$

Substitution of (37a) and (37b) into (33) and equating the sum (34a), (34b) to expression (33) give

$$U_0 + U_1\cos\theta = -\omega\frac{2D_0}{\pi\varepsilon} - \omega\frac{2D_1}{\pi k\varepsilon^2}\cos\theta. \tag{38}$$

Since this equation should be satisfied for all values of the angle θ,

$$U_0 = -\omega\frac{2D_0}{\pi\varepsilon}, \tag{39a}$$

$$U_1 = -\omega\frac{2D_1}{\pi k\varepsilon^2}. \tag{39b}$$

It is known [11], on the other hand, that a pulsating source radiates a sound pressure wave in the form

$$p_0 = \frac{j\omega\varrho Q_0}{4\pi r}\exp[j(\omega t - kr)], \tag{40}$$

where Q_0 is the amplitude of the volume velocity of the source when its dimensions tend to zero and r is the distance from the source.

It is now possible to form an equivalent cylindrical source (Fig. 4) of the same volume velocity Q_p, whose dimensions are very small compared to the wavelength. The change in the shape of the source from spherical to cylindrical shape has, in view of the relation $\Lambda \gg \varepsilon \to 0$, no significance. It is therefore possible to write (see Fig. 4)

$$dQ_0 = 2\pi\varepsilon U_0\, dy. \tag{41}$$

In turn, the acoustic pressure of the wave radiated by an oscillating source at a long distance from the source has the form [11]

$$p_1 = jk\frac{b}{r}\cos\theta\exp[j(\omega t - kr)], \tag{42}$$

where b denotes a dipole moment equal to

$$b = \frac{j\omega\varrho\varepsilon^3\exp(jk\varepsilon)}{(2-k^2\varepsilon^2)+j2k\varepsilon}U_1 \underset{\varepsilon\to 0}{=} j\frac{\omega\varrho\varepsilon^3}{2}U_1. \tag{43}$$

Introducing the mass of an oscillating sphere, $M = \varrho 4\pi\varepsilon^3/3$, it is possible to write

$$b = j\frac{3\omega M U_1}{8\pi}. \tag{44}$$

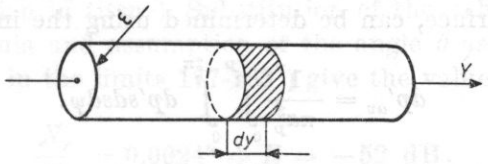

Fig. 4. An equivalent cylindrical wave source with the radius ε and the length dy

Expressions (42) and (44) show that equivalent oscillating sources must have the same momentum with constant frequency. It is therefore possible to form a substitute equivalent cylindrical source. In view of the relation $\Lambda \gg \varepsilon \to 0$, the shape of the source is insignificant. The momentum of an equivalent oscillating source can be written in the form

$$dMU_1 = \varrho\pi\varepsilon^2 U_1 dy. \tag{45}$$

Comparison of expressions (40), (41) and (39a) and (42), (44), (45) and (39b) gives the acoustic pressure of the wave radiated by the two equivalent cylindrical sources considered above, with the length dy, i.e.

$$dp' = -j\left(\frac{\omega^2\varrho D_0}{\pi r} + \frac{3}{4}\frac{j\omega^2\varrho D_1}{\pi r}\cos\theta\right)\exp[j(\omega t - kr)]dy. \tag{46}$$

Considering relations (13a) and (12), it is finally possible to write the expression for the sound pressure of the wave radiated by the element dy placed on the Y axis of a blood vessel. This pressure is equal to the pressure of the wave

reflected from the vessel

$$dp' = \left(\frac{D_0^*}{\pi r} + \frac{3}{4}\frac{jD_1^*}{\pi r}\cos\theta\right)\frac{k\varrho c w a_p^2}{2f}\exp\left\{j\left[\omega t - kf\left(1+\frac{y^2}{2f^2}\right) - kr\right]\right\}\times$$
$$\times\frac{2J_1(ka_p y/f)}{ka_p y/f}\,dy, \tag{47}$$

where

$$D_0^* = D_0/\Phi_M, \tag{47a}$$
$$D_1^* = D_1/\Phi_M. \tag{47b}$$

6. Ultrasonic waves incident on the transducer

The coordinate system now can be changed by setting its centre at the point G (Fig. 2) and reversing the sense of the X axis.

The sound pressure of the wave incident on the piezoelectric transducer T, averaged over its surface, can be determined using the integral

$$dp'_{av} = \frac{1}{\pi a_p^2}\int_0^{a_p}\int_0^{2\pi} dp' s\,ds\,d\psi. \tag{48}$$

The waves radiated by equivalent sources placed on the axis of the vessel penetrate obliquely the wall of the vessel, whereas the solution obtained in chapter 3 applies to a plane problem and therefore can be used only for a perpendicular penetration of the wave through the walls of the vessel. The resulting differences in phase and amplitude are so small as to be neglected, which follows from the geometry of the problem assumed ($f \gg a_p$ and $\Lambda \gg a$).

In formula (47) r can be expressed by s and ψ (see Fig. 2). Subsequently the expression for dp' thus changed can be inserted into formula (48) and integration carried out in this formula with respect to the variables s and ψ in the way used in chapter 2. This gives the mean acoustic pressure caused on the surface of the transducer by the wave radiated by cylindrical sources of length dy placed on the Y axis of the blood vessel.

Carrying out, in turn, further integration with respect to the variable y within the limits $\pm\infty$, all the contributions of the elementary waves radiated by the equivalent sources can be gathered. This integration leads to the final result in the form:

$$p'_{av} = \left(D_0^* + \frac{3}{4}jD_1^*\cos\theta\right)\frac{k\varrho c w a_p^2}{2\pi f^2}\exp\{j(\omega t - 2kf)\}\times$$
$$\times\int_{-\infty}^{+\infty}\left[\frac{2J_1(ka_p y/f)}{ka_p y/f}\right]^2\exp\left(\frac{-jky^2}{f}\right)dy. \tag{49}$$

In formula (20) given by the present autor in a former paper [4] a mistake was made and π^3 should be replaced with 2π, as it is here in equation (49).

The ratio of the power of the wave incident on the transducer N_r to the power of the wave radiated by this transducer N_t will be determined. In view of the geometry of the system assumed, sufficient approximation is provided in this case by the formulae for a plane wave. Thus

$$\frac{N_r}{N_t} \cong \frac{|p'_{av}|^2 \pi a_p^2}{2\varrho c} : \frac{w^2 \varrho c \pi a_p^2}{2} = \left[\frac{|p'_{av}|}{w\varrho c}\right]^2 \tag{50}$$

or, after substitution of the value p'_{av} from expression (49), finally,

$$\frac{N_r}{N_t} = \left|\left[D_0^* + j\frac{3}{4} D_1^* \cos\theta\right] \frac{ka_p^2}{2\pi f^2} \int_{-\infty}^{+\infty} \left[\frac{2J_1(ka_p y/f)}{ka_p y/f}\right]^2 \exp(-jky^2/f)dy\right|^2 . \tag{51}$$

The above formula permits the calculation of signal losses of an ultrasonic wave on its path from the transducer to the blood vessel and back (without considering attenuation in tissue). Substitution of the values a_p, f, k and $D_{0,1}^*$ into the above formula and assumption of the angle θ as 180° approximately (in practice it varies in the limits 177-183°) give the value

$$\frac{N_r}{N_t} = 0.0024^2 \doteq R = -52 \text{ dB}. \tag{52}$$

R represents here the loss in the wave signal radiated, which occurs as a result of that the wave partly goes round the vessel, partly penetrates into it and of that the reflected wave diverges so that only a slight part of the power of the wave returns to the transducer. The quantity R can be called the reflection loss.

7. Detectability of a blood vessel. Discussion

Assumption of an output voltage of the transducer of 250 V and a typical sensitivity of the ultrasonograph receiver of 10^{-5} V gives a ratio of these quantities equal to $W = 2.5 \cdot 10^7 \doteq 148$ dB. The loss caused by the transducing of ultrasonic electrical impulses was assumed as $T = -15$ dB.

Fig. 5 shows the signal level generated by the transmitter and its transducing loss T, the reflection loss R and the attenuation loss A_l in the tissues penetrated. The present hypothetical vessel can be detected at a distance of 10 cm from the surface of the body with attenuation in tissue of 1.8 dB/cm (obstetrics [1]). In the case of attenuation of 3.7 dB (muscle tissue, perpendicular to fibres [7]) the signal will only be stronger by 7 dB than the noise level and it will be more difficult to detect the vessel. When the focal length f is shortened from 10 to 8 cm (dynamic focussing) and the blood vessel is placed there,

the reflection loss R decreases by only about 1 dB, while the attenuation loss A_l decreases by as much as 16 dB. The detectability of a blood vessel would thus increase greatly.

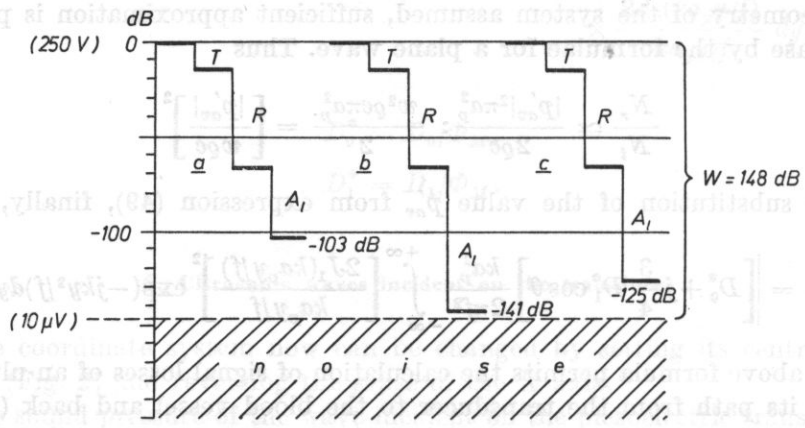

Fig. 5. The signal losses in the detection of a cylindrical blood vessel with a diameter of 0.1 mm by the ultrasonic echo method

T – transducing loss, *R* – reflection loss, A_l – attenuation loss in tissues penetrated, *W* – transmitter voltage to receiver voltage sensitivity ratio

a – distance 10 cm, attenuation in tissue 1.8 dB/cm; *b* – distance 10 cm, attenuation in tissue 3.7 dB/cm; *c* – distance 8 cm, attenuation in tissue 3.7 dB/cm

It is important to note that the tissues penetrated are inhomogeneous. A number of echoes result from reflections from small anatomical structures (muscle fibres, arterioles, capillaries). In view of this, the signal received from a given blood vessel can, nevertheless, remain undetected amoung other signals.

8. Conclusions

The analysis performed has confirmed the previous conclusions of the author [3] regarding the detectability of small blood vessels. The signals received from a very small blood vessel with a radius of 0.1 placed at a distance of 10 cm from the transducer give potentially detectable signals at a frequency of 2.5 MHz.

The substitution of a focussed ultrasonic beam for a parallel one and the consideration of the shear elasticity of soft tissues, in addition to their bulk elasticity, introduced quantitative changes in the detectability of blood vessels. In the present investigation the reflection loss R was -52 dB, while in the previous study their value was -67 dB. In this case the signals received from the vessel under consideration are stronger by 15 dB. The strength of these signals depends critically on the distance between the vessel and the surface of the body, in view of attenuation loss in the tissues penetrated.

The quantitative results obtained here are estimated only, mainly because of the lack of data describing the acoustic parameters of tissues (e.g. the walls of the vessel). In view of this, the difference between the propagation velocities of waves in the tissue surrounding the vessel and in blood has been assumed as the reason for the reflection of ultrasonic waves from the vessel. It is necessary to note, however, that the conditions assumed here are less favourable for the reflection of ultrasonic waves from a blood vessel than in practice.

References

[1] J. ETIENNE, L. FILIPCZYŃSKI, A. FIREK, J. GRONIOWSKI, J. KRETOWICZ, G. ŁYPACEWICZ, J. SAŁKOWSKI, *Determination of ultrasonic focused beams used in ultrasonography in the case of gravid uterus*, Ultrasound in Medicine and Biology, **2**, 119-122 (1976).

[2] L. FILIPCZYŃSKI. *Reflection of plane elastic waves from a cylinder with a free surface*, Proc. II Conference on Ultrasonic Technique, PWN, Warsaw 1957, pp. 21-27.

[3] L. FILIPCZYŃSKI, *Detectability of small blood vessels and flat boundaries of soft tissues in the ultrasonic pulse echo method*, Archives of Acoustics, **6**, 1, 45-62 (1981).

[4] L. FILIPCZYŃSKI, *Detectability of blood vessels with ultrasonic echo method: Physical considerations*, Proc 4-th European Congress on Ultrasonics in Medicine, Ed. A. Kurjak, A. Kratochvil, Dubrovnik 1981, Excerpta Medica, Amsterdam, 81-85.

[5] L. FILIPCZYŃSKI, J. ETIENNE, *Theoretical study and experiments on spherical focusing transducers with Gaussian surface velocity distribution*, Acustica, **28**, 121-128 (1973).

[6] L. A. FRIZELL, E. L. CARSTENSEN, J. F. DYRO, *Shear properties of mammalian tissues at low megaherz frequencies*, JASA, **60**, 1409-1411 (1976).

[7] A. S. GOSS, R. L. JOHNSTON, R. DUNN, *Compilation of empirical ultrasonic properties of mamalian tissues*. II, JASA, **68**, 93-107 (1980).

[8] P. MORSE, *Sound and vibration*, McGraw Hill, New York 1948.

[9] H. T. O'NEIL, *Theory of focusing radiators*, JASA, **21**, 516 (1943).

[10] Lord RAYLEIGH, *Theory of sound*, London 1945.

[11] R. N. RSHEVKIN, *Kurs lektsij po teorii zwuka*, Moscow 1960.

Received on July 7, 1981; revised on January 19, 1982.

ARCHIVES OF ACOUSTICS
7, 3-4, 271-301 (1982)

ACOUSTOOPTIC CONVERSION OF TE AND TM MODES IN A DIFFUSIVE PLANAR WAVEGUIDE

MIECZYSŁAW SZUSTAKOWSKI, BOGUSŁAW ŚWIETLICKI

WAT (00-908 Warszawa, ul. Lazurowa 224)

This paper gives the results of calculations of the accoustooptic effect in a planar graded index waveguide obtained from the diffusion of titanium to a Y-cut $LiNbO_3$. The effect of TE and TM modes are considered. The effectiveness of diffraction ($TE_m \rightarrow TE_m$, $TM_m \rightarrow TM_m$) and conversion ($TE_m \rightarrow TE_n$, $TM_m \rightarrow TM_n$, $TE_m \rightarrow TM_m$) of modes, depending on the acoustic power, is investigated. Calculations are carried out for acoustic wave of 360 MHz frequency.

1. Introduction

Papers [1-5], published recently on the earliest developments of acoustooptic elements in integrated optics, show wide applications of these elements possible in integrated systems of information transmission and processing. In these elements the acoustooptic effect occurs through surface acoustic waves (SAW) acting on a light beam conducted by a waveguide. In view of the complex character of this effect (modal character of light propagation, anisotropic medium), different functions can be implemented in these elements, giving a large family of acoustooptical elements of integrated optics, such as modulators, deflectors, mode convertors, spectrum analysers etc.

The present work contains the results of calculations of acoustooptical diffraction and conversion of modes in a planar modulator with a variable profile of the diffraction coefficient $n(y)$. These calculations took into account three phenomena occurring in the acoustooptical effect in anisotropic crystals:

— photoelastic effect,
— electrooptical effect,
— corrugation of waveguide surface.

The process of conducting a light beam by a waveguide has a modal character, i.e. the light beam conducted has a relevant field distribution in waveguide cross-section.

In view of this, the acoustooptical effect in waveguides can be divided into:

1. mode diffraction (e.g. $TE_0 \rightarrow TE_0$, $TM_0 \rightarrow TM_0$),
2. mode conversion (e.g. $TE_0 \rightarrow TE_1$, $TE_0 \rightarrow TM_0$).

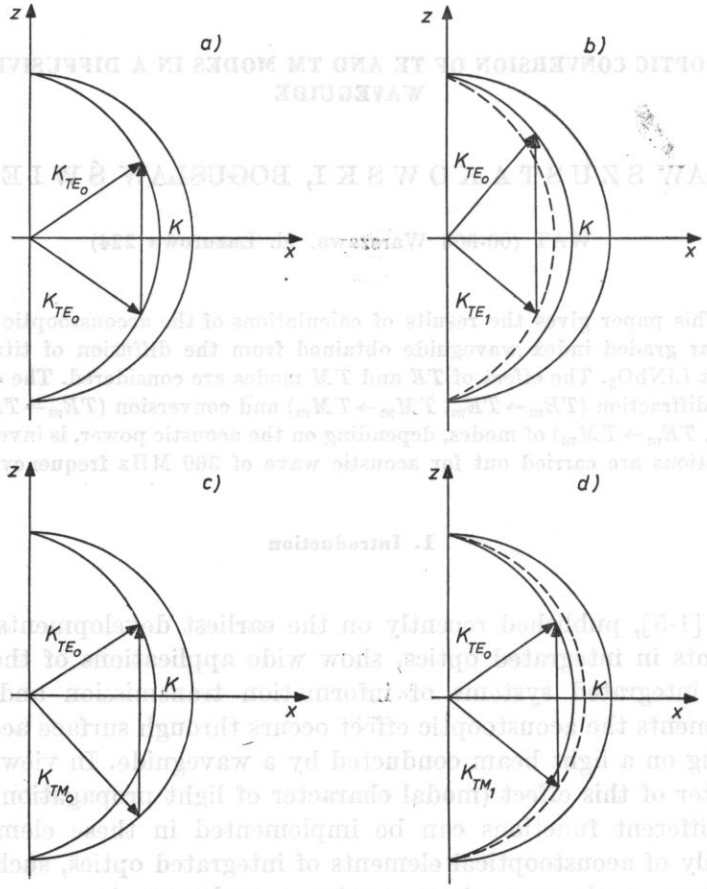

Fig. 1. Relations between wave vectors: a) diffraction of modes, b) conversion of modes (change in mode number), c) conversion of modes (change in polarisation), d) conversion of modes (change in polarisation and mode number)

Fig. 1 shows a relation between the vave vectors of the acting modes and the wave vectors of acoustic waves K in the cases mentioned above. It is necessary to note that in the case of conversion it is possible to distinguish between change in mode number (e.g. $TE_0 \rightarrow TE_1$, Fig. 1b), change in polarisation (e.g. $TE_0 \rightarrow TM_0$, Fig. 1c) and change in polarisation related to change in mode number (e.g. $TE_0 \rightarrow TM_1$, Fig. 1d).

2. Theoretical basis of calculations

Fig. 2 shows the geometry of the system.

The calculation of the effectiveness of the acoustooptical effect in a waveguide with a variable profile $n(y)$ requires the determination of the spatial distributions of the electric field of the light beam $E_m(y)$ and the fields related to SAW propagation, i.e. the displacement field $S(y)$ and the electric field in the piezoelectric material $E^a(y)$.

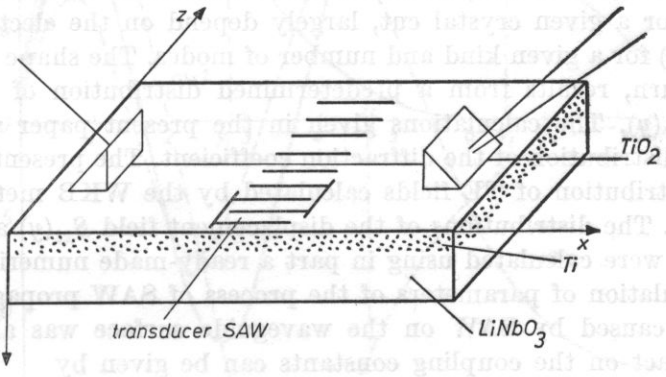

Fig. 2. A schematic diagram of the acoustooptical planar light modulator

The effectiveness of the acoustooptical effect in a waveguide with a variable profile $n(y)$ is given by the expression (6)

$$\eta = \Gamma_{nm}^2 L^2 \sin^2 TL/(TL)^2, \tag{1}$$

where L is the length of the path of the effect, Γ_{nm} is the coupling coefficient, $T^2 = \Gamma_{mn}\Gamma_{nm}$, m, n are mode numbers.

The coupling coefficients Γ_{mn} and Γ_{nm} are given in the following form

$$\Gamma_{mn} = \frac{\pi}{\lambda_0 n_m \cos\theta_m} \frac{\int E_m(y)\,\Delta\varepsilon(y)\,E_n(y)\,dy}{\int E_m^2(y)\,dy},$$
$$\Gamma_{nm} = \frac{\pi}{\lambda_0 n_n \cos\theta_n} \frac{\int E_n(y)\,\Delta\varepsilon(y)\,E_m(y)\,dy}{\int E_n^2(y)\,dy}, \tag{2}$$

where $\Delta\varepsilon(y)$ is change in the tensor of dielectric permittivity; n_m and n_n are the diffraction coefficients for the modes of the orders m and n; θ_m and θ_n are the angles of anisotropic Bragg diffraction.

The change in the dielectric permittivity $\Delta\varepsilon$ of a crystal caused by the acoustic wave field has the form [7]

$$\Delta\varepsilon_{rs} = -\varepsilon_{ri}(p_{ijkl}S_{kl} - r_{ijk}E_k^{(a)})\varepsilon_{js}, \tag{3}$$

where p_{ijkl} and r_{ijk} are, respectively, components of the tensor of photoelastic and electrooptical constants; S_{kl} are components of the displacement tensor; $E_k^{(a)}$ are components of the vector of the intensity of the electric field in piezoelectric material. In expression (3), the first term describes the photoelastic effect, while the second defines the electrooptical effect.

The integrals occurring in formulae (2) for the coefficients Γ_{mn} and Γ_{nm}, called the integrals of field overlap, have direct influence on the effectiveness of the interaction of surface acoustic and optical waves. Their numerical values vary in the limits $0-1$ and, with a constant distribution of the field of acoustic wave $S(y)$ for a given crystal cut, largely depend on the electric field distribution $E_m(y)$ for a given kind and number of modes. The shape of the function $E_m(y)$, in turn, results from a predetermined distribution of the diffraction coefficient $n(y)$. The calculations given in the present paper were taken for a Gaussian distribution of the diffraction coefficient. The present investigations used the distribution of TE fields calculated by the WKB method and given in paper [8]. The distributions of the displacement field $S_{kl}(y)$ and the electric field $E_k^{(a)}(y)$ were calculated using in part a ready-made numerical programme for the calculation of parameters of the process of SAW propagation [9]. The corrugation caused by SAW on the waveguide surface was also considered.

Its impact on the coupling constants can be given by

$$\Gamma_{mn}^{(c)} = \frac{\pi}{\lambda_0 n_m \cos\theta_m} U_2(0) \frac{E_m(0)(\varepsilon - I)E_n(0)}{\int E_m^2(y)\,dy},$$
$$\Gamma_{nm}^{(c)} = \frac{\pi}{\lambda_0 n_n \cos\theta_n} U_2(0) \frac{E_n(0)(\varepsilon - I)E_m(0)}{\int E_n^2(y)\,dy}, \tag{4}$$

where $U_2(0)$ is the value of the component U_2 of the displacement on the surface $y = 0$ and I is a unity matrix.

3. Calculated results

The calculations were taken for several fundamental modes of TE and TM modes. The distributions of the fields $E_m(y)$ for the TE modes were taken from paper [8] in order to make easier the interpretation of the results (Fig. 3).

In the case of the interaction of modes $TE_m \rightarrow TE_n$, the description of the effect only requires the determination of the distribution of one component $\Delta\varepsilon_{33}$ of the tensor of dielectric permittivity. This distribution is shown in Fig. 3b. The electrooptical effect $\Delta\varepsilon_{33}^{(e)}$ dominates as a result of a large value of the constant r_{33} compared to that of the photoelastic p_{33} ($r_{33} = 0.308$; $p_{33} = 0.088$ [10]) for this orientation of $LiNbO_3$ (Fig. 2).

Fig. 4 shows the distribution of the field $E_m(y)$ and the distributions of the components $\Delta\varepsilon(y)$ which describe the interaction of modes $TM \rightarrow TM$.

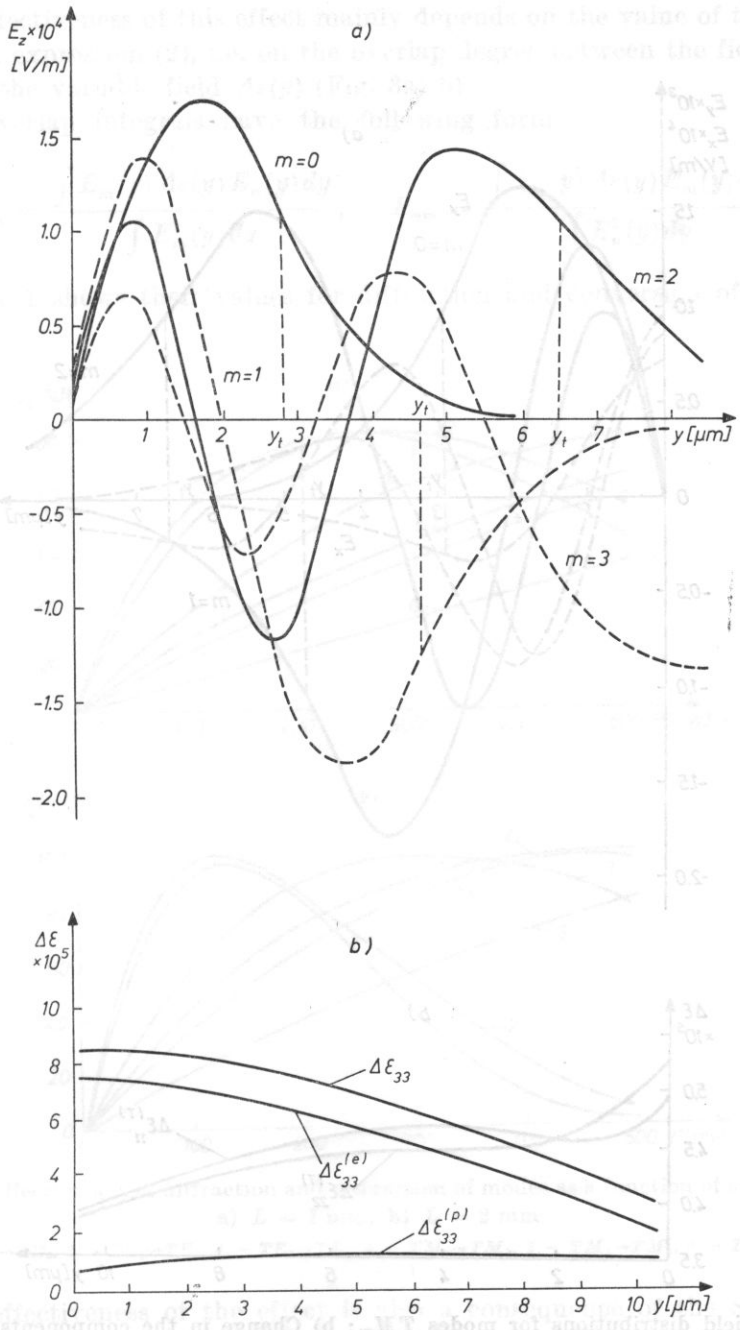

Fig. 3. a) Field distributions for modes TE_m in an $LiNbO_3$: T_i waveguide. The index m represents the number of a mode; b) Change in the component $\Delta\varepsilon_{33}(y)$ of dielectric permittivity: $\Delta\varepsilon^{(p)}$ — change caused by the photoelastic effect, $\Delta\varepsilon^{(e)}$ — change caused by the electrooptical effect

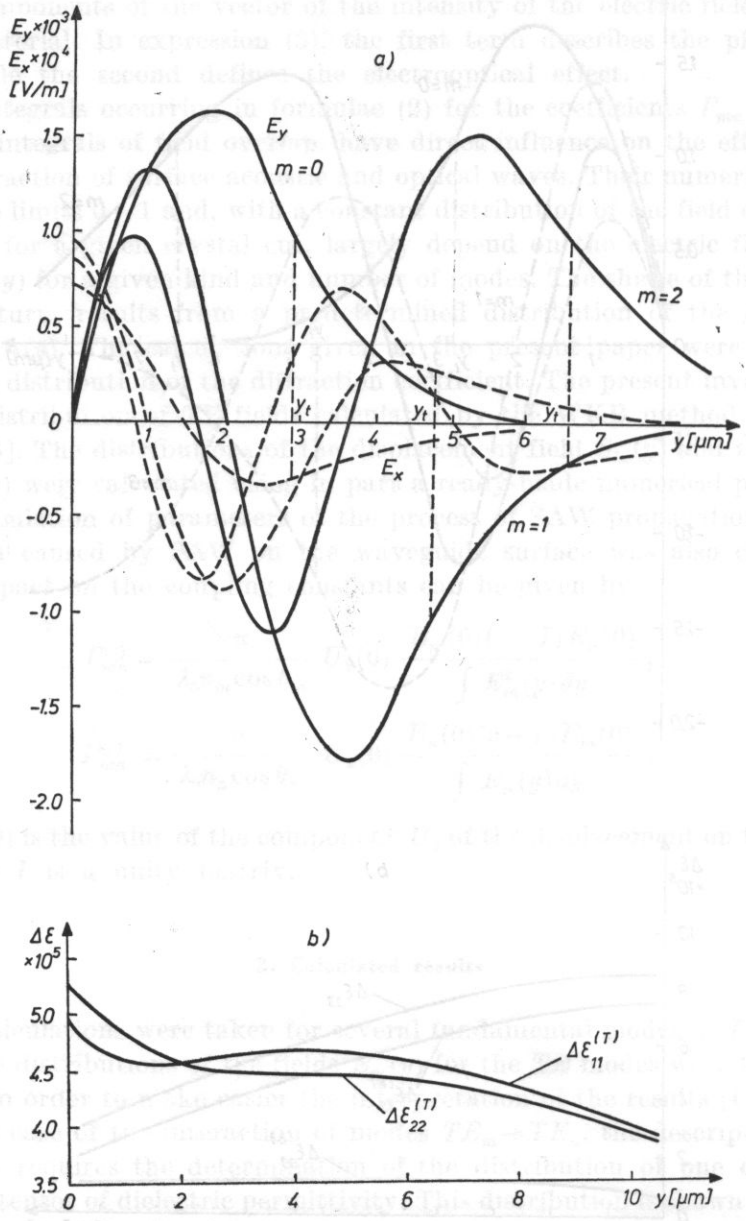

Fig. 4. a) Field distributions for modes TM_m; b) Change in the components $\Delta\varepsilon_{11}(y)$ and $\Delta\varepsilon_{22}(y)$ of dielectric permittivity

The effectiveness of this effect mainly depends on the value of the overlap integrals in expression (2), i.e. on the overlap degree between the fields $E_m(y)$, $E_n(y)$ and the variable field $\Delta\varepsilon(y)$ (Fig. 3a, b).

The overlap integrals have the following form

$$F_{mn} = \frac{\int E_m(y)\,\Delta\varepsilon(y)\,E_n(y)\,dy}{\int E_m^2(y)\,dy}, \qquad F_{nm} = \frac{\int E_n(y)\,\Delta\varepsilon(y)\,E_m(y)\,dy}{\int E_n^2(y)\,dy}, \tag{5}$$

while Table 1 shows their values for diffraction and conversion of particular modes.

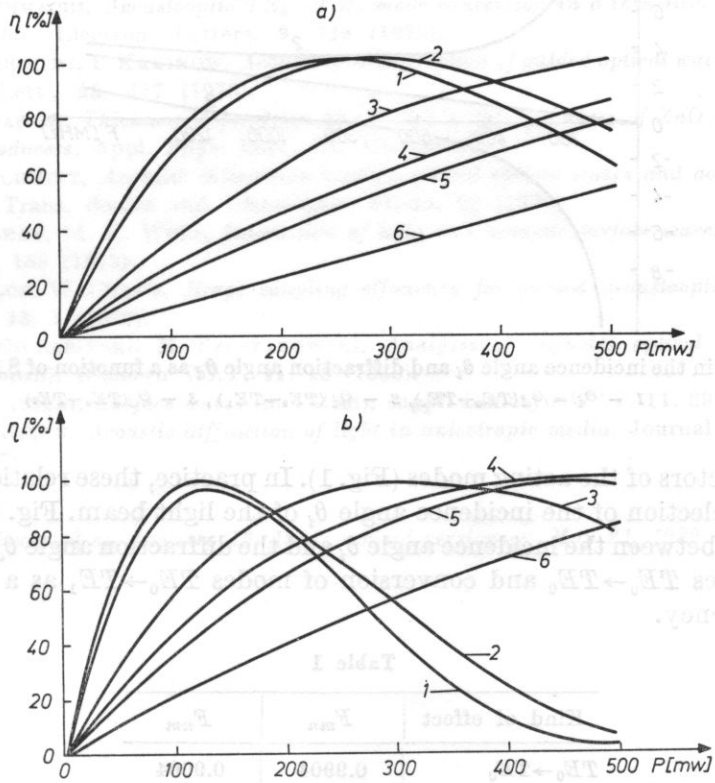

Fig. 5. The effectiveness of diffraction and conversion of modes as a function of acoustic power
a) $L = 1$ mm, b) $L = 2$ mm
1 – $TE_0 \to TE_0$, 2 – $TE_1 \to TE_1$, 3 – $TE_0 \to TE_1$, 4 – $TM_0 \to TM_0$, 5 – $TM_1 \to TM_1$, 6 – $TM_0 \to TM_1$;

The effectiveness of the effect is also a consequence of the SAW power and the length of the path of the effect $(\eta \sim \sin^2(\Gamma\sqrt{P}L))$.

Fig. 5 shows the results of calculations of the effectiveness as a function of the acoustic power P for the length of the path $L = 1$ mm (Fig. 5a) and $L = 2$ mm (Fig. 5b). Comparison of Figs. 5a and 5b shows that a change of

1 mm in the length of the effect path L, which is equivalent to a 1 mm widening of the acoustic beam, leads to a change in the acoustic power required for a hundred percent effectiveness from 250 mW ($L = 1$ mm) to 125 mW ($L = 2$ mm). The corrugation of the waveguide surface is so slight ($\Gamma^{(c)} \approx 10^{-2}\Gamma$) that it can be neglected in the present case. The implementation of particular kinds of effects shown in Fig. 5 requires the satisfaction of respective relations among

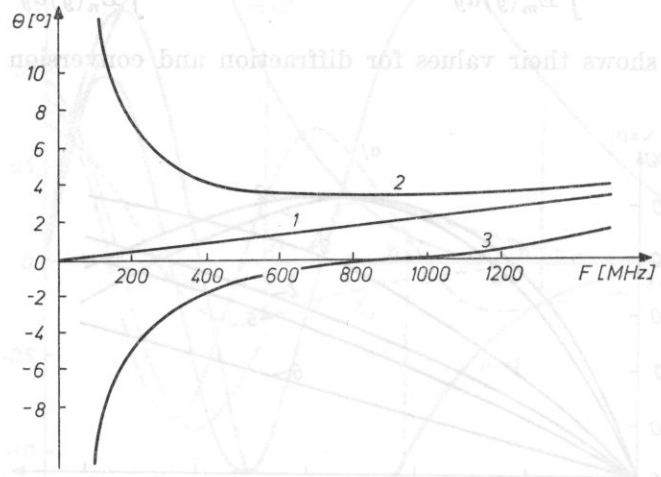

Fig. 6. Change in the incidence angle θ_i and diffraction angle θ_d as a function of SAW frequency
$1 - \Theta_i = \Theta_d(TE_0 \to TE_0)$, $2 - \Theta_i\,(TE_0 \to TE_1)$, $3 - \Theta_d(TE_0 \to TE_1)$

the wave vectors of the acting modes (Fig. 1). In practice, these relations are satisfied by a selection of the incidence angle θ_i of the light beam. Fig. 6 shows the relationship between the incidence angle θ_i and the diffraction angle θ_d for diffraction of modes $TE_0 \to TE_0$ and conversion of modes $TE_0 \to TE_1$ as a function of SAW frequency.

Table 1

Kind of effect	F_{mn}	F_{nm}
$TE_0 \to TE_0$	0.9904	0.9904
$TE_1 \to TE_1$	0.9145	0.9145
$TE_0 \to TE_1$	0.600	0.648
$TM_0 \to TM_0$	0.439	0.439
$TM_1 \to TM_1$	0.403	0.403
$TM_0 \to TM_1$	0.141	0.176

It follows from the behaviour of the relations $\theta_i = f(F)$ and $\theta_d = f(F)$ (Fig. 6) that, in the frequency range $F = 400$-1300 MHz, with a practically

constant incidence angle θ_i, the diffraction angle θ_d varies from -2 to $+2°$.

This is an essential practical conclusion which can be used in the implementation of an acoustooptical planar deflector.

All the calculation whose results are given above were taken for a chosen SAW frequency, $F = 360$ MHz, and the light wavelength $\lambda_0 = 0.6328$ μm.

References

[1] L. Kuhn, M. Dakss, *Deflection of an optical guided wave by surface acoustic wave*, Appl. Phys. Lett., **17**, 265 (1970).

[2] Y. Ohmachi, *Acoustooptic $TE_0 - TM_0$ mode conversion in a thin film of amorphous tellurium dioxide*, Electron. Letters, **9**, 539 (1973).

[3] R. Schmidt, I. Kaminow, *Acoustooptic diffraction of guided optical waves in $LiNbO_3$*, Appl. Phys. Lett., **23**, 417 (1973).

[4] H. Sasaki, *Thickness dependence of effective coupling factors of ZnO thin-film surface-wave transducers*, Appl. Phys. Lett., **25**, 476 (1973).

[5] R. Schmidt, *Acoustic interaction between guided optical waves and acoustic surface waves*, IEEE Trans. Sonics and Ultrasonics, **SU-23**, 22 (1976).

[6] E. Lean, ed. E. Wolf, *Interaction of light and acoustic surface waves*, in *Progress in Optics*, **XI**, 158 (1973).

[7] W. Loh, W. Chang, *Bragg coupling efficiency for guided acoustooptic interaction*, Appl. Optics, **15**, 1 (1976).

[8] W. Ciurapiński, M. Szustakowski, *Analysis of diffusive optical waveguide in $LiNbO_3$* (in Polish), Biuletyn WAT, **11**, 15 (1980).

[9] E. Danicki, *Surface waves* (in Polish), suppl. Biuletyn WAT, **11**, 291 (1976).

[10] D. Dixon, *Acoustic diffraction of light in anisotropic media*, Journal Appl. Phys., **38**, 5149 (1967).

Received on January 16, 1981; revised version on May 21, 1982.

ARCHIVES OF ACOUSTICS
7, 3-4, 281-286 (1982)

AN IMPROVED PIEZOELECTRIC CERAMIC TRANSDUCER FOR ULTRASONIC APPLICATIONS IN AIR

V. N. BINDAL, MUKESH CHANDRA

National Physical Laboratory
(Hillside Road, New Delhi-12, India)

The design considerations of a new type of piezoelectric ceramic transducer for transmitting and receiving ultrasonic waves in air have been reported. This transducer contains a bilaminar assembly consisting of a piezoelectric ceramic disc and a metallic plate which oscillates in flexural mode. This bilaminar assembly mounted at its nodal circle can be designed to operate at a fixed frequency in the range of 25 to 50 kHz.

The constructional details and the working of the transducer have also been given. The resonant frequencies f_{exp} observed experimentally for transducers having good transmitting and receiving sensitivities are found to be in good agreement with the values f_{cal} derived from theoretical considerations.

This closed-type transducer is rugged and compact and can be employed with advantage in several indoor as well as outdoor uses in automation, sensing and remote control applications.

1. Introduction

Ultrasonic transducers [1-4] for use in air have been of much interest in recent times for a number of automation, sensing and remote control applications [5-7], since ultrasonic waves have some definite inherent advantages over the other known conventional techniques.

This paper describes an improved type of ultrasonic transducer [8] developed at the National Physical Laboratory, New Delhi. The design of the transducer is so modified that the vibrating element oscillates freely without having any clamping effect and is completely sealed to avoid the adverse effect of environmental conditions in open fields. The design considerations and the performance of the transducer have also been discussed.

2. Design considerations

The ultrasonic transducer under report comprises a bilaminar assembly of a piezoelectric ceramic disk of lead zirconate titanate (NPLZT-5) [9] developed at the laboratory and a suitably designed metallic circular plate. The oscillation frequency f_r [kHz] of the bilaminar assembly of a nodal diameter d[cm] shown in Fig. 1 is given by the relation [10]

$$f_r = [kh_2/d^2][1+(3/2)A+(3/4)A^2]^{1/2},$$

where

$$A = [(E_1/E_2)(h_1/h_2)^2-1]/[(E_1/E_2)(h_1/h_2)+1],$$

E_1, E_2 are the Young's moduli [N/m^2] and h_1, h_2 are the thicknesses [cm] of the piezoelectric ceramic and aluminium discs respectively. For this bilaminar assembly, k is equal approximately to 434 for the oscillation frequency under consideration.

In an earlier work [3] the oscillating bilaminar assembly was held in position by being supported on the outer periphery between the cork washer and foam. As the amplitude of vibration is minimum at the nodal plane in any oscillating element, it is considered proper that instead of keeping the element in its peripherial area, it may be mounted at the nodal circle.

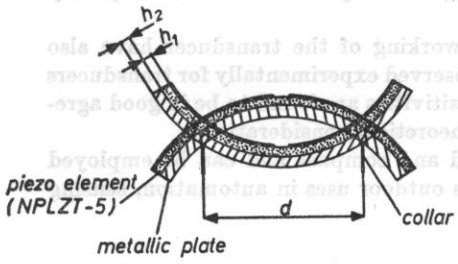

Fig. 1. Sectional view of the oscillation mode of the bilaminar disc at resonant frequency

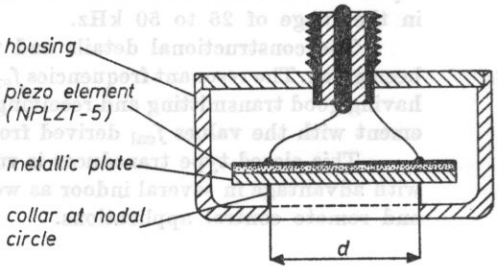

Fig. 2. Schematic diagram of the improved transducer

In view of this, a modification is incorporated in the metallic disc of the bilaminar assembly by providing a thin metallic collar at its nodal circle, as shown in Fig. 1. The calculation of the nodal diameter [13] has been done on the basis of known relations for thin plates. The ceramic disc has two semicircular electrodes on one face and a single electrode on the other. This bilaminar assembly is found to be oscillating freely in flexural mode on excitation by an *a.c.* signal of desired frequency. It is enclosed firmly and rigidly in a metallic housing, making a closed type transducer as shown in Fig. 2. The photograph of the transducer is shown in Fig. 3.

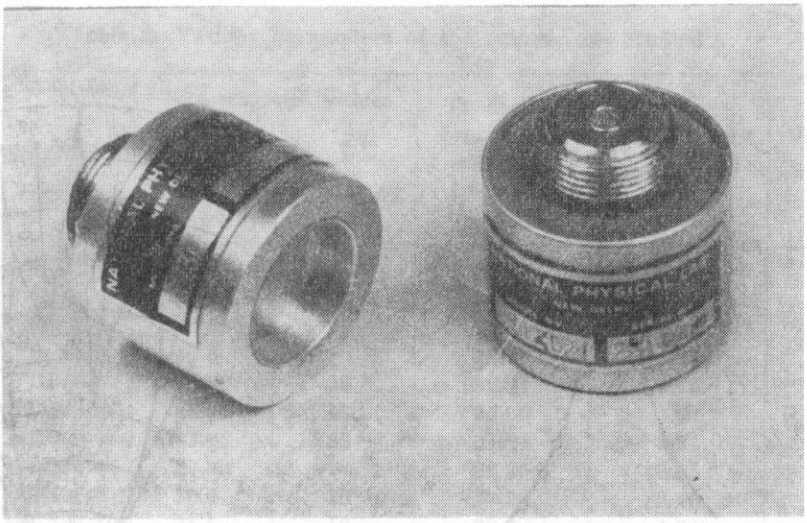

Fig. 3. A pair of improved piezoelectric transducers for ultrasonic applications in air

3. Performance

A series of ultrasonic transducers were made for checking the performance. Typical curves showing the transmitting response and pressure distribution, measured at a distance of 30 cm from the transducer are shown in Figs. 4 and 5, respectively. It is seen from the transmitting response that the transducer produces a sound pressure level of 110 dB and has a narrow 3 dB band width of 0.4 kHz at a resonant frequency of 33.8 kHz, with a Q of about 80. The measured pressure distribution as a function of angular orientation for a typical transducer shows an angular width of $\pm 30^\circ$ for the main lobe.

The results measured experimentally and calculated theoretically are summarised in Tables 1 and 2. It can be seen that the measured resonant frequency f_{exp} of the transducers which have high sensitivity are in good agreement with the results calculated theoretically f_{cal}. The difference $f_{exp} - f_{cal}$ for these transducers is much less than 3.75% of the measured resonant frequency f_{exp}. On the other hand, the transducers for which the difference $f_{exp} - f_{cal}$ of the values observed and calculated of the oscillation frequency is large, varying from more than 5.86 % to as high as 13.78% are also weak in transmitting and receiving sensitivities.

Care was taken so as to avoid either an uneven epoxy layer or any air bubbles entrapped between the two constituents of the bilaminar assembly during fabrication, which could cause poor response of the transducer. It is observed that inspite of taking all the precautions during fabrication of transducers, some of the transducers show poor performance as transmitters and receivers. Moreover, any deviation of the physical constants of the constituents

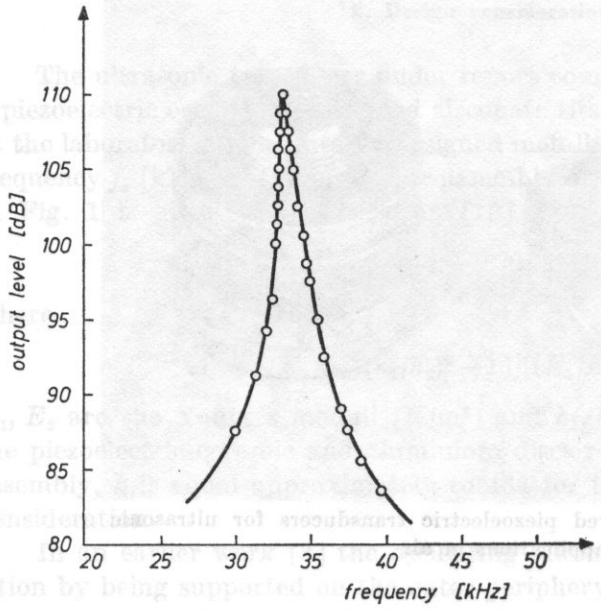

Fig. 4. Transmitting response of a typical transducer

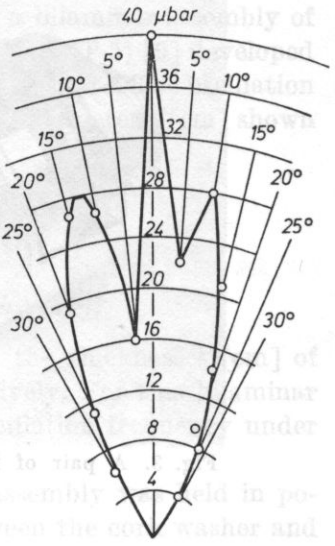

Fig. 5. Measured pressure distribution as a function of angular orientation for a typical transducer

of the bilaminar assembly from one sample to another is also likely to cause differences between the observed and calculated values of the resonant frequencies. It is, therefore, suggested that the desired resonant frequency of the transducer should be adjusted by decreasing either the thickness or the diameter of the metallic plate.

Table 1. Various (dimensional) parameters of the ultrasonic transducers studied

Sample no.	Transducer	Piezoelectric ceramic discs (NPLZT-5)		Aluminium disc		Nodal diameter d [mm]
		thickness [mm]	diameter [mm]	thickness [mm]	diameter [mm]	
1	UT-302-1	1.10	22.1	1.10	24.0	17.50
2	UT-302-2	1.10	22.0	1.10	22.8	17.40
3	UT-302-3	1.05	22.2	1.35	24.5	17.05
4	UT-302-4	1.10	22.1	1.50	25.0	17.05
5	UT-302-5	1.15	22.5	1.45	22.5	16.80
6	UT-302-6	1.18	23.0	1.50	22.5	16.50
7	UT-302-7	1.25	22.2	1.35	22.0	16.80
8	UT-302-8	1.05	22.0	1.20	23.0	17.50
9	UT-302-9	1.15	22.1	1.20	24.0	17.60
10	UT-302-10	1.15	22.0	1.30	23.0	17.60

Table 2. Various parameters of the transducers studied

Sample no.	Transducer	Experimental values: resonant frequency f_{exp} [kHz]	Experimental values: sensitivity [μA]	Theoretical value of oscillation frequency f_{cal} [kHz]	Difference ($f_{exp} - f_{cal}$)	Variation [%]
1	UT-302-1	26.57	35	25.81	0.76	2.85
2	UT-302-2	27.60	25	26.25	0.35	1.26
3	UT-302-3	30.40	25	29.39	1.01	3.32
4	UT-302-4	32.30	40	32.66	0.36	1.11
5	UT-302-5	32.92	30	32.77	0.15	0.455
6	UT-302-6	33.08	18	35.02	1.94	5.86
7	UT-302-7	33.05	22	31.81	1.24	3.75
8	UT-302-8	29.90	15	26.25	3.65	12.20
9	UT-302-9	30.6	10	27.20	3.40	11.10
10	UT-302-10	34.5	10	29.7	4.74	13.73

The modification in the design of the transducer has resulted in improving its transmitting and receiving sensitivities by 8 to 10 % compared with the performance of the transducer reported on earlier.

4. Conclusion

The new ultrasonic transducer developed at NPL is a compact, rugged and inexpensive source of ultrasonic waves in air. It is also an excellent receiver of these waves and is capable of detecting fairly weak ultrasonic signals generally needed in a number of automation, sensing and remote control systems. Apart from these applications, the transducer is suitable in various university experiments such as the verification of Bragg's law of diffraction [11, 12] for ultrasound, the demonstration of the constructive and destructive interference of ultrasonic waves and the determination of ultrasonic velocity in air.

The study shows that the accurate positioning of the nodal circle of the oscillating bilaminar assembly and its mounting there are very critical for its proper transmitting and receiving sensitivities. Care should, therefore, also be taken in the selection of the nodal circle in the proper position. The lead wire for taking connections should be fixed at the nodal circle with a minimum amount of solder to avoid any undesirable loading effect. The transducer, being closed-type and completely sealed, is suitable for both indoor and out door uses.

The technical know-how for the manufacture of the ultrasonic transducer is available through the National Research and Development Corporation of India, New Delhi. The process has already been transferred to two industrial organisations for commercial exploitation. Further work on the development of some other types of ultrasonic transducer for use in air is also in progress.

Acknowledgment. The authors are thankful to Dr. A. R. VERMA, Director, National Physical Laboratory, New Delhi and Dr. G. C. JAIN, Scientist (Director), National Physical Laboratory, New Delhi, for their keen interest in the work. The authors are also thankful to Dr. Janardan SINGH for piezoelectric materials and to Sh. GURMUKH SINGH for help in some measurements.

References

[1] F. MASSA, *Ultrasonic transducers for use in air,* Proc. IEEE, **53**, 1363 (1965).

[2] V. N. BINDAL, Indian Patent No. 116564, 1968.

[3] V. N. BINDAL, *Ultrasonic transducer for automation, sensing and remote control applications,* Research and Industry, **21**, 80 (1976).

[4] V. DOMARKAS, A. MASONIS, A. PETRAUSKAS, *New type of electroacoustic transducers for gases,* Proceedings Ultrasonic International 1977, 180.

[5] H. SAIN, *Ultrasonic sensing,* Ultrasonic, **2**, 179 (1964).

[6] P. GREGUSS, *The applications of airborne and liquid-borne sounds to industrial technology,* Ultrasonics, **2**, 5 (1964).

[7] J. COULTHARD, *Ultrasonic sensing of object in gaseous media,* Ultrasonics, **6**, 167 (1968).

[8] V. N. BINDAL, Mukesh CHANDRA, Indian patent No. 144413, 1977.

[9] G. C. JAIN, V. N. BINDAL, J. SINGH, V. SINGH, N. NARAYANSWAMY, N. C. SONI, *The frequency and temperature dependence of dielectric and electromechanical properties of piezoelectric materials developed at NPL,* Conference Papers, International Conference and Exhibition on Ultrasonics, July 19-20, 1980, 43.

[10] Y. TOMITA, T. YAMAGUCHI, Rev. Elect. Comm. Lab., **13** (1965).

[11] *Physics Demonstration Experiments,* **II**, ed. H. F. MEINERSE, Ronals Press Company, New York 1979.

[12] V. N. BINDAL, Indian Patent No. 122862, 1969.

[13] H. LAMB, *The dynamic theory of sound,* Dover Publ. Inc., New York 1925.

Received on November 22, 1981.

XXVIII OPEN SEMINAR ON ACOUSTICS
Gliwice, 7-11 September, 1981

XXVIII Open Seminar on Acoustics (OSA 81) was held in Gliwice on 7-11 September, 1981. It was organized by the High Silesian Division of the Polish Acoustical Society and the Institute of Physics, Silesian Technical University. The Organizing Committee was headed by Dr. Wiesław KASPRZYK. The Organizing Committee also included Zdzisław JAKUBCZYK, M. Sc., — financial problems, Dr. Eng. Marian NOWAK — foreign correspondence and care of foreign guests and Dr. Józef TABIN — review of papers submitted to the Organizings Committee and edition of seminar proceedings.

130 persons, including 5 foreign guests, took part in the Seminar. The foreign guests were: Dr. Paul FRANÇOIS (France), Dr. Nazar AL-RAWAS (Iraq), Dr. Hamon DETLEV (GDR), Dr. Kaetzmer DIETER (GDR) and Dr. Ruser DETLEV (GDR). Sixty four papers, including three general ones, were delivered. In addition a film was shown on the history and research in the Institute headed by Dr. P. FRANÇOIS.

The Seminar was held in three paralell sessions, each beginning with a leading paper on a given subject.

Section A — physical acoustics, acoustooptics, crystals, sonochemistry, non-destructive testing, piezoelectric and piezomagnetic transducers.

Section B — electroacoustics, acoustics of speech and hearing and musical acoustics.

Section C — hydroacoustics, ultrasound in medicine, noise and vibration.

The papers which had been accepted for delivery by divisions of the Polish Acoustical Society and submitted to the Organizing Committee were published — due to the efforts of the Organizing Committee — in one volume and a supplement (in 150 copies). The proceedings included 90 papers submitted to the Organizing Committee. The traditional Marek Kwiek Competition was organized for which only 3 papers were entered; of which two were distinguished. Dr. Z. KLESZCZEWSKI supervised the Competition in terms of organization and substance.

Dr. J. BERDOWSKI was the Scientific Director of the Seminar, with the assistance of M. STROZIK, M. Sc, The Secretariat of the Seminar, Dr. J. GMYREK, A. KLIMASEK, M. Sc., A. KWAŚNIEWSKI, M. Sc., Dr. R. HNATKÓW and Mr. J. ROCZNIAK, saw to the organization and catering. The technical chores were performed by technicians K. KASPRZYK and J. WIERZBICKI.

On 7-9 September the Seminar was accompanied by an exhibition of acoustic equipment organized by Brüel and Kjaer which enjoyed a great interest.

Two organizational meetings: of the Executive Board of the Polish Acoustical Society and the Plenary Congress of the Delegates of the Polish Acoustical Society in which a new Executive Board was elected, were held on the first day of the Seminar.

A meeting of the Committee on Acoustics of the Polish Academy of Sciences was held on 9 September, 1981.

The Seminar was inaugurated officially on 8 September, 1981. On behalf of the Organizing Committee the guests and participants were welcomed by its president Dr. W. KASPRZYK and subsequently on behalf of the Executive Board by the new President of the Polish Acoustical Society, Prof. Z. JAGODZIŃSKI. Prof. F. KUCZERA inaugurated the Seminar with his general paper *Acoustic properties of a liquid in terms of the theory of a liquid state.* On 9 and 10 September, the sessions also began with general papers: *Application of acoustic methods in mining* by Dr. A. LIPOWCZAN and, *50 years of acoustooptics in Poland* by Prof. A. ŚLIWIŃSKI.

The subjects of papers delivered in the sections were very differentiated, including in effect all the fields of acoustics. The papers delivered and discussion showed the present state of acoustic research and the perspectives for its development.

During the meeting a new Executive Board of the Committee was elected.

The Organizing Committee wishes to express its gratitude to all those who assisted it in its activities and made possible the organization of the OSA'81.

Joachim Gmyrek
(Gliwice)

THE MAREK KWIEK PRIZE

On December 1, 1981 the Jury of the Marek Kwiek Prize, Dr. Eng. Ryszard GUBRYNOWICZ – chairman, Doc. Dr. Hab. Edward OZIMEK and Dr. Eng. Jerzy ETIENNE – members, considered the papers entered for the prize and delivered at the XXVIIIth Open Seminar on Acoustics OSA'81 at Gliwice.

The Jury granted no prize of Ist or IInd degree and distinguished the following papers: Jacek MARSZAL, *An analog delay line for a multi-beam time-space sonar processor*; Zbigniew SOŁTYS, *A model of a sound source working in an interior.*

Chairman of the Jury
Dr. Eng. R. Gubrynowicz

Papers in sections

Section A (chairmen: Z. KLESZCZEWSKI, J. RANACHOWSKI, A. ŚLIWIŃSKI)

W. KASPRZYK, *Analysis of the work of an acoustic atomizer by the method of geometrical points.*
H. KRÓL, *An ultrasonic atomizer of fluid fuels in carburettor of internal combustion engines.*
K. TECHMAŃSKI, A. KOŁODZIEJ, B. KIBORT, B. MAJEWSKI, *Attempts to apply ultrasonic technique in the production of TV units.*
I. AUERBACH, W. SZACHNOWSKI, *Non-destructive ultrasonic control of plastic rotor blades.*
E. GIELATA, *Dimensionless acoustic criterion numbers in description of a thin-walled tube.*
R. PŁOWIEC, S. ERNST, M. WACIŃSKI, *The elasticity of diols, glycerols and glycerol electrolytes over the GHz range.*
W. BOCH, *Acoustic investigations of aqueous solutions of $ZnSO_4$ and $LiCl$.*
J. KOPYŁOWICZ, R. PŁOWIEC, *Anomalies of water viscosity determined by an ultrasonic viscometer.*
M. ŁABOWSKI, *Investigation of the acoustic properties of chosen critical mixtures.*

E. SOCZKIEWICZ, *Propagation of acoustic waves and stochastic characteristics of inhomogeneous media.*

T. ZAMORSKI, *The effect of the curvature of the wave-front on the transmission properties of a horn for frequencies close to the cut-off frequency.*

Z. KLESZCZEWSKI, A. KWAŚNIEWSKA, Z. JAKUBCZYK, *Acoustic and acoustooptic properties of semiconductor crystals.*

J. BERDOWSKI, M. STROZIK, *An acoustooptic modulator using surface waves.*

A. BORKOWSKI, W. PAJEWSKI, *The phase velocity of surface and pseudosurface waves in a quartz crystal.*

R. BUKOWSKI, Z. KLESZCZEWSKI, A. MLECZKO, *The diffraction of light of very high intensity by acoustic waves.*

Z. KLESZCZEWSKI, M. TOMASZEWSKI, *Nonlinear elastic and piezoelectric properties of certain crystals.*

M. ADAMSKI, J. DEPUTAT, *Structural sensitivity of the elasto-acoustic coefficient.*

L. LEWANDOWSKI, *The coefficient of attenuation of acoustic waves in solid stochastic media.*

Z. KUBIK, *A system for the measurement of the acousto-electric effect in a layered structure.*

Section B (chairmen: H. HARAJDA, W. JASSEM)

W. JASSEM, *A regressive model of isochronism in a speech signal.*

A. HAJDUKIEWICZ, *Investigation of visual analogies of a simple sound.*

H. HARAJDA, *The amplitude envelope of the sound of consonants in a lecture hall.*

H. KUBZDELA, *Automatic recognition of words based on binary spectograms.*

I. PECIAK, *Investigation of the masking level and reproduction quality of speech in a system of encoding telephone conversations by four-frequency periodic phase inversion using correlation-spectral methods.*

Z. SOŁTYS, *A model of a sound source working in an interior.*

AL-RAWAS, *Effect of angle of azimuth of a sound and/or its repetition coloration.*

T. LIPIŃSKI, K. MUZALEWSKI, *Amplitude distortions in time-frequency compression and expansion.*

R. MAKOWSKI, *Objective investigations of the effect of localization of sound sources.*

I. SOBOLEWSKI, *Estimation of the autocorrelation function of stationary and ergodic processes.*

I. C. TARGOŃSKI, *Detectability of a sinusoidal signal against a noise background by the free choice method.*

J. ŻERA, T. BOEHM, T. ŁĘTOWSKI, *Conditions of coupling a transducer with the loading medium.*

Section C (chairmen: T. CEYPEK, Z. JAGODZIŃSKI, A. LIPOWCZAN, B. NOSOWICZ)

B. NOSOWICZ, T. WRONA, W. GLIŃSKI, *Chosen examples of designs for noise abatement in Silesian industry.*

A. RUDIUK, *The problem of noise certificate of aircraft.*

D. TRYNKOWSKA, R. MICHALSKI, *Technical parameters and real-ear attenuation of ear muffs.*

W. BEBLO, *Vibrational dosimetry.*

J. DYŻEWSKI, A. HAJDUKIEWICZ, W. WITKOWSKI, *Investigation of the acoustic properties of the music theatre in Gdynia.*

Z. JUSZCZYK, *The usefulness of ultrasonic investigations in diagnostics of some disorders of the abdominal cavity.*

J. KAZIMIERCZAK, *Acoustic identification of events in a working machine.*

W. CHOLEWA, *Application of the Camac system in vibroacoustic investigations.*

E. ZALEWSKA-PACIOREK, *Analysis of the path of a sound ray in a perpendicular-walled interior.*

D. RUSER, *A listing of stochastic measurement methods with information reduction in hydrolocation.*

A. KOWALSKI, *Classification of underwater objects.*

J. MARSZAL, *Analog delay line with sampling for a multi-beam time-space processor of a sonar.*

F. CHINCHURETA, W. MARTIN, R. SALAMON, A. STEPNOWSKI, *Transmission of broad-band signals in hydrocommunication systems.*

A. DYKA, *Experimental investigations of a filter for improving the depth resolution of hydrolocation systems.*

E. KOZACZKA, *Application of the cepstrum function in the investigation of the evolution of pulse hydroacoustic signals.*

J. MARSZAL, R. SALAMON, *A digital time-space processor with the "end-fire" order of microphones.*

J. MORAWIEC, E. KOZACZKA, *Application of the pulse method for determining the sensitivity characteristics of hydrophones.*

K. MUŻA, *Investigation of chosen characteristics of a measurement basin by means of a pulse sound source.*

J. TABIN, *The reflection of elastic waves.*

A. BORKOWSKI, A. PILARSKI, *Analysis of the angular dependence of the coefficient of reflection of ultrasonic waves on the interface between a liquid and a solid.*

B. SIKORA, M. HAGEL, *The reflection of ultrasonic waves from the blurred boundary between two media.*

J. TABIN, *New aspects of the reflection of elastic waves from a sphere.*

J. TABIN, *The directionality of the detection of ultrasonic waves by an oblique probe.*

R. SALAMON, F. CHICHURETA, *Analysis of layered system by the method of differential equations.*

A. KOŁODZIEJSKI, E. KOZACZKA, *Investigations of vibration of a cylindrical liner excited by a vibrating system of pulses.*

Z. KACZKOWSKI, *Dimensions vs resonance frequencies of chosen singleaperture piezoelectric transducers.*

W. LIS, *The effect of the casing on the pulse response of a transducer.*

A. DOBRUCKI, C. SZMAL, I. MORAŃSKI, *The effect of braces and absorption on the vibration of the walls of loudspeaker casings.*

S. BARTNICKI, E. DANICKI, *The effect of the mass of electrodes on the propagation of surface acoustic waves.*

A. STEPNOWSKI, Z. WOJAN, *The frequency response of a cylindrical transducer for radial and longitudinal polarisation.*

DOCTORAL DISSERTATIONS OF POLISH ACOUSTICIANS

ANDRZEJ PUCH

The effect of the operating conditions of axial dynamic generator with the horn and pressure chamber common for all stator channels on its accoustic parameters

This thesis presents a theoretical model (based on electroacoustical analogies) of the acoustic system of a dynamic flow generator in which the horn and pressure chamber (both of annular cross-section) are common for all stator channels. Experimental tests proved the correctness of the model derived in the range described by the assumptions under which it was built. Moreover, the effect of the shape of rotor and stator ports on the power and acoustic efficiency have been analysed. In the case of the port shapes giving rectangular time-depen-

dence of active air-flow area, the twofold increase of power and acoustic efficiency of generator was obtained. The case of power and efficiency drop was also determined in the range of higher frequencies.

Under supervision of Roman Wyrzykowski, D. Sc.,
at the Institute of Physics, Gdańsk University, 1978.

MARIA WYKOWSKA

Equivalent models of machines treated as cylindrical sources of noise

The present work is an attempt to replace a sound source consisting of three electric machines of different dimensions, connected in series by means of elastic couplings on driving shafts, by a cylindrical source. The criterion of directivity is adopted to find a solution to the problem. This criterion is based on the principle of conformability of the measured directional pattern of a real source with the patterns obtained from calculations performed for the adopted model.

Under supervision of Zbigniew Engel, D.Sc.,
at the Institute of Mechanics and Vibroacoustics,
Academy of Mining and Metallurgy, Cracow 1978.

TOMASZ ZAMORSKI

Finite length horn effect on the operating conditions of acoustic siren

The subject of the dissertation is an analysis of the horn part in the construction of dynamic axial generators, so called dynamic axial sirens. The work consists of two parts: the theoretical and experimental. The theoretical part is devoted to an analysis of acoustic wave propagation in hyperbolical horns of annular cross section with the emphasis placed upon the effects of the finite horn length. The experimental part of this work starts with a description of the experimentally examined siren. The experimental methods of determining the power and the acoustic efficiency of generator are also discussed. The results of the power and efficiency measurements have been compared to the discussion carried out in the theoretical part. It was proved that this discussion gives a reliable description of the horn properties as well as it allows foreseeing the influence of these properties upon the generator power and efficiency. The paper ends with a formulation of a set of criteria for the optimum horn choice in the future siren constructions.

Under supervision of Roman Wyrzykowski, D. Sc.,
at the Institute of Physics, Warsaw Technical University, 1979.

URSZULA JORASZ

Psychoacoustic analysis of the Doppler effect in the case of a monochromatic signal

The starting point for theoretical considerations and experimental investigations performed is a specific case of the Doppler effect for a tonal signal. Psychoacoustic experimental investigations consist in the study of a stationary observer's perception of a signal emitted by a moving source; more specifically, a study of the perception of pitch variations in a signal under the conditions of time variation of the loudness of this signal. The investigations were performed in laboratory using a purpose-built electronic model of a moving source.

It follows from investigations that dynamic generalized frequency discrimination thresholds, dependent, on the parameters of the motion of the source with respect to the observer, i.e. the motion velocity, distance, and on whether the source approaches or moves away from the observer were determined. In addition initial data were obtained for further investigations of the coupling between the loudness and pitch of tones in dynamic conditions.

Under supervision of Halina Ryffert, D. Sc.,
at the Department of Acoustics, Mickiewicz
University, Poznań 1980.

ALICJA CZAJKOWSKA

Psychoacoustic analysis of the perception and evaluation of simultaneous variations in the intensity and frequency of a tone

The investigations presented in this work were based on the conception of the existence of a mutual coupling between simultaneously evaluated variations in the loudness and pitch of the same tonal signal with varying intensity and frequency. As an example, some elements of this coupling, related to the perceptibility and evaluation of the magnitude of variations in loudness and pitch, were investigated for a chosen tone. The results obtained were expressed in the form of new, so-called generalized, discrimination thresholds and the curve of loudness and pitch variations sensed to be equal. These permitted to find that it is possible to sum up the subthreshold effects caused by simultaneous intensity and frequency variations in a signal and to obtain thus a superthreshold effect in the form of a sensation of pitch variation. For greater variations in the physical parameters a sort of mutual "masking" of simultaneous loudness and pitch variations of the same tone was found, while in the case when both variations were perceptible it was found that it was possible to compare them in terms of magnitude.

Under supervision of H. Ryffert, D. Sc.,
at the Department of Acoustics, Mickiewicz
University, Poznań 1980.